

**Thesis submitted for the degree of  
Doctor of Philosophy  
University of Leicester**

**By**

**Moses Gerishom Otunga**

**July 2002**

UMI Number: U601307

All rights reserved

INFORMATION TO ALL USERS

The quality of this reproduction is dependent upon the quality of the copy submitted.

In the unlikely event that the author did not send a complete manuscript and there are missing pages, these will be noted. Also, if material had to be removed, a note will indicate the deletion.



UMI U601307

Published by ProQuest LLC 2013. Copyright in the Dissertation held by the Author.  
Microform Edition © ProQuest LLC.

All rights reserved. This work is protected against  
unauthorized copying under Title 17, United States Code.



ProQuest LLC  
789 East Eisenhower Parkway  
P.O. Box 1346  
Ann Arbor, MI 48106-1346

## **PREFACE**

The content of this dissertation is original, except where specific reference is made to the work of others. No part of this dissertation has been submitted to any other University.

**Moses Gerishom Otunga**  
British School of Leather Technology,  
University College Northampton

## ABSTRACT

The influence of drying leather at 30% strain on the tensile strength and crack resistance of the grain layer of chromium tanned bovine leather was examined. The effect of drying under different strains was also examined. Bovine wet blue splits were stretched (by 30%) either along one axis (uniaxial) or two perpendicular axes (biaxial) and dried in this stretched condition. The strength and the fracture toughness of the resulting crust leather, was then evaluated. Drying leather under 30% uniaxial strain resulted in an increase in the tensile strength for samples cut along the stretch axis. However the variation of tensile strength with angle of cutting the specimen with respect to the stretch axis can be described by the Tsai-Hill theory that is applicable to fibre composite materials.

The essential work of fracture approach was applied for the first time to leather specimens cut both longitudinally and transversally to the stretch axis. For all the samples examined, a strong anisotropy in the fracture behaviour was observed. The fracture resistance for cracks propagating along the stretch direction in uniaxial samples was lower than in the transverse direction, this fracture anisotropy being enhanced at higher applied strains. Drying under uniaxial strains above 15%, resulted in an increase in the fracture toughness for cracks running transversally to the strain direction, but at the same time, it seriously reduced the fracture resistance for cracks propagating along the strain direction resulting in global yielding, a phenomenon that rendered the evaluation of fracture resistance by use of essential work of fracture approach unattainable. Drying under biaxial strains above 15% seriously reduced the fracture resistance of leather both perpendicular to and parallel to the backbone.

The application of optical microscopy to observe the propagation of cracks through the grain layer led to the conclusion that drying under biaxial strain can cause a reduction in crack resistance due to changes in the size and nature of a highly orientated fibrous zone close to the crack tip. X-ray diffraction studies were made in order to relate the fracture behaviour to leather structure. The X-ray data was correlated with experimental data in order to investigate the influence of pre-stretching on the strength and hence quality of leather during manufacture and their relationship to the fibrous collagen microstructure.

## **ACKNOWLEDGEMENTS**

I would like to thank my supervisor, Prof. Geoff Attenburrow for his invaluable guidance and encouragement during the course of my studies. I would like to acknowledge the support of all the colleagues in the department who in one way or another contributed to the development of this dissertation. I would like to thank Paul Taylor for his assistance with the construction of the experiment test equipment.

I am also most grateful to many people who helped, advised, or discussed my research. In particular I would like to thank Prof. Keith Meek for many useful suggestions for improvement.

I am indebted to the graduate school for providing the necessary funding for this research work.

Finally, I wish to dedicate this dissertation to my late parents, mother Beninah and father Howard for their countless sacrifices for the sake of my education.

## TABLE OF CONTENTS

<b>CONTENTS</b>	<b>PAGE NUMBER</b>
TITLE	i
PREFACE	ii
ABSTRACT	iii
ACKNOWLEDGEMENTS	iv
CONTENTS	v
NOMENCLATURE	xi

### CHAPTER ONE: INTRODUCTION

1.1 LEATHER MANUFACTURE	2
1.1.1 Pre-tanning operations	2
1.1.1.1 Curing	2
1.1.1.2 Soaking	3
1.1.1.3 Unhairing and Liming	3
1.1.1.4 De-liming	4
1.1.1.5 Bating	4
1.1.1.6 Pickle	4
1.2 TANNING OPERATIONS	4
1.3 POST-TANNING OPERATIONS	5
1.3.1 Dyeing	5
1.3.2 Fatliquoring	5
1.3.3 Drying	6
1.4 LEATHER QUALITY	6
1.5 AREA YIELD	6
1.6 FRACTURE TOUGHNESS	7
1.7 OBJECTIVES AND AIMS OF THE RESEARCH	8
References	9

### CHAPTER TWO: LITERATURE OVERVIEW

2.1 THE STRUCTURE OF THE SKIN	12
2.1.1. Microstructure of collagen fibres	13
2.1.2. The structure of the collagen fibre network	14

2.1.3. The collagen fibre composite	14
2.2 THE CONVERSION OF SKIN INTO LEATHER	15
2.3 AREA YIELD AND LEATHER QUALITY	15
2.4 DRYING OF LEATHER AFTER PROCESSING	16
2.4.1 Hang drying (tension free drying)	16
2.4.2 Vacuum drying	16
2.4.3 Toggle drying	17
2.4.4 Drying with air using a drier and a drying chamber	17
2.4.5 Cross-linking during drying	17
2.5 MECHANICAL PROPERTIES OF LEATHER	18
2.5.1 Linear set	18
2.5.2 Set in collagen fibre aggregates	18
2.5.3 Set of bulk leather	19
2.5.4 Dependence of set on location on the hide	19
2.5.5 Influence of moisture and temperature	20
2.6 SPECIMEN LOCATIONS AND ORIENTATION	21
2.6.1 Specimen location on the hide	21
2.6.2 Specimen orientation on the hide	21
2.7 BIAXIAL TESTING OF LEATHER	22
2.8 CHARACTERIZATION OF FRACTURE ENERGY	24
2.8.1 Fracture mechanics	25
2.8.1.1 Tearing energy	26
2.8.1.2 Fracture energy of notched specimens	27
2.8.1.3 Essential work of fracture	28
2.8.2 Fracture mechanisms	28
2.8.2.1 Fibre fracture and fibre pull out	29
2.8.2.2 Work of fibre debonding	30
2.8.2.3 Fibre orientation	30
2.8.2.4 Angle of weave	31
2.9 MICROSCOPY	31
References	33

## **CHAPTER THREE: GENERAL TESTING TECHNIQUES**

3.1 MATERIALS	41
3.2 GENERAL EXPERIMENTAL PROCEDURES	41
3.2.1 Sample preparation	41
3.2.2 Thickness measurement	45
3.2.3 Specimen strain distribution monitoring	45
3.2.4 Tear tests and sample geometry	46
3.2.5 Crack propagation and fracture tests	47
3.2 TESTING EQUIPMENT	48
3.3.1 Uniaxial testing equipment	48
3.3.2 Biaxial testing equipment	49
3.4 MICROSCOPY.	51
3.4.1 Optical microscopy	52
3.4.2 Scanning electron microscopy	52
3.4.3 X-ray diffraction methods	52
References	54

## **CHAPTER FOUR: TENSILE STRENGTH**

4.1 INTRODUCTION.	56
4.2 FAILURE CRITERIA FOR FIBRE COMPOSITES	57
4.2.1 Limit criteria	58
4.2.2 Interactive criteria	60
4.3 PREDICTION OF COMPOSITE STRENGTH	60
4.3.1 Tsai-Hill theory	61
4.4 COLLAGEN FIBRE ORIENTATION IN LEATHER	62
4.5 FAILURE MECHANISMS IN COMPOSITES	62
4.6 EXPERIMENTAL	63
4.7 RESULTS AND DISCUSSION	63
4.7.1 Variation of tensile strength with position	63
4.7.2 Stress-strain curves for wet blue leather	65
4.7.3 Relationship between elongation and strength	66
4.7.4 Effect of drying on stress-strain curves	67

4.7.5 Effect of specimen size	69
4.7.6 Effect of orientation angle on strength	70
4.7.7 Failure mechanisms	74
4.7.8 X-ray diffraction studies	78
4.8 CONCLUDING REMARKS	81
References	82

## **CHAPTER FIVE: MODELLING ELONGATION AT BREAK**

5.1 INTRODUCTION	88
5.2 ELONGATION AFTER STRAIN DRYING	89
5.3 MECHANICAL PROPERTIES OF COLLAGEN FIBRE AGGREGATES	89
5.4 DEFORMATION MECHANISMS	89
5.5 POISSON'S RATIO	90
5.6 ELONGATION TO BREAK MODEL	91
5.7 RESULTS AND DISCUSSION	95
References	100

## **CHAPTER SIX: FRACTURE TOUGHNESS EVALUATION**

6.1. INTRODUCTION.	104
6.1.1 Fracture mechanics	105
6.1.1.1. Notch sensitivity	106
6.1.1.2 Stress intensity approach	107
6.1.1.3 Energy balance approach	108
6.1.2. Characterization of fracture in ductile materials	109
6.1.2.1. The J-integral	109
6.1.2.2. Essential work of fracture	110
6.1.3. Tear behaviour	114
6.1.3.1. Tear specimen geometry	114
6.1.3.2. Tear test fracture toughness evaluation	115
6.1.3.3. Correlation between fracture toughness tests	116

6.2. EXPERIMENTAL PROCEDURES FOR THIS WORK	117
6.2.1 Materials	117
6.2.2 Crack Propagation tests	118
6.3. RESULTS AND DISCUSSION	118
6.3.1. Effect of uniaxial stretching on EWF	118
6.3.2. Effect of biaxial stretching on EWF	120
6.3.3. Effect of fatliquors on EWF	122
6.3.4. Effect of applied strain on EWF	126
6.3.5. Fracture toughness from tear tests	129
6.3.6. Effect of specimen size and geometry	130
6.3.7. Load displacement curves	132
6.3.8. Notch sensitivity	136
6.3.9. Effect of uniaxial drying on fracture toughness	138
6.3.10. Effect of biaxial drying on fracture toughness	140
6.3.11. Validity of the results	140
6.3.12. Fracture mechanisms	143
6.3.12.1 Frictional sliding and fibre pull-out	144
6.3.12.2 Fibre fracture	144
6.4. CONCLUSION	145
References	146

## **CHAPTER SEVEN: CONCLUDING REMARKS AND FUTURE WORK**

7.1 CHARACTERIZATION OF LEATHER QUALITY	151
7.1.1 Area Yield	151
7.1.2 Freely dried leather	152
7.1.3 Leather dried under uniaxial strain	152
7.1.4 Leather dried under biaxial strain	153
7.1.5 Leather quality from trouser tear test	153
7.1.6 Leather strength	153
7.1.7 Elongation to break	154
7.1.8 Influence of fatliquors	154
7.1.9 Fracture mechanisms	155
7.2 FURTHER RESEARCH	157

## NOMENCLATURE

<b>Symbol</b>	<b>Definition</b>
a	Notch length,
a/w	Ratio of notch length to specimen width,
B	Thickness of leather samples,
E	Tensile modulus
$F_f$	Fracture force
G	Strain energy release rate
$G_{IC}$	Critical strain energy release rate
K	Stress intensity factor,
$K_{IC}$	Critical stress intensity factor, mode I loading,
L	Gauge length of leather samples,
R	Fracture surface energy
W	Width of leather samples,
$W_e$	Essential work of fracture
$W_f$	Total work of fracture
$W_p$	Non-essential work of fracture
$\mu$	Poisson's ratio,
$\lambda$	Fibre length,
$\lambda_0$	End-to-end fibre length before straining
$\lambda_c$	Fibre contour length
$\lambda_\theta$	End-to-end fibre length after pre-straining
$\sigma_f$	Nominal fracture stress
$\sigma_{un}$	Nominal breaking stress of un-notched specimens
$\theta$	Angle between test piece and pre-strain axis
$\theta'$	Angle between line joining fibre ends and pre-strain axis prior to straining
$\sigma_\theta$	Tensile strength at an angle $\theta$ to the pre-strain axis
$\sigma_1$	Tensile strength at $\theta = 0^\circ$
$\sigma_2$	Tensile strength at $\theta = 90^\circ$

$\sigma_N$	Nominal breaking stress for a notched specimen
$\sigma_{UN}$	Breaking stress for a notched specimen
$e_{ld}$	Longitudinal drying strain
$e_{td}$	Transverse drying strain
$e_{bu}$	Total longitudinal strain at break
$e_{b\theta}$	Elongation at break at test angle $\theta$
$\sigma_{1u}$	Longitudinal tensile strength
$\sigma_{2u}$	Transverse tensile strength
$\tau_{12}$	Shear strength
$\omega_f$	Specific total work of fracture
$\omega_e$	Specific essential work of fracture
$\omega_p$	Specific non-essential work of fracture
$\beta$	Shape parameter
$r_p$	Radius of the plastic zone

#### **Abbreviation**

#### **Definition**

EWf	Essential work of fracture
SEM	Scanning electron microscope
LEFM	Linear elastic fracture mechanics
SENT	Single edge notch tension
DENT	Double edge notch tension
FPZ	Fracture process zone
PDZ	Plastic damage zone

# CHAPTER ONE

---

## INTRODUCTION

1.1 LEATHER MANUFACTURE	2
1.1.1 Pre-tanning operations	2
1.1.1.1 Curing	2
1.1.1.2 Soaking	3
1.1.1.3 Unhairing and Liming	3
1.1.1.4 De-liming	4
1.1.1.5 Bating	4
1.1.1.6 Pickle	4
1.2 TANNING OPERATIONS	4
1.3 POST-TANNING OPERATIONS	5
1.3.1 Dyeing	5
1.3.2 Fatliquoring	5
1.3.3 Drying	6
1.4 LEATHER QUALITY	6
1.5 AREA YIELD	6
1.6 FRACTURE TOUGHNESS	7
1.7 OBJECTIVES AND AIMS OF THE RESEARCH	8
References	9

## **1.1 LEATHER MANUFACTURE**

Leather is made from hides and skins that are normally purchased either straight from the slaughterhouse or in preserved form. The manufacturing process is a combination of many mechanical and chemical operations that can be divided into three broad areas, namely pre-tanning operations, tanning operations and post-tanning operations. Tanning is a general term used to refer to the numerous processing steps involved in converting animal hides and skins into finished leather. During tanning, collagen fibres in hides and skins, are reacted with tanning agents to prevent them from decaying and at the same time make them resistant to wetting and also keep them durable and supple. The most common tanning agents are chromium salts and vegetable tannins extracted from tree barks. There are however other tanning agents such as alum, syntans (man made chemicals) and formaldehyde to mention a few. A detailed description of these operations can be found in the leather technician's handbook [Sharphouse, (1995)]. However an overview of the steps involved in leather making will now be presented.

### **1.1.1 Pre-tanning operations**

The purpose of these operations is to increase the amount of water in the hide, to an amount close to that of the "living" hide, remove foreign bodies and loosen the structure. This loosening makes it easier for the tanning agents, fats, dyestuffs and other substances, to penetrate into the hide. In the beam house, non-collagenous proteins are removed from within the hide, as are the epidermis, hair, melanins and components of cell walls, however the collagen fibre skeleton remains unaffected.

#### ***1.1.1.1 Curing***

Tanneries and abattoirs are not normally at the same location and therefore it is not possible to start tanning skins and hides as soon as the animal has been flayed. Before being transported from the abattoirs, the skins and hides have to be protected from putrefaction and rotting that would otherwise take place once the animal is dead. The process that is carried out to protect the skins is known as curing, and there are several

ways in which this can be done. Skins can be chilled and transported in refrigerated trucks. This process is expensive but eliminates the need to use chemical preservatives.

In another approach, skins are laid out on stones in the sun to dry. With this method, there is very little control of the speed of drying due to the unevenness of the stones and it is therefore common for the skins to dry unevenly. One way around this is to stretch the skins across wooden frames. These frames can then be hung in the shade until dry. However, as a rule sun-dried skins do not generally make good quality leather. Skins may also be cured, by immersing them into a salt solution in large container and then stirring constantly, until the brine penetrates the skins. The concentration of salt is kept high, by continually adding salt to the brine solution. The skins are then taken out and dried ready for shipping. This is a very good method for preserving skins, but quite expensive.

### ***1.1.1.2 Soaking***

Soaking is the first stage that aims to clean and wash the hides and skins with water so as to completely re-hydrate them (to return the skins to the state they were in at slaughter). During this stage some of the unwanted non-collagenous materials (blood, dirt and dung) present in/on the hides and skins are removed.

### ***1.1.1.3 Unhairing and liming***

The cleaned skins still have their hair on. The hides and skins are chemically unhaired by applying sodium sulphide and calcium hydroxide. Excess lime is added to raise the solution to a pH of about 12.5 resulting in a swelling of the skin structure, which allows removal of some of the remaining non-collagenous proteins and loosening of the collagen structure.

#### ***1.1.1.4 De-liming***

The liming operation makes the skins very alkaline. In order to begin tanning, the alkalinity has to be lowered considerably. The chemical used for this is ammonium chloride. As the lime in the skin is neutralised by the ammonium chloride, the skin starts to de-swell. As a result, the inter-fibrillary and keratin proteins that were destroyed during liming are washed out of the skin.

#### ***1.1.1.5 Bating***

Bating is a treatment of the hide with proteolytic enzymes to remove additional non-collagenous proteins from the surface of the hide. Bating is carried out in order to soften the skin even further, through the enzymatic removal of muscle fibres. When it is finished, the grain will be smooth and relaxed.

#### ***1.1.1.6 Pickle***

This process brings the skin to the right acidity for tannage. Sulphuric and formic acids are added to bring the skin to a pH below 3. Salt is also added at this stage to prevent swelling

## **1.2 TANNING OPERATIONS**

The tanning process converts the collagen, the major protein of the hide, into a putrefaction resistant condition. There are several tanning processes, which can be summarised as chromium, vegetable and syntan or combined tanning processes. Today, the majority of leathers are chrome tanned in drums using chrome salts (basic tri-valent chromium hydrated sulphate complexes). Vegetable tannage has been eclipsed by chromium as the major tanning material. However, it is still employed for shoe soles and saddlery and some speciality leathers. Syntans are increasingly employed as

auxiliaries in association with chrome and vegetable tannins, or may be employed as principal tanning agents for certain speciality leathers.

After the tanning process, the hides or skins can be transported to other locations; this leather state is known as wet blue (if they are chrome tanned). After tanning some additional operations are required, which in general aim at levelling the hides and skins to give them a uniform thickness.

### **1.3 POST-TANNING OPERATIONS**

After tanning, wet blue may be dyed, fatliquored or retanned. The excess liquid moisture is then driven out of the leather by a samming machine and then dried by various techniques. Before drying fatliquors are incorporated to replace the natural oils of the skin. This minimises the formation of inter-fibre adhesions during drying. After drying, the leather is then treated mechanically to soften it. The specific post-tanning operations vary from tannery to tannery and also depend on the desired end use of the leather being manufactured. This is why most tanneries sell their leather after the wet blue stage so that different clients can carry out the post tanning operations to suit their requirements.

#### **1.3.1 Dyeing**

When the tanning process is complete, the tanned hides and skins can be dyed to the desired colour.

#### **1.3.2 Fatliquoring**

Fatliquoring is usually the last operation in the aqueous phase before drying. This process is generally carried out using either fish oils or synthetic oils that have been emulsified to allow their use in aqueous solutions. The fatliquoring process largely determines the mechanical and physical properties of the leather. If the leather is dried without fatliquoring, it becomes hard and tinny, because the fibres are not lubricated. The function of the fatliquoring is to separate the fibres in the wet state so that they do not stick together too much during drying.

### **1.3.3 Drying**

Skins are dried out following their initial tannage to form crust leather, as this is a convenient point at which to grade the skins. The method, and degree of drying is dependent on the type of leather being produced, with any future transportation of the skins also an important issue. Leather may be dried by any of the five common methods. Air-drying is the simplest method. The leather is hung and placed on racks and dried by the natural circulation of air around it. In toggle drying, the leather is spread on special screens placed in a drier that has controlled temperature and humidity. In a pasting unit, leathers are pasted on large sheets of plate glass, porcelain, or metal and sent through a drier with several controlled temperature and humidity zones. In vacuum drying, the leather is spread out, grain down, on a smooth surface to which heat is applied. A vacuum hood is placed over the surface, and a vacuum is applied to aid in drying the leather. High frequency drying involves the use of high frequency electromagnetic field to dry the leather.

## **1.4 LEATHER QUALITY**

Although the properties of leather depend on the structure of the skin from which it was made, its quality is influenced by the post-tanning operations that are carried out for various reasons. Drying is one of the most important processing steps affecting leather quality. Most leather properties such as softness and tightness of the grain are affected by drying. The method of drying has to be adapted to the characteristics required of the leather.

## **1.5 AREA YIELD**

In the manufacturing of the leather, the raw material is purchased by weight, whereas the price of the finished product is determined by area; therefore any permanent improvement in the area yield must be of considerable commercial importance. Stretching leather during processing has been practiced for many years with the aim of increasing area yield from production and most of the post-tanning operations such as

samming, setting, staking and toggle drying tend to produce a degree of stretch in the leather [Jaret et al (1988)] and may result in area yield [Sykes, (1992)]. However, whilst in-process stretching may improve yield there is concern that it may also degrade the quality of the finished leather. Quality can be measured in terms of strength, fracture toughness or softness depending on the desired end use. Although most significant gains to area yield are made through tensile stresses applied to wet leather, the extent of stretching during drying may be limited by the quality deterioration measured by either fracture toughness, strength or stiffness depending on the anticipated end use. Earlier work on thin strips of leather has shown that tensile modulus and tensile strength are markedly affected when leather is dried under strain [Wright and Attenburrow, (1997)]. The perfect method of drying is that which yields the required leather with the largest area without affecting the quality required for its end use.

## **1.6 FRACTURE TOUGHNESS**

Leather is utilised in the making of shoes, clothing, upholstery and bags. All of these uses require not only good tensile strength but resistance to crack propagation as well. How easily starter cracks propagate in the grain layer depends on its notch sensitivity. However there are marked differences in notch sensitivity between the grain and the corium [O'Leary and Attenburrow (1996)]. This was explained in terms of the observed differences in crack tip configuration of these two layers. It is therefore essential to evaluate the susceptibility to both cracking and tearing of leather that has been pre-stretched during processing. There is also an urgent need to develop a method that can be used to successfully determine crack resistance of leather.

Fracture toughness approaches do not require detailed knowledge of events that accompany crack propagation. Ideally fracture toughness is the sum of all the various dissipative work components arising from the various fracture mechanisms per unit cross-sectional area of the new fracture surfaces created. This subject is of obvious importance to material scientists, because an understanding of micro-structural events that lead to fracture is essential to the development of materials with optimum toughness.

## 1.7 AIMS AND OBJECTIVES OF THE RESEARCH

The main aims of this study were: (a) to provide underpinning knowledge which would help establish the conditions required to give the highest area yield without compromising on leather quality and (b) to establish the relationship between fracture properties, tear resistance, notch sensitivity and grain crack resistance, elongation at break and tensile strength and the underlying fibre structure so as to model the fracture process. In order to achieve these aims an intensive study of strength and fracture behaviour of leather dried under strain was conducted. The specific objectives were to:

- Develop appropriate experimental techniques and the relevant equipment [chapter three]
- Establish using microscopy or otherwise how the fracture mechanisms responsible for changes in strength with strain induced changes in the fibrous microstructure. [Chapter four]
- To develop/apply new scientific approaches to characterise crack resistance in leather [chapter six].
- Quantitatively determine how the degree of set or pre-strain in leather affects its strength [chapter four]
- Quantitatively determine how the degree of set or pre-strain in leather affects its fracture toughness or tear properties [chapter six].
- Quantitatively determine how the degree of set or pre-strain in leather affects its elongation at break [chapter five].
- To apply theoretical developments (sometimes from the composites field) to better understand the nature of the strength changes observed [chapters four and six].

## References

Attenburrow, G.E., "The Rheology of Leather-A review", *Journal of the Society of Leather Technologists and Chemists*, (1992), vol. 77, pp. 107-113

Jaret, R.M. and Sykes, R.L., "Analysis of Video Recordings to Investigate Mechanical Operations", *Journal of the Society of Leather Technologists and Chemists*, (1988), **72**, pp. 94-96

O'Leary, D.N. and Attenburrow, G.E. "Differences in Strength between the Grain and Corium Layers of Leather", *Journal of Materials Science*, (1996), **31**, pp. 5677-5682

Sharphouse, J.H., *Leather Technicians handbook*, Leather Producers Association, (1971)

Sykes, R.L., "Leather Research-Where Now?" *Journal of the Society of Leather Technologists and Chemists*, (1992), **76**, pp. 149-156.

Wright, D.M. and Attenburrow, G.E., "The Set and Mechanical Behaviour of Partially Processed Leather Dried under Strain", *Congress Proceedings of the International Union of Leather Chemists and Technologists (IULTCS), London*, (1997), pp. 686-702

Wright, D.M. and Attenburrow, G.E., "The Deformation and Set of Partially Processed Leather", *Proceedings of the XXII Congress of the International Union of Leather Chemists and Technologists*, Friedrichshafen, Germany, (1995)

# CHAPTER TWO

---

## LITERATURE OVERVIEW

2.1 THE STRUCTURE OF THE SKIN	12
2.1.1. Microstructure of collagen fibres	13
2.1.2. The structure of the collagen fibre network	14
2.1.3. The collagen fibre composite	14
2.2 THE CONVERSION OF SKIN INTO LEATHER	15
2.3 AREA YIELD AND LEATHER QUALITY	15
2.4 DRYING OF LEATHER AFTER PROCESSING	16
2.4.1 Hang drying (tension free drying)	16
2.4.2 Vacuum drying	16
2.4.3 Toggle drying	17
2.4.4 Drying with air using a drier and a drying chamber	17
2.4.5 Cross-linking during drying	17
2.5 MECHANICAL PROPERTIES OF LEATHER	18
2.5.1 Linear set	18
2.5.2 Set in collagen fibre aggregates	18
2.5.3 Set of bulk leather	19
2.5.4 Dependence of set on location on the hide	19
2.5.5 Influence of moisture and temperature	20
2.6 SPECIMEN LOCATIONS AND ORIENTATION	21
2.6.1 Specimen location on the hide	21
2.6.2 Specimen orientation on the hide	21
2.7 BIAXIAL TESTING OF LEATHER	22
2.8 CHARACTERIZATION OF FRACTURE ENERGY	24
2.8.1 Fracture mechanics	25
2.8.1.1 Tearing energy	26
2.8.1.2 Fracture energy of notched specimens	27
2.8.1.3 Essential work of fracture	28
2.8.2 Fracture mechanisms	28
2.8.2.1 Fibre fracture and fibre pull out	29

2.8.2.2 Work of fibre debonding	30
2.8.2.3 Fibre orientation	30
2.8.2.4 Angle of weave	31
2.9 MICROSCOPY	32
References	33

## 2.1 STRUCTURE OF THE SKIN

All animal skins have the same basic structure consisting of two distinct layers, the outermost epidermis and the underlying dermis. The dermis can be further divided into three parts as shown in figure 2.1. The grain layer is beneath the epidermis and is composed of densely woven fibre bundles, which have a fine construction. Beneath the grain layer is the corium layer, which is composed of a network of thicker bundles of strong fibres. In between the grain layer and the corium layer is a zone referred to as the grain-corium boundary in which the collagen fibres progressively reduce in thickness from the thicker corium fibres to the fine grain fibres. The grain and corium layers have been found to have distinctly different mechanical properties (tear strength, tensile strength and notch sensitivity) [O'Leary, (1995)].

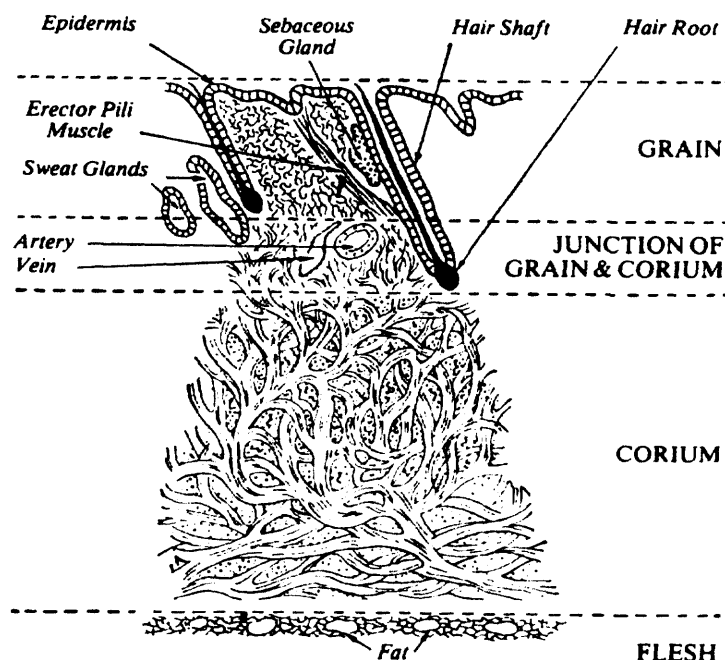


*Figure 2.1; Structure of the skin [cf. Sharphouse, Leather technicians handbook, published by leather producers association, Northampton, (1971)]*

G

Both the corium and grain fibres are made up of collagen. Collagen is the basic structural fibre in all connective tissue. It is often the most abundant protein in animals and is widely distributed in the structural elements of the body. The most important properties of collagenous tissues are mechanical. The understanding of mechanical properties of such tissues requires knowledge of their microstructure as well as of their macrostructure. The unique characteristics of leather are due largely to its fibrous structure, which is an interwoven, three-dimensional network of fibres inherent in the natural raw materials; hides and skins.

### 2.1.1 Microstructure of collagen fibres

Collagen is a fibrous protein whose basic chemical constituents are glycine, proline, and hydroxyproline with some other amino acids present in variable proportions [Baer et al (1991)]. These chains of amino acids are about 290 nm in length and form a triple helical structure. Five hierarchical fibrous units are reported in corium material of bovine leather [Alexander et al, (1993)]. The individual units of this hierarchical structure were shown to have varying diameters as shown in table 2.1 below.

**Table 2.1:** *Hierarchy of structure within the skin [cf. Alexander et al., (1993)]*

<b>Structural unit</b>	<b>Typical diameter</b>
Fibre bundle	60-200 $\mu\text{m}$
Fibre	30-60 $\mu\text{m}$
Fibril bundle	3-6 $\mu\text{m}$
Fibril	100-200 nm
Micro fibril	10 nm

The most fundamental units of collagen fibres have been shown to be the micro-fibrils with diameters of about 0.01  $\mu\text{m}$ . The micro-fibrils aggregate to form fibrils whose diameters range from 0.1 to 0.2  $\mu\text{m}$ . The fibrils in turn aggregate to form the fibril bundle with diameters ranging from 3 to 6  $\mu\text{m}$ . The fibril bundles are also aggregated to form the fibre with typical diameters in the range 30-60 $\mu\text{m}$ . The fibres finally aggregate

to form the fibre bundles of diameters within the range 60-200 $\mu$ m. It is from these collagen fibres and fibre bundles that a fibre network is constructed.

### **2.1.2 Structure of the collagen fibre network**

The construction of the collagen fibre network is characterized by continual branching. The collagen fibril bundle divides into two parts and each of these join with another to form another fibril bundle. This principle also operates on the level of the fibres. A fibre separates into two parts and both of these join with another, changing direction from the original fibre. It is this branching of the collagen structure that gives the corium layer a woven structure [Heidemann, 1993].

### **2.1.3 The collagen fibre composite**

In a natural skin, collagen fibrils are surrounded by an extracellular matrix, which maintains the integrity and architecture of the collagen. The primary component of this matrix is a high molecular weight hyaluronic acid with a highly branched aggregate of proteoglycans. It is now known that a proteoglycan, dermatan sulphate is distributed over the surface of collagen fibrils in a regular and highly organized manner. Dermatan sulphate is found at the surface of all fibrils whether they are the larger central corium fibre bundles or the individual fibrils immediately below the epidermis [Haines, (1983)].

Dermatan sulphate has a marked influence on collagen stability. It is the ability of the proteoglycans to absorb water that swells the matrix and supports the collagen fibrils. The mechanical properties of the matrix are regulated by its water content, which in turn affects the properties of the composite tissue as a whole. In this hydrated state the collagen fibril is extremely flexible. As noted earlier the inter-fibril and inter-fibre spaces of the network contain hyaluronic acid and proteoglycans, especially dermatan sulphate. These substances probably form a coat on the surface of the fibrils and act mainly as a lubricant to lower the friction between fibres during the movement of the skin.

## **2.2 THE CONVERSION OF SKIN INTO LEATHER**

During the complex process of converting skin into leather, non-collagenous tissues and proteoglycans such as dermatan sulphate are removed causing the collagen fibre structure to be opened up [Stanley, (1992)]. The individual fibrils and fibril bundles that make up the fibres of the collagen network are separated. The remaining collagen network is then tanned in order to crosslink the collagen molecules of the fibrils as already explained in section 1.1.

## **2.3 AREA YIELD AND LEATHER QUALITY**

Leather is sold mainly on an area basis and therefore maximizing area yield is the aim of the trade, provided this is not done at the expense of quality. Leather is made to meet various end use purposes that need varying qualities that must not be sacrificed at the expense of area yield. Apart from the raw hide from which leather is made, the major components determining leather quality [Daniels, (1993)] are

- The chemical processing from the raw hide to the tanned condition
- The modification of the basic tanning method by a variety of retanning and fatliquoring materials.
- Mechanics associated with the process vessels and leather making machinery
- The drying techniques employed.

Each of these components needs to balance with the others. If one or more of these components does not harmonize with the required characteristics, then it is necessary to attempt to build these properties into the leather using the remaining options. With chrome leathers it is general practice to manufacture or purchase a versatile wet-blue which can be adapted to a reasonably wide range of leathers as opposed to a specialised tanning procedure. Thus enhancement of wet-blue towards a set of target properties is normally achieved by using the correct mechanical and drying techniques.

## **2.4 DRYING OF LEATHER AFTER PROCESSING**

Drying is one of the operations during leather making that has a great effect on leather quality. Leather softness, tightness of the grain, area yield and many other properties are a consequence of the drying conditions employed, especially, temperature, humidity and time. In a hydrated state, leather is fully lubricated with water that is held between the elements of the fibre. In this state it can be moulded into any shape. However, as the leather is dried, the fibres approach each other and have a tendency to stick together to an extent that depends on how the water is removed. The method of drying is therefore adapted to the characteristics of the required leather. An ideal method of drying is one that gives maximum area yield without compromising quality.

### **2.4.1 Hang drying (tension free drying)**

During hang drying, leather is hung in ambient air and is allowed to dry over days. It is through simple stress free hang drying at moderate temperatures that a majority of the soft textured leathers are made. These leathers tend to be plump and have fine break characteristics but with corresponding loss of potential yield due to the fibres setting at a higher angle of weave owing to lack of tension in the drying cycle.

### **2.4.2 Vacuum drying**

The most widely adopted post-tanning drying procedure in Europe is vacuum drying followed by hang drying. During vacuum drying, wet leather is laid flat with the grain surface down, on a flat heated plate and then covered with an airtight hood and then a vacuum is applied. The rapid removal of water in this operation, coupled with combination of contact time, temperature and pressure exerted on the fibre structure has a significant effect on the grain appearance. Vacuum drying is often followed by toggle drying or tension free drying to improve softness and break and also to remove the firmness that usually accompanies vacuum drying.

### **2.4.3 Toggle drying**

Toggle drying is the operation in which leather is stretched on special frames using clamps and then allowed to dry with time. The tension applied during the toggling operation can retain much of the yield gained and preserve a better shape. This tension also increases the firmness, coarseness of the grain and the break characteristics.

### **2.4.4 Drying with air using a drier or a drying chamber**

This is accomplished by passing both air (at appropriate temperature and humidity) and leather in opposite directions in a drier. In this operation the incoming air at first comes in contact with nearly dry leather leaving the drier. At this stage, the drying potential of air is the highest. As it becomes increasingly more saturated, the same air comes stepwise in contact with increasingly wetter leather. To increase its water uptake capacity in several of its final stages, the air has sometimes to be reheated.

### **2.4.5 Cross-linking during drying**

During drying leather loses moisture to the atmosphere and capillary forces cause it to shrink. Recent studies [Komanowsky, (1990)], indicate that below 9% moisture content, the macrostructure shrinks to the extent that close approach of the fibrils allows the formation of permanent cross-links and compressive forces on the fibrils to be developed. This bonding together of collagen molecules in close proximity renders leather less soft.

## 2.5 MECHANICAL PROPERTIES OF LEATHER

The use of leather in boot and shoe uppers depends upon its viscoelastic properties that permit it to be shaped upon the last in shoe manufacture. This allows it subsequently to extend and contract more or less elastically in response to the stresses imposed during wear. A number of investigators [Mitton and Price (1970), Upstone and Ward (1969) and Whittaker (1975)] have examined the set and viscoelastic properties of leather on the basis of hysteresis observed at low strain cycling.

### 2.5.1 Linear set

When viscoelastic materials are extended by the application of tensile stresses and then released, they do not immediately return to their original length but retain a certain amount of the initial extension normally referred to as set. If we consider a sample of initial length,  $L_0$  which is extended until its length is  $L_i$  and is held for a period of time at that length. Upon release the sample retracts to a length  $L_f$ , set may then be defined as the recovered strain divided by the applied strain and expressed as a percentage as indicated below:

$$LinearSet = 100 \left[ \frac{L_f - L_0}{L_i - L_0} \right] \quad (2.1)$$

If a disc of leather is considered instead of a strip, the area changes can be used instead of the linear extensions in which case plastic deformation can be measured by area set.

### 2.5.2 Set in collagen fibre aggregates

A significant amount of work has been carried out on the mechanical properties of tanned collagen fibres teased from the corium material. Results of studies [James et al (1965)] on heat setting of chrome-tanned collagen fibres indicate that set of single fibres resembles set in pieces of upper leather, but whereas heat setting of leather results in high values of set, the influence of heat setting on the single fibres was relatively small. Similar studies [Millar et al (1967)] in which chrome-tanned collagen fibres were

extended and set by either heating them in an oven or steam/air mixture, the fibres showed similar changes in set as those observed with strips of leather. These results suggest the crucial role played by the presence of water between the individual units of leather fibres.

### **2.5.3 Set of bulk leather**

Set increases with the amount of applied strain, however linear set is considerably lower than area set for low values of applied strain [Butlin, (1963)]. These observations can be explained in terms of the way the fibre feltwork deforms [Attenburrow, (1992)]. In linear straining, the feltwork is capable of more straining prior to the fibres themselves becoming strained whereas in area straining, less feltwork deformation can occur before the fibres come under strain. The implication of this argument is that it is necessary for the fibres to be strained in order to achieve higher values of set.

Recent studies [Wright and Attenburrow, (1995)] on the mechanical behaviour of partially processed leather dried under strain indicate that high degrees of set are produced by drying under strain and that the leathers produced in this way have an increasing stiffness whose magnitude corresponds to the original stress-strain curve of the wet blue leather. Leather dried under strain was also observed to exhibit a lower elongation at break due to the prior deformation of the fibre network.

### **2.5.4 Dependence of set on location on the hide**

Several studies [Poplewell and ward, (1963) & Miller and Mitton, (1967)] have examined the variation of set with location on the hide. Poplewell and Ward (1963) measured linear set at various positions over a side and found little systematic variation with hide location of the percentage set, although there was a considerable variation between neighbouring specimens. Later Mitton and Millar (1967) examined linear set and area set of chrome side leather for samples cut parallel and perpendicular to the backbone. In both cases their results confirmed Poplewell and Ward's conclusions that linear set and area set are highly variable quantities. In part, the variability was

attributed to locational differences dependent on anatomical features, but much of it seemed to be in the nature of random fluctuations that were large even for neighbouring specimens.

### **2.5.5 Influence of moisture and temperature**

The effect of dry heat setting and moist heat setting on the degree of set has been examined by a number of workers [Holmes and Ward (1971), Guy (1976) and Upstone and ward (1969)]. Holmes and Ward (1971) studied the influence of dry heat setting and moist heat setting processes used in the lasting of shoe upper leathers. Dry heat setting produced area set as high as 50-60% as compared to steam heat setting which barely achieved an area set of about 40% after the same period of recovery. They attributed this phenomenon to strain recovery that occurred immediately upon release of heat set samples due to their high moisture content. It is also clear from their results that area set increases substantially with the applied strain. They attempted to relate the percent area set with the linear strains imposed in the two perpendicular directions. It was observed that the area set was dependent on the various levels of percent linear strain in the direction parallel to the backbone

Guy (1976) examined the effect of heat setting on the deformation and mechanical hysteresis energies of commercial full chrome side leather samples subjected to cyclic deformation of up to 2.5% strain. It was found that the majority of permanent set was confined to the first extension cycle. He suggested that viscoelasticity and flow deformation could be the most important hysteresis mechanisms for leather. Hence the total energy of deformation to a given strain is composed of the energy of elastic deformation, the energy loss due to visco-elasticity and the energy loss due to plastic flow.

Upstone and Ward (1969) examined the form of the load extension curves in the low (1-2%) strain region for a number of leathers and the effect on this curve of moisture, heat setting and various tanning processes. The results of the various experiments both with leather and with synthetic substitutes showed that for many materials the first 1-2% extension gives a markedly non-linear load extension curve. There was considerable

variation between neighbouring strips, suggesting the importance of the local fibre structure. Contrary to expectation, heat setting failed to modify the stress strain behaviour of the leather except that the toe region departed from linearity more after heat setting than before.

## **2.6. SPECIMEN LOCATION AND ORIENTATION**

A number of workers [Mann et al (1951), Kanagy et al (1952) and Maeser (1960)] examined the differences that occur in the tensile properties of leather due to location and orientation of the specimen on the hide as discussed below.

### **2.6.1 Specimen location on the hide**

Maeser (1960) studied the effect of hide location and cutting direction on the tensile properties of upper leathers. He found out that the agreement in tensile strength between two sides of a single hide is generally much better than that between two adjacent blocks cut from the same side of the hide. He concluded that the tensile properties of leather naturally vary over the hide according to a definite pattern which is the same for all bovine hides regardless of the age, sex, or size of the animal from which the skin is taken or the tanning procedures used in making the hides into leather. Mann (1951) and Kanagy (1952) reported similar observations.

### **2.6.2 Specimen orientation on the hide**

It is common practice in testing leather to cut specimens either parallel or perpendicular to the backbone. Leather is made up of a network of interweaving collagen fibres and it was formerly assumed that this interweaving is random. Evidence [Osaki, (1999)] however has been accumulated to show that the interweaving of fibres follows a definite pattern in the skin. The fibre pattern causes variation in different locations on the hides of all physical properties and in particular that of strength. The tensile strength usually is greater when it is determined in a direction parallel to the backbone, which indicates that the orientation of the fibres is predominantly in this direction.

At a given location on the hide, there must therefore be some direction along which specimens can be cut to give a maximum value of a given physical property; and by the rules of symmetry, specimens cut in a direction perpendicular to the direction of maximum would be expected to give the minimum value of the same property [Maeser, (1960)]. Since fibres run predominantly parallel to the backbone, the angle between the backbone and the direction along which specimens must be cut to obtain the maximum value of a property can be designated as the principal angle. This principal angle is envisaged to be unique for a particular physical property at a given hide location, for example, the principal angle for the tensile strength will not necessarily be the same as the principal angle for elongation. Maeser (1960) devised a method of sampling which gives the directions a specimen should be cut at any given skin location to obtain either the maximum or the minimum of the tensile strength or any other tensile property. Specimens cut at an angle of  $45^{\circ}$  to the backbone showed the lowest variations.

## **2.7 BIAXIAL TESTING OF LEATHER**

Despite the fact that the process of shoe lasting is a complex multi-dimensional deformation, many of the experimental investigations of the shoe upper leather have concentrated on the determination of uniaxial tensile failure stresses and strains [Kanagy, (1955) & Roddy, (1956)]. In part this is due to the variability of the physical properties of leather over the area of a single hide, and between different hides which has presented a major obstacle in evaluation of the laws of leather deformation in the laboratory and therefore still needs experimental investigation.

During the lasting process the shoe upper experiences large deformations for which the uniaxial tensile stress test cannot be used to correctly express the two dimensional stress-strain relationships. Few studies [Butlin (1963)] however have been carried out on two dimensional stress-strain behaviour of leather. The apparatus used in both investigations did not enable independent extensions to be applied in two directions. In most of its uses, leather does not deform uniformly in two dimensions as occurs in the dome plasticity apparatus. The dome plasticity apparatus also has the disadvantage that it is not possible to make direct stress-strain measurements.

Although apparatus were later designed [Poplewell and Ward (1963)] to measure the applied load at constant extension, the rate of testing could not be ascertained from these apparatus. Due to the short periods of testing (15 minutes) it was difficult to differentiate plastic flow (set) from visco-elastic behaviour. Similar apparatus were also used [Mitton and Millar (1967)] to measure linear set. Area set was measured on a dome plastimeter. The rate of testing could not be ascertained from the dome plastimeter apparatus.

The plastimeter apparatus was also used to investigate the elastic properties of leather in two dimensions [Ward and Chinn (1971)], however the rate of straining could not be ascertained from this apparatus. The strains were increased step-wise in one direction, while employing a constant strain in the second direction.

Later investigations on the influence of area strain on area set [Ward and Chinn (1971)] using similar apparatus showed that area set increases substantially with the area strain and that there is a tendency of the percent area set to approach an asymptote as the area strain approaches 20%. An attempt was made to relate the percent area set with the linear strains imposed in the two perpendicular directions. This showed that the area set was dependent on the various levels of percent linear strain in the direction parallel to the backbone. From their results it can be concluded that the higher the percent linear set in the variable strain direction, the higher will be the percent linear set in the constant strain direction. This means that there is an interaction between the two directions of straining.

A biaxial testing facility has been used to investigate the mechanical behaviour of shoe upper leathers [Lin and Hayhurst (1993)]. They concluded that shoe upper is an orthotropic material under bi-axial stress situations in both the butt and belly regions. The directional difference of the stress-strain behaviour in the butt region was less pronounced than that in the belly region. This was attributed to the fibre network structure in the two principal directions being relatively more equal for the butt region.

## 2.8 CHARACTERIZATION OF FRACTURE ENERGY

The fracture resistance of any material is an important factor in determining the end uses for which the material will be suitable. There is need to establish a physical quantity that can better represent the strength characteristics of leather. The ideal physical quantity should not be sensitive to sampling angle, and should reflect the fracture resistance of leather. The physical quantity should also be able to characterize the toughness of leather and correlate well with other specific strength requirements such as tear strength and tensile strength. The approach here is to use an energy concept. Fracture energy is normally used as a measure of fracture toughness. Recent investigations [Liu et al, (1999)] aimed at characterizing the fracture resistance of leather by measuring the energy required to fracture a sample using the area under the force displacement curve, indicated that the sampling angle has little effect on the fracture energy as compared to tensile strength and elongation at break both of which depend on the sampling angle. In this study however crack propagation studies were not undertaken. For crack propagation to occur, there has to be a balance of energy between the increase in energy required to produce new crack surfaces and the decrease in the elastic stored energy [Griffiths, (1920)]. The elastic stored energy is not distributed uniformly throughout the specimen but is concentrated in the region of small cracks.

If the energy required to form a new surface is assumed to be associated with the breaking of chemical bonds, then the surface energy calculated is much lower than the value obtained from tensile or cleavage experiments. This is because a large contribution to the surface energy arises from viscous flow and alignment of polymer chains. Account must also be taken of the energy loss from the system associated with the kinetic energy of crack propagation. The Griffith theory is therefore not immediately applicable to leather, since during tearing, energy is being irreversibly lost by viscoelastic and flow processes. This energy dissipation is however confined largely to the tip of the growing tear and will depend on the shape of the tip, rather than the shape of the tear specimen and the detailed manner in which the tearing forces are applied.

When all the energy interchanges during the fracture process are balanced out, an amount will be found to be lost after crack extension. This is the work of fracture, which

when divided by the increase of the area,  $A$  of one side of a crack is called the fracture toughness,  $R$ . Fracture toughness is a characteristic material property and can vary with strain rate, temperature, environment and microstructure [Atkins and Mai, (1985)]. However the interrelation between the applied load, the corresponding displacement, the associated crack area and the relevant fracture toughness, during crack propagation may be determined from the Griffith's energy balance approach. There are however two major approaches that are normally used to study the fracture process of materials, namely:

- Fracture Mechanics and
- Fracture Mechanisms.

### **2.8.1 Fracture mechanics**

Fracture mechanics is the theoretical formulation of the conditions of deformation under which a crack will propagate in a continuous medium. Fracture mechanics does not therefore require a detailed knowledge of the micro-mechanisms of fracture. The complicated crack tip events that occur during fracture are conveniently glossed over in the macroscopic fracture toughness term,  $R$ . It must be appreciated that fracture toughness is the sum of all the various dissipative work components arising from the various fracture mechanisms per unit cross-sectional area of fracture referenced to the area of the main crack. A number of factors must be satisfied before engineering fracture mechanics can be applied to a given class of material [Andrews, (1980)], namely

- the strain must be proportional to the stress ( linearity)
- all deformations up to a certain limit are elastic i.e. reversible (no energy is lost in a stress-strain cycle). This also implies that all deformations are fully recoverable
- the elastic strains are infinitesimally small
- a material departing from linear elastic behaviour must do so by undergoing fully irrecoverable plastic flow.
- the material is isotropic in its mechanical properties.

Leather is not only anisotropic but also exhibits large recoverable deformations in which significant energy loss (hysteresis) takes place in a loading/unloading cycle. True plastic

flow and true linear elasticity does not occur in leather and hence linear elastic fracture mechanics (LEFM) fails to provide a suitable framework in which to consider the fracture of leather. Consideration of fracture in leather is mainly concerned with its physical aspects and hence requires a theory of fracture that contains explicit parameters describing its physical and molecular properties. Here conventional fracture mechanics also fails because it characterizes a material's fracture resistance in terms of an empirical parameter that has no explicit relationship to its physical properties.

### ***2.8.1.1 Tearing Energy***

The ability to withstand tearing forces is one of the most significant mechanical properties required for leather products, particularly those used for upholstery. The study of tear characteristics of leather is important because a common mode of mechanical failure of footwear and clothing in service is a tearing of some form. It has been generally accepted that the loads required to initiate or propagate a tear or the maximum tearing load are measures of the tear resistance of the material [Guy and Marriott (1974)]. However a better criterion of resistance to tearing is the energy required to initiate and propagate the tear.

During tearing experiments, the load is applied at a constant rate of specimen extension. The total tearing energy is the sum of the energy required to initiate the tear and energy required to propagate the tear and is dependent on the distance travelled by the tear.

Results from studies on several test specimen shapes have shown that the tearing energy is independent of the specimen geometry but markedly dependent on the diameter of the crack tip. The ratio of tearing energy to diameter of crack tip is however approximately constant [Rivlin and Thomas (1953)]. The tearing of leather has in many respects been likened to the tear behaviour of some elastomers [Mitton (1945)]. Indeed the tearing of leather resembles that of some elastomers, in that it is not catastrophic, but the initiation energy depends on the rate of tearing and the diameter of the tip of the tear [Guy and Marriott, (1974)]

### ***2.8.1.2 Fracture energy of notched specimens***

The study of a material's response to the presence of notches is essential not only in material selection but also in the evaluation of the service behaviour and life expectancy of components designed from that material. When a material is notch sensitive, the presence of a small crack or notch causes a stress concentration at the tip of the crack. This stress concentration promotes fracture at applied stresses that are lower than those required to fracture an unnotched specimen. In contrast, the effect of a notch in a notch-insensitive material is to reduce the nominal breaking stress. However this reduction is only in direct proportion to the reduction in cross-sectional area as a consequence of the notch presence [Kelly & Macmillan, 1986].

Recent studies [O'Leary and Attenburrow, (1996)] have demonstrated that the corium layer of crust leather is a notch insensitive material. This has been attributed to fibre orientation in the corium that takes place at the crack tip when leather is subjected to tensile stresses. Hence there is need to investigate the notch sensitivity of leather whose fibres have been subjected to some pre-orientation by drying under strain. The same authors have however shown that when leather is split at the grain-corium boundary, the grain only material so obtained is notch sensitive.

In a perfectly notch-insensitive material, the nominal applied stress necessary to produce failure falls linearly with notch length. The relationship between nominal fracture stress  $\sigma_f$  and notch length,  $a$ , as proposed by Kelly and Macmillan is given by

$$\sigma_f = \sigma_{UN} \left[ 1 - \left( \frac{a}{w} \right) \right] \quad (2.2)$$

in which  $\sigma_{UN}$  is the nominal breaking stress of un-notched specimen, and  $w$  is the width of the specimen.

### **2.8.1.3 Essential work of fracture**

Essential work of fracture was originally proposed by Broberg [Broberg, (1968)] and later developed by Mai and Cotterell [Mai and Cotterell, (1986,1987)] for fracture toughness characterization of ductile materials. As a result of their work, the essential work of fracture (EWF) is increasingly being used for the fracture toughness determination of a wide range of ductile materials [Saleemi and Nairn, (1990), Hashemi, (1997), Tanaka and Yamauchi, (2000)].

According to the EWF theory, the total energy ( $W_f$ ) required to break a notched specimen is the sum of two terms, called the essential ( $W_e$ ) and the non-essential ( $W_p$ ) work of fracture. The total fracture energy ( $W_f$ ), which is the integral of force over displacement during a fracture test, can therefore be expressed by:

$$W_f = W_e + W_p \quad (2.3)$$

The essential work of fracture is related to the energy required for the creation of new fracture surfaces and is therefore a pure crack resistance parameter and thus regarded as fracture toughness. The non-essential work or the plastic work is related to energy dissipated in the region surrounding the fracture surfaces where various types of deformations (crazing, micro-voiding and shear) may take place. Therefore ( $W_e$ ) is surface related, whereas ( $W_p$ ) is a function of the deformed plastic volume surrounding the crack surfaces. This approach is presented in detail in chapter 5.

### **2.8.2 Fracture Mechanisms**

The term fracture mechanism is normally used in relation to the physical or molecular processes that occur in the vicinity of a propagating crack eventually leading to fracture. This approach requires knowledge of material responses as the crack propagates and that in turn requires localised measurements. Such measurements generally require complex microscopic techniques in order to determine the response of a material at the crack tip. Mechanisms of interest in stress strain relationships are disruption of

adhesions between fibres, fibre breakage, fibre pull-out, increases in fibre orientation and notch tip blunting.

### ***2.8.2.1 Fibre fracture and fibre pull-out***

In fibrous composites, fibre fracture occurs when a matrix crack approaches a continuous fibre of uniform strength whose ends are embedded in the matrix at distances greater than the transfer length, experiences a transfer stress by shear from the matrix which is equal to or greater than its fracture stress. It must however be noted that most fibres have flaws at various places along their length and that there is a statistical variation of fibre strength along its length so that a fibre in the path of the crack will be broken either where it crosses the plane of the crack (where the stress is greatest) or at a flaw in the fibre which is near, but not necessarily on the plane of the crack. It is evident that fibre fracture occurs in leather failure and it is reasonable to equate a composite matrix with the feltwork of fibres in which an individual fibre is embedded and attached.

Fibre pull out occurs when a fibre, large enough to receive stress by shear from the fibre feltwork, reaches its fracture stress and fractures ahead of the propagating crack. Fibre pull-out has been observed [O'Leary and Attenburrow (1996)] from the collagen fibre feltwork of both the corium and the grain layers of bovine leather. During fibre pull-out, irreversible work is expended against friction in pulling the length of fractured fibre through the fibre feltwork until it becomes completely liberated. Thus high levels of fibre pull out in a fracturing material ensure high levels of energy absorption during the fracture process. Fibre fracture is a prerequisite for fibre pull-out. For fibre pull out to occur, the fibre must fracture ahead of a propagating tear [Kelly & Macmillan, 1986]. Accordingly, fibres ahead of the tear have to be sufficiently large to receive stress by shear from the fibre feltwork to attain fracture stress.

### ***2.8.2.2 Work of fibre debonding***

Work of fibre debonding may be defined as the work done in the breaking of inter-fibre adhesions. For leather there is essentially no matrix. However the feltwork of tanned collagen fibres enables stress and strain transmission during mechanical deformation and so a pseudo matrix can be assumed to exist. In a tendon, the dissociation of large fibres from their matrix as well as the dissociation of fibrils within larger fibres has been observed [Torp et al (1975)]. If de-bonding occurs at each hierarchical level within the fibre as well as the fibre debonding from the matrix, the energy required in the process of debonding is elevated thus increasing the fracture toughness

### ***2.8.2.3 Fibre orientation***

When leather is deformed, the fibrils and whole fibres (fibril bundles) which are initially stuck to each other, slide or move apart or are torn from fillers and excess solidified tanning agent in spaces in the leather structure [Kronick and Maleef (1992)]. At the same time the fibres turn into the direction of the stretch. For a notched specimen fibre orientation results in blunting of the notch with an associated change in the morphology of the crack tip material often over quite large regions, both of which affect the fracture resistance of a material.

Progressive fibre orientation is dependent upon the initial alignment of fibres (with respect to the direction of applied strain) before the material is strained. When the majority of the fibres are already aligned in the same direction as the applied strain, they have little scope to orientate towards the strain axis (i.e. they are already aligned in this direction). Hence the fibres themselves are directly strained at low levels of nominal strain. However if many fibres are aligned at large angles to the direction of the applied strain, the fibres may orientate towards the strain axis. This orientation would ensure higher levels of nominal strain are achieved before straining the fibres themselves.

The level of fibre orientation is also dependent on fibre mobility. The mobility of individual fibres within the 3-dimensional feltwork of fibres is restricted by such factors as the level of fibre lubrication, fibre diameter, the fibre packing density and the subsequent restriction placed on the fibres by other fibres within the feltwork.

#### ***2.8.2.4 Angle of weave***

Angle of weave is the average angle between the leather surface and the interweaving fibres within the leather structure. The angle of weave plays an important role in determining the breaking strength and elongation at break of leather. For high tensile strength the fibres need to interweave at a low angle so that the load can be transferred along the fibre axis. The tensile strength of leather is a function of the number of fibres in the woven fibre network that are oriented in the direction of the applied load.

Leather with fibres at a high angle of weave show a little resistance to extension [Ward and Brooks, (1966)]. For extensions of up to 60% before rupture, the structure of the fibre network was observed to be held together by interlacing fibres at other angles. On the other hand, leather with fibres of low angle of weave was reported to have small breaking extension and high breaking stress. For a low angle of weave, it was believed that movement of the fibres during extension was limited and therefore high stresses develop at low extensions. However observations on the low strain characteristics of leather [Upstone and Ward, (1969)] could not relate the alignment of the fibres to the applied loads or to the low strain behaviour. It must however be appreciated that as the specimen is stretched the fibres oriented in the direction of the applied load approach each other so that the extent to which the cross section of the specimen narrows is inversely proportional to the number of fibres already oriented in that direction. Extension then requires stretching of the fibres rather than changes of angle between them. In most circumstances, tensile strength is inversely proportional to elongation so that a high strength usually indicates low elongation, whereas a low strength indicates high elongation.

## 2.9 MICROSCOPY

The optical microscope and scanning electron microscope (SEM) have both been used to investigate the fracture mechanisms that take place during fracture of a given material. Scanning electron microscopy has been used to examine the morphology of individual fibrils in dry leather [Stanley, (1992)]. However treatment of leather samples to facilitate examination in the microscope introduces artefacts into the structure that could compromise the interpretation of the photomicrographs [Haines, (1983)]. Conventional light and scanning electron microscopy has been used to establish the hierarchical structure of collagen fibres [Alexander et al, (1993)]. Light microscopy was used to assess the gross structure and angles of weave of the fibre bundles and the opening up of the fibres. The higher magnifications possible with SEM allow the hierarchical structure to be clearly seen.

Very few studies have used microscopy to characterize the in situ fracture mechanisms involved in the fracture of leather. However the optical microscope has been used [O'Leary and Attenburrow, (1996)] to examine tear propagation in notched leather samples. Use of SEM was limited to the examination of fracture surfaces. Fracture surface micrographs provided a basis for understanding the fracture process in each layer of leather by visual assessment of properties such as fibre pull out and fracture surface roughness.

## References

Alexander, K.T.W., Covington, A.D., Garwood, R.J. and Stanley, A.M., "The Examination of Collagen Ultrastructure by Cryo-Scanning Electron Microscopy", *XXII IULTCS Congress Proceedings*, Brazil, (1993), pp 1-12

Andrews, E.H., "A generalised Theory of Fracture Mechanics", *Journal of Materials Science*, (1974), **9**, pp 887

Andrews, E.H. and Billington, E.W., "Generalised Fracture Mechanics, Part 2 Materials Subject to General Yielding", *Journal of Materials Science*, (1976), **11**, pp 1354

Andrews, E.H. and Fukahori, Y. "Generalised Fracture Mechanics-Part 3 Prediction of Fracture Energies in Highly Extensible Solids", *Journal of Materials Science*, (1977), **12**, pp 1307

Andrews, E.H., "The Mechanical Properties of Biological Materials-Fracture", *Symposia of the Society for Experimental Biology*, (1980), **34**, pp 13

Atkins, A.G. and Mai, Y.M., "Elastic and Plastic Fracture", (1988), John Wiley and Sons, Chichester

Attenburrow, G.E. and Wright, D.W., "Studies of the Mechanical Behaviour of Partially Processed Leather", *Journal of the American Leather Chemists Association*, (1995a), **89**, pp. 391-402

Attenburrow, G.E., "The Rheology of Leather-A Review", *Journal of the Society of Leather Technologists and Chemists*, (1993), vol. **77**, pp107-114

Baer, E., James, J., Cassidy, J. and Hiltner, A. "Hierarchical Structure of Collagen Composite Systems: Lessons from Biology", *Pure and Applied Chemistry*, (1991), vol. **63**, No. **7**, pp. 961-973

Bailey, J.E., "Mechanical Properties of Composites- Micromechanics", Handbook of Polymer Fibre Composites, Longman scientific and technical (UK), Jones, F.R. editor, (1994), pp 212-230

Butlin, J.G. " The Plasticity and other Related Properties of Upper Leather", *Journal of the Society of Leather Trades Chemists*, (1963), **47**, pp. 3-38

Daniels, R., "Drying Leathers", *World Leather*, (1993), December/January, pp. 12-17

Gordon, J.E., *Structures or Why Don't Things Fall Down*, (1978), Penguin, London

Griffith, A.A, "The Phenomenon of Rupture and Flow in Solids", *Philosophical Transactions of the Royal Society London*, (1920), **A221**, pp 163

Guy, R. and Marriott, "The Measurement of Elongation at Break in Leather Testing" *Journal of the Society of Leather Technologists and Chemists*, (1974), vol. 58, pp137-144

Guy, R. "The Effect of Heat Setting on Low Stress/Strain Characteristics of a Full Chrome Side Leather", *Journal of the Society of Leather Trades Chemists*, (1976), vol 56, pp. 246-260.

Guy, R. and Marriott, "A Comparison of Two Tear Tests for Leather" *Journal of the Society of Leather Technologists and Chemists*, (1975), vol. 59, pp30

Haines, B.M, "The Skin before Tannage-Procter's View and Now", *Journal of the Society of Leather Technologists and Chemists*, (1983), vol. 68, pp 57-70

Hashemi, S., "Ductile Fracture of Polymer Films", *Plastics, Rubber and Composites Processing and Applications*, (1993), Vol. 20, No. 4, pp229-237

Hashemi, S., "Work of Fracture of PBT/PC Blend: Effect of Specimen Size, Geometry, and Rate of Testing", *Polymer Engineering and Science*, (1997), vol. 35, No. 5, pp 912-921

Hashemi, S. and Yuan, Z., "Fracture of Poly(ether-ether ketone) Films", *Plastics, Rubber and Composites Processing and Applications*, (1994), vol. 21, No. 3, pp151-161

Hashemi, S., "Temperature and Deformation Rate Dependence of the Work of Fracture in Polycarbonate (PC) Film", *Journal of Materials Science*, (2000), **35**, pp 5851-5856

Hayhurst, D.R., "A Biaxial-Tension Creep-Rupture Testing Machine", *Journal of Strain Analysis*, (1973), Vol. 8, No. 2, pp119-123

Heidemann, E., "Fundamentals of leather manufacturing", (1993), Eduard Roether K.G., Darmstadt

Hill, R., "A theory of the Yielding and Plastic Flow of Anisotropic Metals", *Proc R Soc Series A*, (1948), pp281-297

Hull, D. and Clyne, T.W., "Strength of Composites" An Introduction to Composite Materials (2<sup>nd</sup> edition), (1996), pp 159-207

James, A., Mitton, R.G. and Miller, M, "Mechanical Properties of Chrome Tanned Corium Fibres", *Journal of the Society of Leather Trades Chemists*, (1965), **49**, p 53

Jaret, R.M. and Sykes, R.L., " Analysis of Video Recordings to Investigate Mechanical Operations", *Journal of the Society of Leather Technologists and Chemists*, (1988), **72**, pp. 94-96

Kanagy, J.R., Randall, E.B., Carter, T.J., Kinmonth, R.H., and Mann, C.W., " Variations of Physical Properties Within and Between Vegetable Retanned Cow and Steer Hides", *Journal of the American Leather Chemists Association*, (1952), **47**, pp. 726-748

Kelly, A. "Interface Effect and the Work of Fracture of Fibrous Composites", *Proceedings of the Royal Society*, London, (1970), **A319**, pp 95

Kelly, A and Macmillan, N.H., "Strong Solids", (1986), Clarendon Press, Oxford

Kendall, K. and Fuller, K.N.G, “J-Shaped Stress Strain Curves and Crack Resistance of Biological Materials”, *Journal of Physics D-Applied Physics*, (1987), **20**, pp 1596

Kinloch, A.J. and Young, R.J., “Fracture Behaviour of Polymers”, Elsevier Applied Science, London, (1990)

Komanowsky, M., “Moisture-Solid Relationships Accompanying the Drying of Leather”, *Journal of the American Leather Chemists Association*, (1990), **85**, pp 6-18

Kronick, P and Maleef, B., “Nondestructive Failure Testing of Bovine Leather by Acoustic Emission “, *Journal of the American Leather Chemists Association*, (1992), **87**, pp 259

Kronick, P. and Beuchler, P., “Fibre Orientation in Calf Skin by Laser Light Scattering or X-ray Diffraction and Qualitative Relation to Mechanical Properties”, *Journal of the American Leather Chemists Association*, (1986), **81**, pp 221-230

Kronick, P., Page, A. and Komanowsky, M., “An Acoustic Emission Study of Staking and Fatliquor”, *Journal of the American Leather Chemists Association*, (1993), **88**, pp 178-186

Liu, C.K., and McClintick, A.D., “An Energy Approach to the Characterization of the Fracture Resistance of Leather”, *Journal of the American Leather Chemists Association*, (1997), **92**, pp103-118

Lin, J. and Hayhurst, D.R., “The Development of a Biaxial Tension Test Facility and its Use to Establish Constitutive Equations of Leather”, *European Journal of Mechanics, A/Solids*, (1993), vol. 12, No. **4**, pp 493-507

Lin, J. and Hayhurst, D.R., “Constitutive Equations for Multi-Axial Straining of Leather under Uniaxial Stress”, *European Journal of Mechanics, A/Solids*, (1993), vol. 12, No. **4**, pp 471-492

Maeser, M. and Dion, O.J., "The Effect of Splitting on Tensile Properties of Leather", *Journal of American Leather Chemists Association*, (1954), **22**, pp. 48

Maeser, M. " The Effect of Hide Location and Cutting Direction on the Tensile Properties of Upper Leathers", *Journal of the American Leather Chemists Association*, (1960), Vol 55, pp 501-522

Mai, Y.W. and Atkins, A.G., "Further Comments on J-shaped Stress-Strain Curves and Crack Resistance of Biological Materials", *Journal of Physics D-Applied Physics*, (1989), **22**, pp 48

Mann, C.W., Randall, E.B., Mandel, J., Kilduff, T.J. and Charles, A.M. "Sampling of Side Upper Leather", *Journal of American Leather Chemists Association*, (1951), **46**, pp. 248-263

Maspoch, M.L., Ferrer, D., Gordillo, A., Santana, O.O. and Martinez, A.B., "Effect of Specimen Dimensions and the Test Speed on the Fracture Toughness of iPP by the Essential Work of Fracture (EWF) Method", *Journal of Applied Polymer Science*, (1999), vol. 73, pp 177-187

Mattei,V. and Roddy, W.T., "Physical Properties of Leather Fatliquored at Different Oil Levels", *Journal of American Leather Chemists Association*,(1957), **52**, pp. 110

Mitton, R.G. and Millar, M., " Linear Set and Area Set of Chrome Side Leather" *Journal of the Society of Leather Trades Chemists*, (1967), **51**, pp. 172-182

Mitton, R.G., "Mechanical Properties of Leather Fibres" *Journal of the Society of Leather Trades Chemists*, (1945), **69**, pp. 169

Mitton, R.G. "The Dependence of Tearing Load on Thickness" *Journal of the Society of Leather Technologists and Chemists*, (1964), **48**, pp. 195

Morgan, F.R., "The Mechanical Properties of Collagen and Leather Fibres", *Journal of the American Leather Chemists Association*, (1960), **55**, pp 4

Mouzakis, D.E., Gahleitner, M. and Karger-Kocsis, J., "Toughness Assessment of Elastomeric Polypropylene (ELPP) by Essential Work of Fracture Method", *Journal of Applied Polymer Science*, (1998), vol. 70, pp 873-881

O'Leary, D., "Differences in Strength Between the Grain and the Corium Layers of Leather", *PHD thesis*, Leicester University, (1995)

O'Leary, D.N. and Attenburrow, G.E. "Differences in Strength Between the Grain and Corium Layers of Leather", *Journal of Materials Science*, (1996), **31**, pp. 5677-5682

Popplewell, D. and Ward, A.G., "The Mechanical Properties of Upper Leather-1 the Measurement of Linear Plasticity", *Journal of the Society of Leather Trades Chemists*, (1963), **47**, pp. 502-511

Stanley, A., "Application of Modern Microscopic Techniques to Leather Manufacturing", *Microscopy and Analysis*, (1992), pp 25-28

Sykes, R.L., "Leather Research-Where Now?", *Journal of the Society of Leather Technologists and Chemists*, (1992), **76**, pp. 149-156.

Tanaka, A. and Yamauchi, T. "Deformation and Fracture of Paper during the in-Plane Fracture Toughness Testing-Examination of the Essential Work of Fracture Method", *Journal of Material Science*, (2000), **35**, pp 1827-1833

Torp, S., Baer, E. and Friedman, B. "Effects of Age and Mechanical Deformation on the Ultrastructure of Tendon", *Structure of Fibrous Biopolymers*, Sythoff and Noordhoff, Netherlands, (1975), p. 223

Upstone, P.J. and Ward, A.G., "The Low Strain Characteristics of Leather", *Journal of the Society of Leather Trades Chemists*, (1969), **53**, pp. 361-375

Vos, A. and Vlimmeren, P.J van., "Topographic Differences in Physical Properties", *Journal of the Society of Leather Technologists and Chemist*, (1973), vol. 57, pp 93-98

Ward, A.G. and Chinn, S.J., "The two Dimensional Deformation of Shoe Upper Materials", *Journal of the Society of Leather Trades Chemists*, (1971), vol. 55, pp. 221-231.

Whittaker, R.E., " The Viscoelastic Properties of Leather and Poromerics", *Journal of the Society of Leather Technologists and Chemists*, (1975), vol. 59, pp. 172-180

Wright, D.M. and Attenburrow, G.E., " The Deformation and Set of Partially Processed Leather", *Proceedings of the XXII Congress of the International Union of Leather Chemists and Technologists, Friedrichshafen, Germany*, (1995b)

Wright, D.M. and Attenburrow, G.E., " The Set and Mechanical Behaviour of Partially Processed Leather Dried under Strain", *Congress Proceedings of the International Union of Leather Chemists and Technologists (IULTCS), London*, (1997), pp. 686-702

Wright, D.M. and Attenburrow, G.E., "Factors Influencing the Plastic Deformation of Leather", *Proceedings of the III Asian International Conference of Leather Science and Technology, Himeji City, Japan*, (1996)

Wu, J. and Mai, Y.W., "The Essential Fracture Work Concept for Toughness Measurement of Ductile Polymers", *Polymer Engineering and Science*, (1996), vol. 36, No. 18, pp 2275-2288

## CHAPTER THREE

---

### MATERIALS AND GENERAL TESTING TECHNIQUES

3.1 MATERIALS	41
3.2 GENERAL EXPERIMENTAL PROCEDURES	41
3.2.1 Sample preparation	41
3.2.2 Thickness measurement	45
3.2.3 Specimen strain distribution monitoring	45
3.2.4 Tear tests and sample geometry	46
3.2.5 Crack propagation and fracture tests	47
3.3 TESTING EQUIPMENT	48
3.3.1 Uniaxial testing equipment	48
3.3.2 Biaxial testing equipment	49
3.4 MICROSCOPY	51
3.4.1 Optical microscopy	52
3.4.2 Scanning electron microscopy	52
3.4.3 X-ray Diffraction methods	52
References	54

### 3.1 Materials

Partially processed chromium tanned leather (wet blue) from the same batch of four full bovine hides was obtained from a UK tannery. Each of the four hides was divided into two sides by cutting along the line of the backbone from shoulder to tail. One side was used for control samples and the other for experimental samples. The area selected for sampling was as shown in figure 3.1. The selected area on each side was 0.6m perpendicular to the backbone and 1.39m parallel to the backbone.

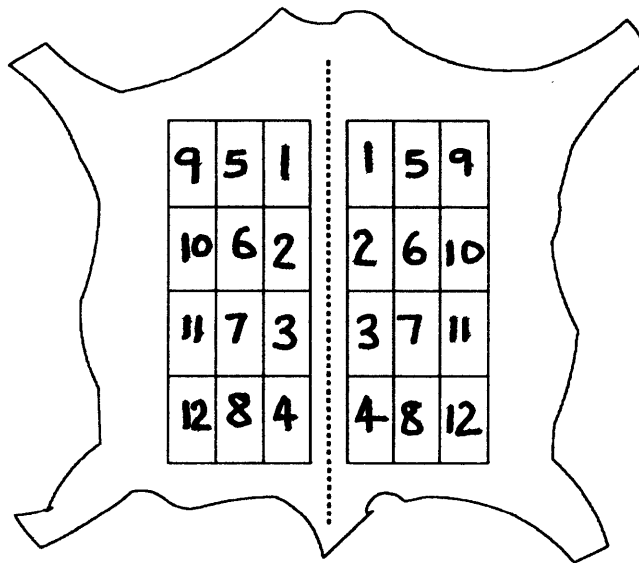


*Figure 3.1: A schematic drawing of a bovine hide showing the sampling area used in this study*

## 3.2 GENERAL EXPERIMENTAL PROCEDURES

### 3.2.1 Sample preparation

The selected area on each side was further divided into twelve rectangular samples of dimensions 300mm by 150 mm, which are shown as red rectangles in figure 3.2. Around each of the twelve rectangular samples, the location of four dumb-bell specimens with dimensions as shown in figure 3.3 was identified. The four dumb-bells, which are shown as blue rectangular strips in figure 3.2 were cut and tested to fracture to give an indication of the mechanical properties to expect in each of the twelve rectangular samples for purposes of experimental planning. The results also assist in

interpreting the variation of mechanical properties with position over the entire side. This dumb-bell sample size conforms to the shape and dimensions specified in the official test method SLP6 of the society of leather technologists and chemists (SLTC).

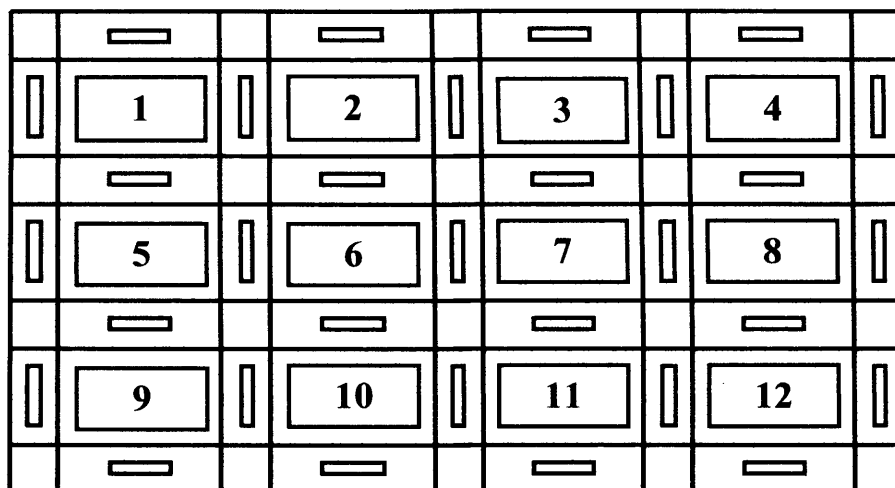


**Figure 3.2:** Schematic drawing showing relative positions of the medium sized tensile test specimens (blue) and the large rectangular samples (red) used in uniaxial strain drying investigations.

For each type of test, the experiments were carried out in three stages. First large samples of appropriate dimensions were cut and then strain dried for 24hrs. From the samples dried under strain, smaller specimens of appropriate dimensions were then cut for various tensile tests. The second stage involved the testing of these tensile specimens cut from the strain dried samples. The third and final stage involved microscopy of the control and experimental samples to characterise the fracture mechanisms. The thickness of each specimen was measured just before the beginning of the test program. A digital micrometer gauge was used to measure the thickness of all specimens for reasons explained in section 3.2.2.

interpreting the variation of mechanical properties with position over the entire side. This dumb-bell sample size conforms to the shape and dimensions specified in the official test method SLP6 of the society of leather technologists and chemists (SLTC).

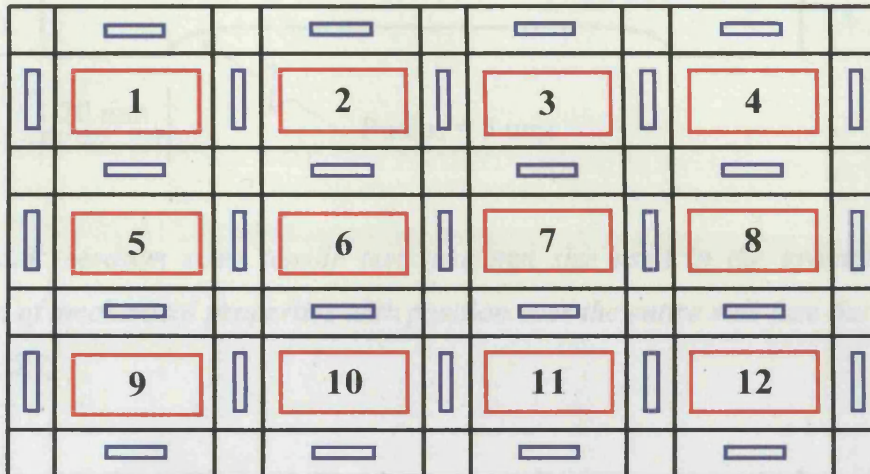


**Figure 3.2:** Schematic drawing showing relative positions of the medium sized tensile test specimens (blue) and the large rectangular samples (red) used in uniaxial strain drying investigations.

For each type of test, the experiments were carried out in three stages. First large samples of appropriate dimensions were cut and then strain dried for 24hrs. From the samples dried under strain, smaller specimens of appropriate dimensions were then cut for various tensile tests. The second stage involved the testing of these tensile specimens cut from the strain dried samples. The third and final stage involved microscopy of the control and experimental samples to characterise the fracture mechanisms. The thickness of each specimen was measured just before the beginning of the test program. A digital micrometer gauge was used to measure the thickness of all specimens for reasons explained in section 3.2.2.

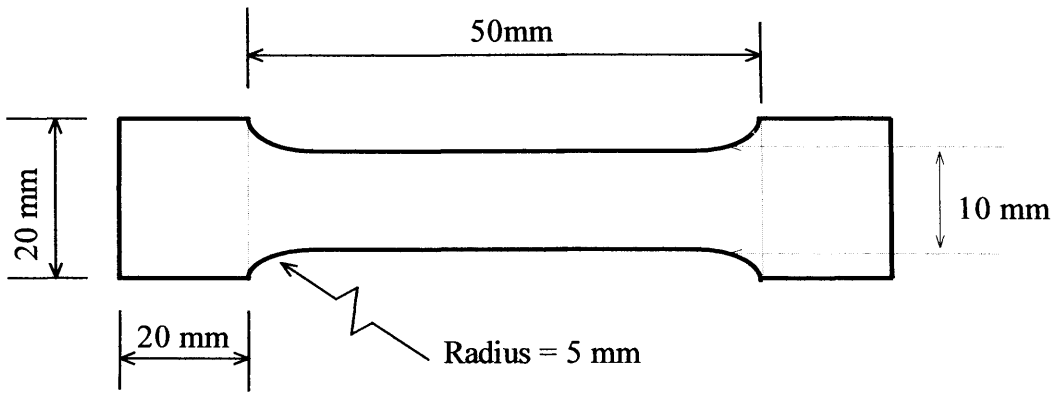


**Figure 3.3:** Medium sized tensile test specimen size used in the evaluation of the variation of mechanical properties with position over the entire side (see the blue strips in figure 3.2)

To obtain samples with straight edges, a cutting die of appropriate profile and dimension for each test type was placed normal to the material and the samples cut using a press. For comparative purposes samples were cut from the two sides and then paired such that each was the exact image of the other across the backbone line. A grid of 10mm by 10mm square was then drawn on each of the rectangular samples (red strips in figure 3.2) using a gold pen to facilitate the monitoring of strain distribution during the drying experiments described below. To prevent slipping of the experimental samples during drying, four holes were cut into the rectangular sample using a circular die as shown in figure 3.4.

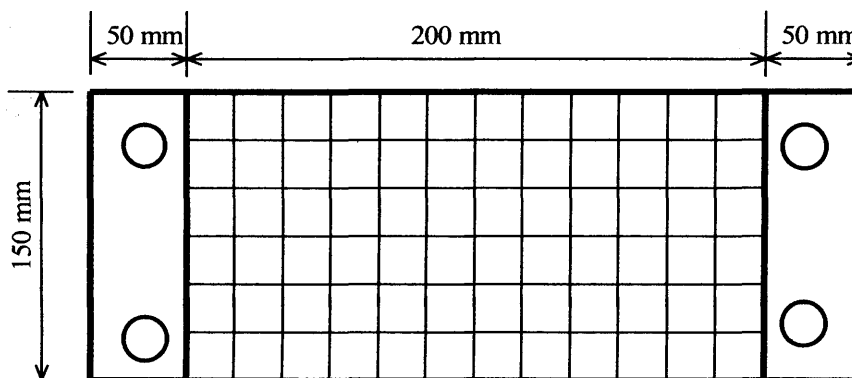


**Figure 3.4** Uniaxial strain drying specimen size, showing holes through which bolts were inserted to prevent slipping under tension.

The specimens were dried by clamping in the jaws of the testing machine (Instron 1122, housed in a room conditioned at 65% RH and 20 C) and strained at a rate of 100mm/min to 30% strain. The specimen was held fixed at this strain for 24 hours after which the jaws of the testing machine were returned to their original position and the strain at which the load fell to zero noted and then used to calculate the immediate set. Originally the samples were dried for a period of 36 hours, but it was found that there was no advantage in drying these samples for longer than 24 hours as the permanent set was the same in both cases.

After strain drying the length of the specimens was monitored for one week to determine the degree of permanent set induced in the material. The control samples were dried freely for the same period and under the same conditions. Each of the dried rectangular samples was used to perform a complete set of tensile tests in order to minimise the variation of mechanical properties with position over the entire side. To achieve this, small dumb-bell specimens (figure 3.5) that conform to the SLP6 official test method, were cut from the dried samples.

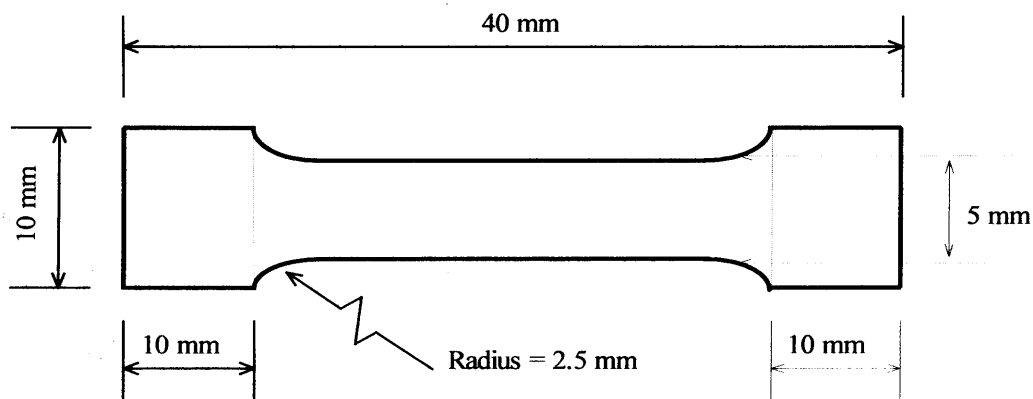


**Figure 3.5:** *Small tensile test sample size used in the evaluation of the variation of mechanical properties with angle of cutting the specimen from the dried large sample*

Each of the dumb-bell specimens was cut at various angles with respect to the stretch axis during drying as shown in figure 3.6.

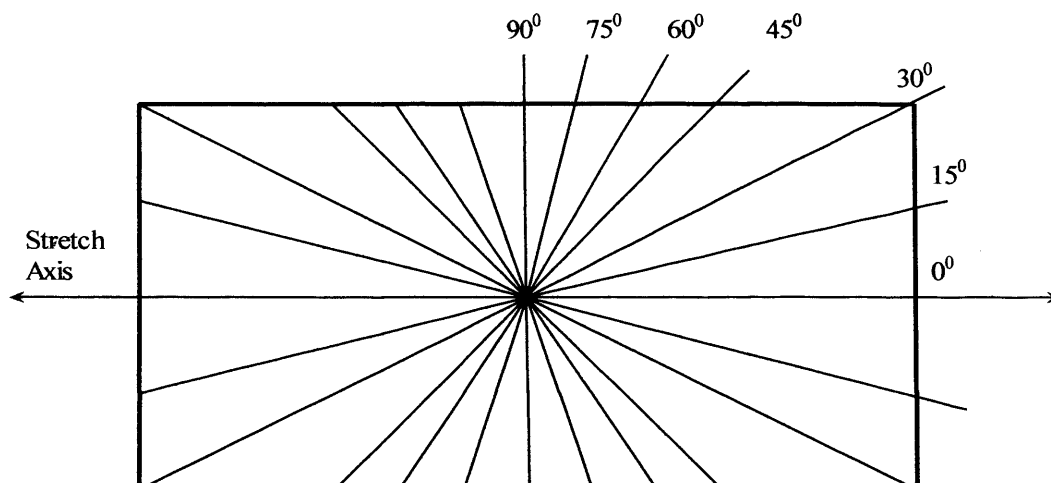


*Figure 3.6 Schematic diagram of a large rectangular sample dried under uniaxial strain showing the angles at which the dumb-bell shaped tensile samples were cut.*

### **3.2.2 Thickness measurement**

The thickness of each specimen was measured using a digital gauge that ensured that the same contact pressure was applied to all the specimens. The thickness measurements obtained using this procedure were in agreement with measurements obtained using the IUP/4 [official method of analysis, (1965)] protocol provided a contact pressure of about  $400 \text{ g/m}^2$  was applied. The digital gauge was preferred over the dial micrometer gauge used in the IUP/4 procedure because of the reproducibility of the thickness measurements. The thickness of each leather specimen was measured after air conditioning at 65% relative humidity, but before commencing the testing protocol.

### **3.2.3 Specimen strain distribution monitoring**

To facilitate the monitoring of strain distribution during fracture toughness tests, an array of 1mm squares was printed on the specimens using a custom made ink stamp as shown in figure 3.7. The stamp was made by etching techniques and then printed on a nylon material. Black printing ink was then applied by a roller on the stamp and then stamped on moist leather. From the deformation of this grid, the strain distribution was

examined in the region around the crack tip as well as over the entire gauge length of the specimen.

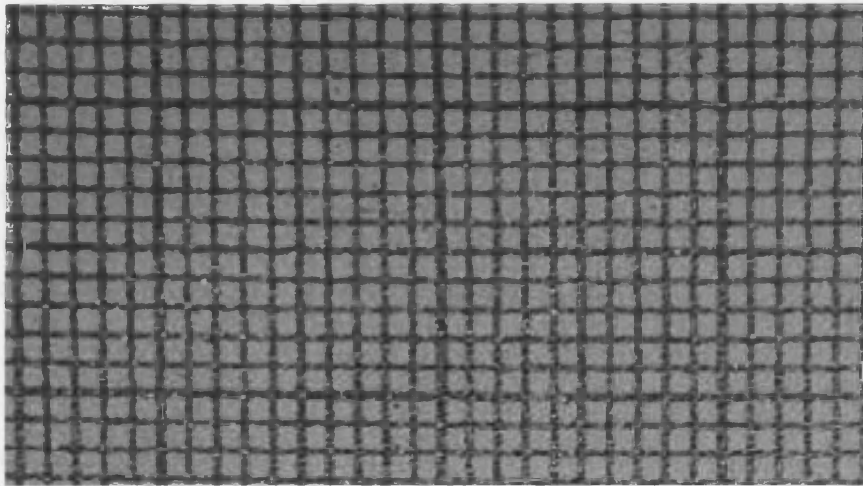


*Figure 3.7: A wet leather sample with a 1 mm square grid stamped on it using a custom made stamp*

### **3.2.4 Tear tests and sample geometry**

Tear tests were conducted to determine the influence of pre-stretch on tear resistance of the leather and the dependence of tear resistance on the direction of sampling at a given location on the hide. The trouser test used during this research was based upon the SATRA method PM30 of 1968. The sample dimensions were as shown in figure 3.8 below. The initial tear was cut either parallel or perpendicular to the backbone depending on the desired test. Tear tests were carried out on the Instron 1122 machine at a rate of 10mm/min.

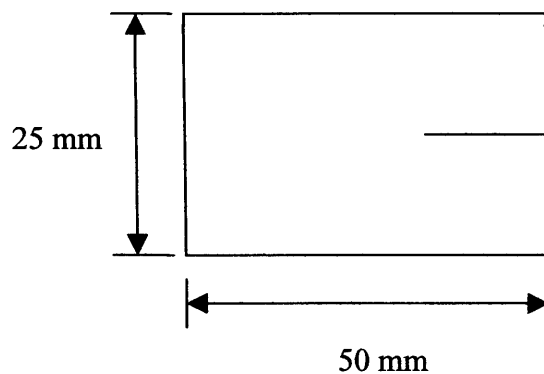


**Figure 3.8:** *Trouser tear test geometry and dimensions*

One leg of the trouser tear specimen was clamped in the upper jaw and the other in lower jaw of the Instron machine thus allowing legs of the specimen to be pulled apart at 180° to each other. Tear data was logged on the computer in terms of load and displacement. Force/displacement curves were recorded automatically on the chart recorder and load displacement values logged on a personal computer (PC). From the general shape of the load/displacement curve for tearing of the specimen the maximum load and the mean load during tearing and fracture energy (area under the curve) were determined.

The tear test requires knowledge of the load at which tear initiates. This was taken to be the point at which the first small step occurs in the load/displacement curve. Specimens were cut close to one another in order to minimize the scatter of tearing parameters due to heterogeneity of the leather. The thickness of all tear samples was measured at three different locations along the expected tear path and the mean value calculated.

### **3.2.6 Crack propagation and fracture tests**

Notched tensile tests were performed in order to evaluate the influence of specimen cutting direction on notch sensitivity of leather and at the same time investigate the notch sensitivity of samples dried at various strain levels. Notched test investigations were performed using single edge notched tension specimen (SENT) as described in section 6.1.1.1. Rectangular specimens of dimensions 16x80 mm were prepared and

notched to different notch lengths. The notches were made using sharp razor blades. After notching the specimens were tested to complete failure at a rate of 10mm/min on an Instron testing machine located in a room conditioned at 20<sup>0</sup> C and 65% RH.

Single edge notched specimens of dimensions 16mm x 80mm were also used to determine fracture toughness of leather using the essential work of fracture approach. These samples were cut from the strain dried samples and then strained at a fixed rate of 10mm/min until complete fracture using an Instron testing machine. Load extension curves were recorded automatically on the chart recorder. From the stress-strain curve so obtained, the load, extension, stress and strain at the point of specimen rupture and the energy required to rupture the specimen was determined by calculating the area under the load-displacement curve. Sections of the fractured specimen were cut normal to the material surface and then examined in a scanning electron microscope for evidence of fibre fracture, fibre pull out and fibre de-bonding from the collagen fibre network structure.

### **3.3 TESTING EQUIPMENT**

The variation of the physical properties of leather over the area of a single hide and between different hides has limited the extent to which established experimental methods and equipment used for other materials can be applied to leather testing. This is further complicated by the fibre orientation that takes place when leather is stretched in tension. The gripping system needs to move freely so as to allow this orientation to occur without constraint near the gripping jaws. Ideally tensile testing of leather would require a gripping system that moves freely because as leather increases in length in response to applied tensile loads, it also contracts laterally. In uniaxial testing this can be overcome by having very long tensile samples and then focussing subsequent analyses at the central portion away from the grips.

#### **3.3.1 Uniaxial testing equipment**

All uniaxial tensile tests were performed using an Instron 1122 universal testing machine at a speed of 10mm/min. Load and displacement data were obtained using a

data logger attached to the Instron machine and then connected to an IBM compatible PC. The data was recorded in two columns as an ASCII text file. Time was recorded in the first column while voltage (which was proportional to the load) was recorded in the second column. The raw data from each tensile test were processed to obtain force and extension from which stress and strain at the point of specimen rupture were determined.

### **3.3.2 Biaxial testing equipment**

Biaxial testing equipment was designed and built in the School of Technology and Design by Paul Taylor. The biaxial testing equipment was used to stretch leather in two independent perpendicular directions by allowing free movement of the leather sample as its dimensions increased in response to applied tensile loads. This biaxial testing equipment, shown in figure 3.9 was screw driven and operated manually. The rate of stretching could not be quantified using this equipment, as it did not have load cells or strain gauges attached to it. However care was taken to ensure that all samples were handled the same way to ensure consistency.

Figure 3.10 shows the shape of biaxial strain drying sample. The grid of 10 mm squares that was drawn on the sample using a gold pen, was used to monitor the strain distribution before, during and after drying. The samples were mounted in the machine by gripping either side of the specimen in five evenly spaced jaws. The specimen was then loaded by turning each pair of perpendicular screws alternately until the required strain was attained as indicated by the change in dimensions of the grid on the sample. The sample was then left in this state to dry for 36 hours in a room conditioned at 20°C and 65% RH.

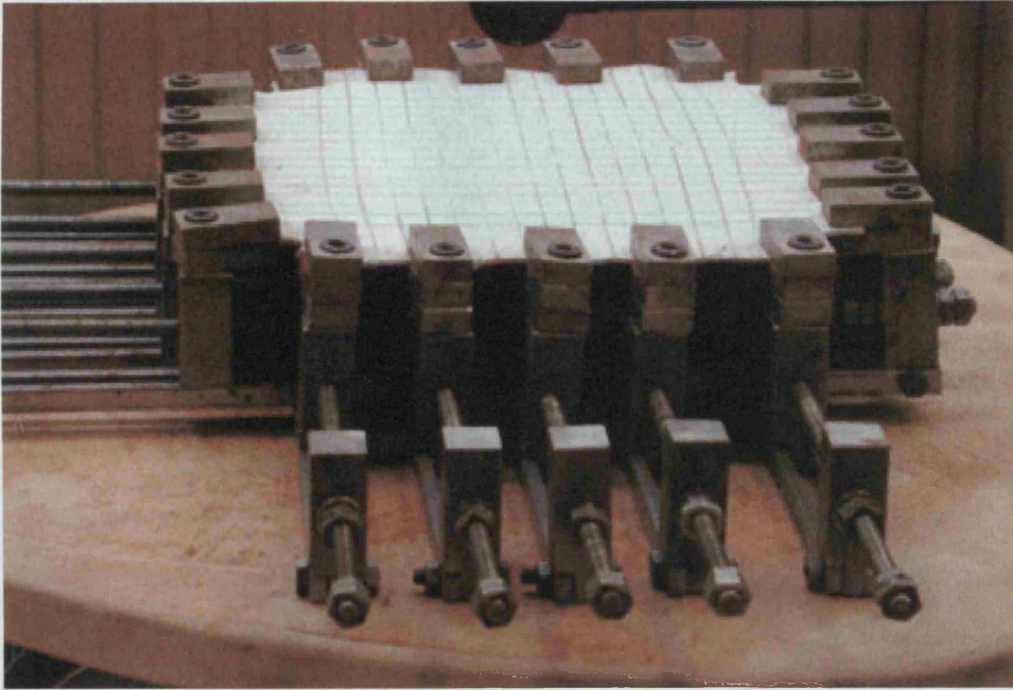


*Figure 3.9: Manually operated biaxial testing machine*

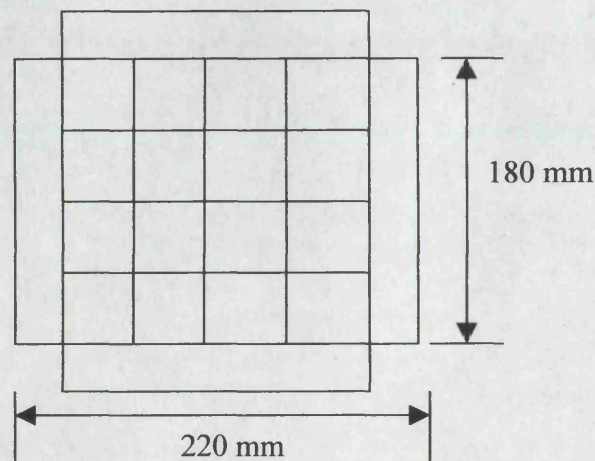


*Figure 3.10: Shape and dimensions of biaxial test specimen.*

Later in this study, a motorised computer controlled biaxial testing machine, designed by Deben Ltd, was obtained in order to overcome the difficulties associated with loading the specimens in the manually operated bi-axial testing machine. This computer controlled biaxial testing machine shown in figure 3.11 had load cells as well as strain gauges and therefore both strain and force could be measured accurately

during stretching. The sample shape and dimensions were as shown in figure 3.10. During loading, the forces developed and the associated displacements in two perpendicular directions were logged on a PC.

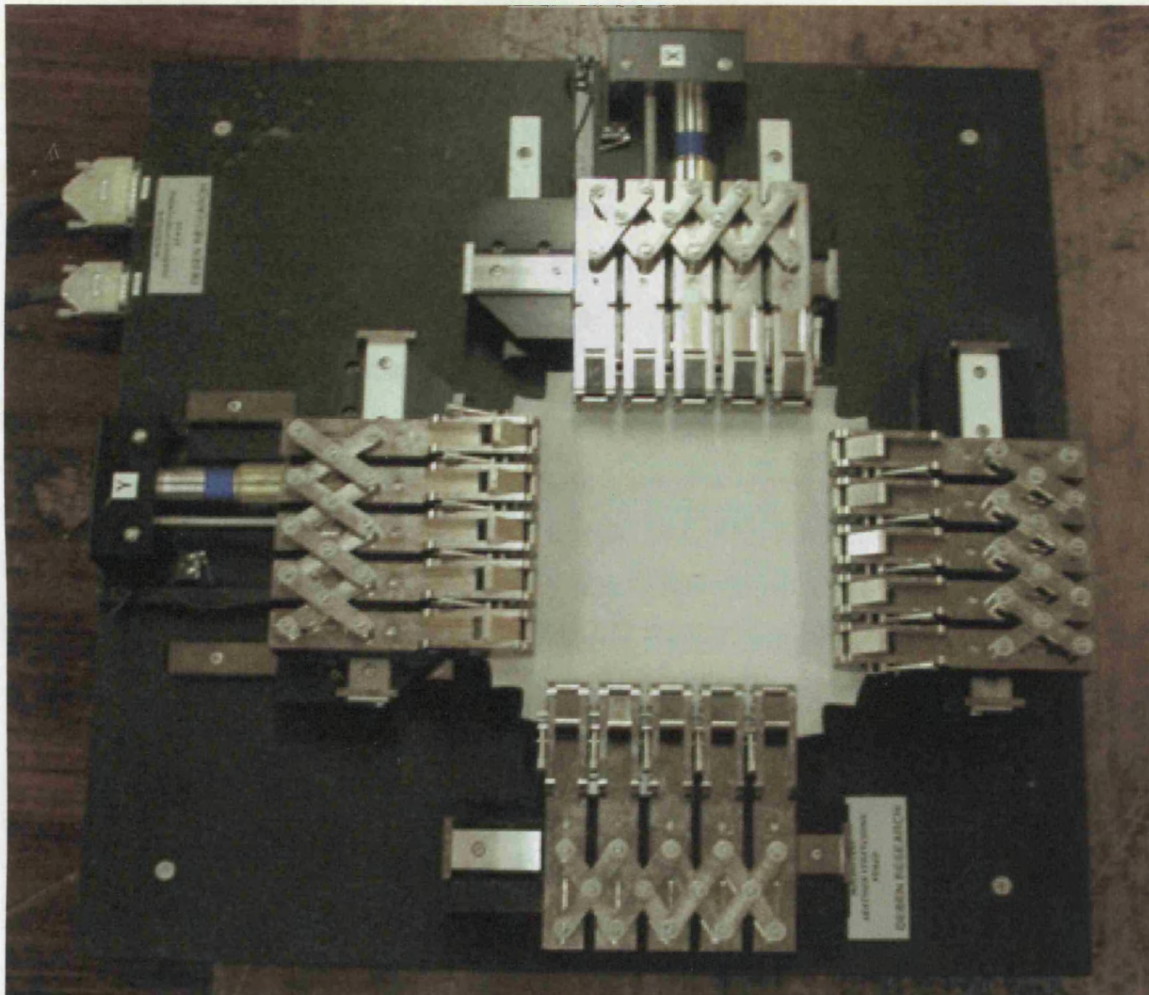


*Figure 3.11: Motorised computer controlled bi-axial testing machine.*

### **3.4 MICROSCOPY**

Various microscopy methods have previously been used to investigate fracture mechanisms and fibre distribution in leather, including optical microscopy [Otunga and Attenburrow, (2000)] X-ray diffraction [Sturrock et al, (2001)], electron microscopy [Alexander et al, (1993)] and microwave methods [Osaki et al, (1993)]. X-ray diffraction applied to leather offers rapid quantitative in situ assessment of the collagen

fibre distribution and can be used to sample a large enough area to give a representative view of the fibre distribution within a macroscopic specimen.

### **3.4.1 Optical microscopy**

A stereo optical microscope was used to examine crack initiation and propagation up to complete fracture of the specimens. The microscope was placed on a screw driven platform and then positioned 2cm from the Instron testing machine that was used to strain the samples. The initiation and subsequent propagation of the crack together with events taking place in the damage zone were then monitored by gently moving the microscope so that the tip of the crack remained in the field of view and in focus. The specimen surface was illuminated with fibre optic halogen lamps.

Throughout the straining of the specimen, microscope images were recorded using a VHS video recorder attached to a video camera that was located on the microscope. The microscope magnified the images by about 100 times. Once the recording was complete, the entire fracture process was then digitised using Pinnacle Systems video capture software and then a CD-ROM made using a CD rewriter.

### **3.4.2 Scanning electron microscopy**

A scanning electron microscope (Hitachi S2500) operated at 10kV was used to observe the fracture surfaces of the specimens. In order to realise this, fractured samples were sectioned normal to the material surface, both parallel and perpendicular to the direction of straining using a sharp razor blade. The sections were placed onto sample stubs and gold coated using a BioRad SEM coating Unit (P53) under an argon atmosphere for 150 seconds at room temperature.

### **3.4.3 X-ray diffraction methods**

Wide angle X-ray diffraction was carried out using Station 7.2 at the Synchrotron Radiation Source at Daresbury, UK. Eight rectangular strips of dimensions 5mm x 10mm were cut from each of the samples dried under 30% strain and the corresponding

control sample. The strips were cut from different regions of each sample in order to give a representative view of fibre distribution over the whole sample region such that the long specimen axis coincided with the pre-stretch axis.

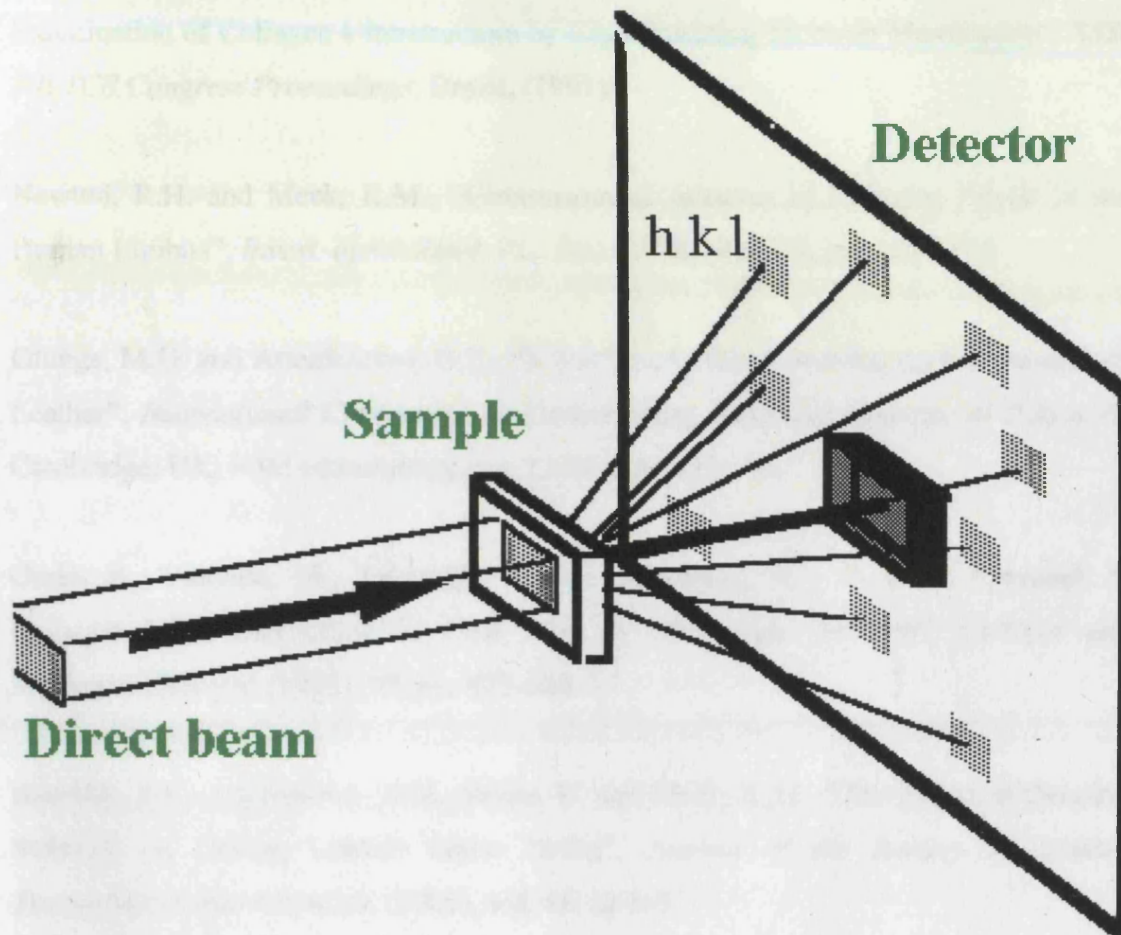


*Figure 3.12: Schematic drawing showing the principle of synchrotron X-ray diffraction*

Each strip was mounted with the largest face normal to the incident beam and with the strain axis in the vertical direction and then examined using the Keele Fibre Camera. X-ray patterns were recorded using a MAR image plate detector. A ~20cm specimen-to-detector distance was used, and calibrated accurately using the 3.04 Angstroms X-ray reflection from calcite powder. The beam was collimated to 1mm diameter, the wavelength was 1.488 Angstroms and the exposure time for each sample was between one and four minutes. Each X-ray pattern showed a clear diffraction ring arising from the lateral packing of the individual collagen molecules. The distribution of scattered intensity as a function of angle around the ring was measured as reported previously [Newton and Meek, (1998)] and averaged over the eight specimens.

## References

Alexander, K.T.W., Covington, A.D., Garwood, R.J. and Stanley, A.M., "The Examination of Collagen Ultrastructure by Cryo-Scanning Electron Microscopy", *XXII IULTCS Congress Proceedings*, Brazil, (1993)

Newton, R.H. and Meek, K.M., "Circumcorneal Annulus of Collagen Fibrils in the Human Limbus", *Invest. ophthalmol. Vis. Sci.*, (1998), Vol. 39, pp1125-1134

Otunga, M.G. and Attenburrow, G.E., "Influence of Prior Stretching on the Strength of Leather", *International Conference on Deformation, Yield and Fracture of Polymers*, Cambridge, UK, IOM communications, (2000), pp 397-399.

Osaki, S., Yamada, M., Takasusu, A. and Murakami, K., "A New Approach to Collagen Fibre Orientation in Cow Skin by Microwave Method", *Cellular and Molecular Biology*, (1993), **39**, pp. 673-680

Sturrock, E.J., Attenburrow, G.E., Boote, C. and Meek, K.M., "The Effect of Bending Stiffness on Drying Leather under Strain", *Journal of the Society of Leather Technologists and Chemists*, (2001), vol. 86, pp 6-9

# CHAPTER FOUR

---

## TENSILE STRENGTH

4.1 INTRODUCTION.	56
4.2 FAILURE CRITERIA FOR FIBRE COMPOSITES	57
4.2.1 Limit criteria	58
4.2.2 Interactive criteria	60
4.3 PREDICTION OF COMPOSITE STRENGTH	60
4.3.1 Tsai-Hill theory	61
4.4 COLLAGEN FIBRE ORIENTATION IN LEATHER	62
4.5 FAILURE MECHANISMS IN COMPOSITES	62
4.6 EXPERIMENTAL	63
4.7 RESULTS AND DISCUSSION	63
4.7.1 Variation of tensile strength with position	63
4.7.2 Stress-strain curves for wet blue leather	65
4.7.3 Relationship between elongation and strength	66
4.7.4 Effect of drying on the stress-strain curves	67
4.7.5 Effect of specimen size	69
4.7.6 Effect of orientation angle on strength	70
4.7.7 Failure mechanisms	74
4.7.8 X-ray diffraction studies	78
4.8 CONCLUDING REMARKS	81
References	82

## 4.1 INTRODUCTION

As mentioned earlier most tanneries strive to improve leather area yield as it has a direct impact on profitability. This is normally achieved by some degree of in-process stretching. Such stretching can be imparted by a setting machine but may be lost due to subsequent relaxation of the leather [Jarret and Sykes, (1988)]. A durable area increase may be achieved by drying leather under strain [Wright and Attenburrow, (1995)&(1997)]. However, whilst in-process stretching may improve yield there is concern that it may also degrade the quality of the finished leather as determined by physical properties such as tensile strength, stiffness and fracture toughness. These physical properties are likely to depend on the fundamental properties of the individual components of leather and the arrangement of these components in leather. However tensile strength of leather is usually considered as an indicator of leather quality. The prediction of leather strength is not only important to the tanner but also in the design of any component that uses leather. There is need therefore to develop methods of predicting leather strength so as to effectively optimise the leather making processes. A lot of work has been done [Hull & Clyne (1996), Rawlings & Mathews (1994) and Rowlands, (1985)] on the strength prediction of fibre reinforced composite materials but there are no such strength prediction methods for leather.

As has been discussed leather is made up of a network of collagen fibres, which in the un-processed animal skin are set in a matrix of natural binding agents such as proteoglycans, and dermatan sulphate, which is distributed over the surface of collagen fibrils in a regular and highly organised manner. Dermatan sulphate is found at the surface of all fibres whether they are the larger central corium fibre bundles or the individual fibrils immediately below the epidermis [Haines, (1983)]. The natural binding agents are removed during the tanning process to create an open structure of fibres, which is held together by the interwoven arrangement of the fibres. During the later stages of the tanning process, the pores between the fibres are partially filled with oils and greases, which determine the subsequent behaviour of the leather. The partial filling of the zones between adjacent fibres produces a porous matrix structure. Under uniaxial loading this type of structure enables the fibres to rotate and to slide relatively to each other [Lin and Hayhurst, (1993)]. Leather can therefore be considered as a special composite structure made up of an aggregate of collagen fibres in a porous

matrix. In this respect, an understanding of the strength theories of artificial fibrous composites can be used as a point of departure to establishing a failure criterion for leather. It must however be understood that leather does not have just one fibre-matrix interface as in artificial composites but rather there is likely to be interactions at the multiplicity of interfaces between the different structural levels of its constituent fibres.

This chapter considers the damage mechanisms in leather and assembles observations and measurements of strength into a systematic scheme for evaluating the role of various mechanisms in the behaviour of leather under tensile loads. Following this a number of models [Rowlands, (1985)] that have in the past been used to predict the tensile strength of carbon fibre reinforced plastics [CFRP] will be discussed. In particular, the model originally proposed by Hill [Hill, (1950)] will be discussed. The basic tenets of this model will now be presented.

## **4.2. FAILURE CRITERIA FOR FIBRE COMPOSITES.**

The idea of “failure criterion” or “failure theory” is usually introduced to predict the strength of materials under multi-axial loading conditions using strength data obtained from uni-axial tests. A failure criterion encloses the stress states that a material can sustain without failure. In fibre reinforced composite materials, strength is usually determined by the application of failure criteria, which are usually grouped into three classes [Hull & Clyne, (1996)] namely:

- Limit criteria, which assume that failure occurs when a stress or strain parallel or normal to the fibre axis reaches the appropriate critical or limiting value.
- Interactive criteria, for example the Tsai-Hill criterion which attempts to allow for interaction of the various components of stresses.
- Hybrid criteria, which combines selected aspects of limit and interactive methods.

### 4.2.1 Limit criteria

All the existing failure theories for composite materials are simply macro-mechanical design criteria in which the unidirectional strength properties are predicted from the strength properties of the constituent materials. These unidirectional strength properties can also be determined experimentally from simple test conditions.

The application of an arbitrary stress state  $\sigma_{\theta u}$  in a tensile test can give rise to failure as a result of exceeding critical values of axial tensile stress  $\sigma_{1u}$ , transverse tensile stress  $\sigma_{2u}$ , and shear stress  $\tau_{12u}$ . The applied stress can be resolved into the directions of the critical stresses ( $\sigma_1$ ,  $\sigma_2$ , and  $\tau_{12}$ ) as shown in figure 4.1. It is then postulated that failure will occur when one (or all) of these resolved stresses attains a respective maximum value ( $\sigma_{1u}$ ,  $\sigma_{2u}$ , and  $\tau_{12u}$ ) respectively. The later strengths are obtained experimentally under uniaxial loading.

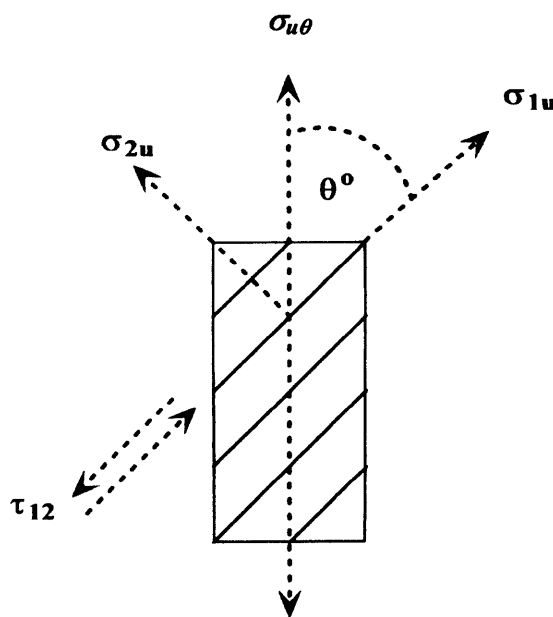


**Figure 4.1:** Schematic drawing showing the orientation of the fibres in the sample with respect to the loading direction (a stress,  $\sigma_{u\theta}$  is applied at an angle  $\theta$  to the fibres as shown).

Thus according to the limit criteria, there are three possible modes of failure for a material tested at an angle  $\theta$  to the fibre direction. Longitudinal tensile fracture will occur when the component of the applied stress  $\sigma_{\theta u}$ , resolved parallel to the fibre axis reaches the longitudinal tensile strength  $\sigma_{1u}$ , of the fibres. This can be expressed as [Bailey, (1994)]

$$\sigma_{1u} = \sigma_{\theta u} \cos^2 \theta \quad (4.1)$$

A second possibility is that of transverse fracture where the applied stress  $\sigma_{\theta u}$ , resolved in the transverse direction reaches the transverse tensile strength,  $\sigma_{2u}$ . This can be expressed as

$$\sigma_{2u} = \sigma_{\theta u} \sin^2 \theta \quad (4.2)$$

Finally failure could occur by shear parallel to the fibres when the resolved stress reaches the shear strength  $\tau_{12u}$ . This can be expressed as

$$\tau_{12u} = \sigma_{\theta u} \sin \theta \cos \theta \quad (4.3)$$

Clearly the strength at a given angle  $\theta$  will be determined by the weakest of these failure modes. For unidirectional lamina, the failure curve shows transition from longitudinal failure at quite a small angle ( $\sim 5^\circ$ ) and a transition from shear failure to transverse failure at quite a large angle ( $18-42^\circ$ ). This result is characteristic of most fibre-matrix combinations and once again the extreme anisotropy of behaviour is evidenced with the rapid fall in strength with increasing value of  $\theta$  [Bailey, (1994)].

The above limit criteria assume that there is no interaction between the various failure modes. However in practice, interaction between these three modes of failure is likely to occur. Tsai-Hill criterion [Rowlands, (1985)], which addresses the interaction between the three modes of failure, and which has proven to be successful in a wide variety of circumstances was applied to leather studied herein and is therefore outlined below.

## 4.2.2 Interactive criteria

The objective of this approach is to allow for the fact that failure loads under multi-axial stress states in the material may differ from failure loads under the action of only uniaxial stress states. Various attempts have been made to predict the failure of long fibre composites under combined stresses, particularly for the plane stress conditions applicable to individual plies in a laminate [Hull and Clyne, (1996)]. A comprehensive review of the approaches adopted has been published [Rowlands, (1985)]. Most of the treatments are based on adaptations of yield criteria developed for metals. Adaptations of these criteria to describe failure of composites must take account of the inherent anisotropy of a fibre composite and of the differences between the mechanisms of metal yielding and composite failure.

Under large deformation, the crystal structure of even initially isotropic metals becomes aligned [Rowlands, (1985)] which renders the behaviour to be anisotropic. This led Hill to propose an orthotropic yield criterion by modifying von Mises yield criterion for metals with orthotropic symmetry [Hill, (1950)]. In its most general form, Hill's criterion defines failure as

$$\left[ \frac{\sigma_1}{\sigma_{1Y}} \right]^2 + \left[ \frac{\sigma_2}{\sigma_{2Y}} \right]^2 - \frac{\sigma_1 \sigma_2}{\sigma_{1Y}^2} - \frac{\sigma_1 \sigma_2}{\sigma_{2Y}^2} + \frac{\sigma_1 \sigma_2}{\sigma_{3Y}^2} + \left[ \frac{\tau_{12}}{\tau_{12Y}} \right]^2 = 1 \quad (4.4)$$

where  $\sigma_1$ ,  $\sigma_2$ , and  $\tau_{12}$  are imposed stresses, referred to the orthogonal directions in the plane, and the material properties  $\sigma_{1Y}$ ,  $\sigma_{2Y}$ ,  $\sigma_{3Y}$ , and  $\tau_{12Y}$  are the measured yield stresses, in tension and shear, when each is applied in isolation.

## 4.3 PREDICTION OF COMPOSITE STRENGTH

Laminated composites are made up of several plies with similar or differing fibre orientations stuck together. There are two different approaches used to predict the laminate strength, namely, the ply-by-ply approach and the total laminate approach. In the first approach the laminate is considered to consist of bonded layers. Each layer is considered to be homogenous and orthotropic. Lamination theory is used to obtain

stresses and strains in each layer. These stresses and strains are transformed to layer principal axes before the failure criterion is applied to each lamina. The failure envelope is obtained by superimposing the failure envelopes of all the layers, from which the innermost envelope is then determined. In the second approach, the failure criterion is applied directly to the entire laminate by considering it to be homogenous and anisotropic. This approach requires the strength characterization of each laminate under consideration.

### 4.3.1 Tsai-Hill Theory.

In order to predict failure of unidirectional composites, Tsai-Hill theory was derived [Azzi & Tsai, (1965)] from equation 4.4 by replacing the yield stresses by the appropriate measured failure stresses and by assuming that the failure stresses in the 2- and 3-directions are equal, so that equation 4.4 reduces to

$$\left[ \frac{\sigma_1}{\sigma_{1u}} \right]^2 + \left[ \frac{\sigma_2}{\sigma_{2u}} \right]^2 - \frac{\sigma_1 \sigma_2}{\sigma_{1u}^2} + \left[ \frac{\tau_{12}}{\tau_{12u}} \right]^2 = 1 \quad (4.5)$$

Equation 4.5, commonly known as the Tsai-Hill Criterion, is widely quoted in composite textbooks and is often used in laminate analysis [Hull, (1996)]. It defines an envelope in stress space such that if the sum of the terms on the left hand side is equal or greater than unity, then failure is predicted. The failure mechanism is not specifically identified, however inspection of the relative magnitudes of the terms in equation 4.5 gives an indication of the likely contribution of the three modes. For a single applied tensile stress  $\sigma_\theta (= \sigma_x, \text{ at an angle } \theta \text{ to the fibre axis})$  and by substituting equations 4.1 to 4.3, in equation 4.5, we obtain

$$\sigma_\theta = \left[ \frac{\cos^2 \theta (\cos^2 \theta - \sin^2 \theta)}{\sigma_{1u}^2} + \frac{\sin^4 \theta}{\sigma_{2u}^2} + \frac{\cos^2 \theta \sin^2 \theta}{\tau_{12u}^2} \right]^{-\frac{1}{2}} \quad (4.6)$$

Equation 4.6 gives the applied stress at which failure is predicted as a function of loading angle  $\theta$ . In order to apply equation 4.6 to leather, knowledge of the collagen fibre structure and orientation is essential.

#### **4.4. COLLAGEN FIBRE ORIENTATION IN LEATHER**

Leather is made up of an interweaving network of collagen fibres. The interweaving of fibres follows a definite pattern in the skin or hide [Maeser, (1960)]. Since the tensile strength depends on the fibre structure, it is expected that tensile strength should also follow a definite pattern on the skin or hide. It is therefore important to obtain information about the collagen fibre orientation in leather so as to tailor tannery processes to various end uses.

Electron microscopy can be used to determine fibre orientations in small leather samples. However mapping fibre orientation in a complete hide is very difficult because the electron microscope can view only a very small portion of the hide. This limitation has been overcome by using a method based on absorption of polarised microwaves in sheet materials such as paper [Osaki, (1987)], human blood vessels [Yamamoto et al., (1988)], and non-woven fabrics [Osaki, (1989)] Recently the microwave method has been applied to calf-skin [Osaki, (1999)] to map out the distribution of collagen fibre orientation in a whole cow skin. Their results indicate that the collagen fibres are mostly oriented parallel to the calf's spinal column and limbs. To build a model for tensile failure of leather, it is important to establish how this fibre structure responds to applied tensile stresses. A study of the damage mechanisms in tensile loading of leather was therefore undertaken and then compared with damage mechanisms in composite materials.

#### **4.5 FAILURE MECHANISMS IN COMPOSITES**

The application of an arbitrary stress state  $\sigma_x$  to a unidirectional lamina can lead to failure by one or more basic failure processes discussed above. Large tensile stresses parallel to the fibres,  $\sigma_1$ , lead to fibre and matrix fracture, with the fracture path normal to the fibre direction. The strength is usually much lower in the transverse tension and

shear modes and the composite fractures on surfaces parallel to the fibre direction when appropriate  $\sigma_2$  or  $\tau_{12}$  stresses are applied. In these cases, fracture may occur entirely within the matrix, at the fibre/matrix interface or primarily within the fibre. To predict the strength of a lamina or laminate, values of the failure (ultimate) stresses  $\sigma_{1u}$ ,  $\sigma_{2u}$  and  $\tau_{12u}$  have to be determined.

In a unidirectional composite containing only one type of fibre, failure in tension is normally attributed to progressive failure of the component fibres. The fibres have a wide distribution of strengths, so that as the strain is increased, individual single fibres will fail sporadically throughout the composite. At each failure site, there will be a perturbation of the local stress distribution with stress concentration on the surviving fibres close to the fracture site. This leads to an enhanced probability of failure close to the previous failure sites, so that a region of several failed fibres develop. Eventually, one of these regions reaches a critical size, and a catastrophic succession of fibre breaks, travels across the section leading to complete tensile failure.

## **4.6 EXPERIMENTAL**

The materials and sample preparation together with test procedures were as described in section 3.1. However in addition shorter samples of dimensions 100mm x 150mm were dried under strain in order to investigate the influence of sample size on the mechanical properties of leather dried under strain.

## **4.7 RESULTS AND DISCUSSION**

### **4.7.1 Variation of tensile strength with position**

Figure 4.2 shows the variation of normalised tensile strength measured parallel to the backbone with position on the hide for the leather used in this study. The strength was normalised by determining the average tensile strength over the entire hide and then dividing the tensile strength at every location by this average value. Similar observations have been reported for full thickness leather [Vos and Vlimmeren, (1973)] in a review that was performed to examine the topographic differences in physical properties of

different kinds of leather. This research confirms for the first time that similar behaviour is found in grain alone. The samples used in this study were obtained from the official sampling area that excludes the neck, tail and limb regions of the hide.

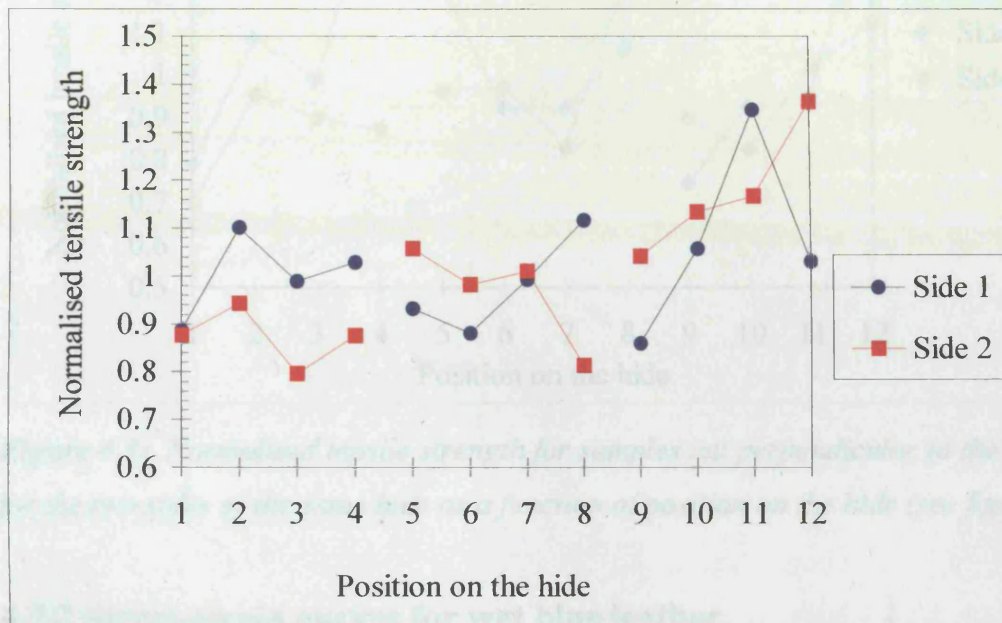


**Figure 4.2:** Normalised tensile strength for samples cut parallel to the backbone for the two sides of the same hide as a function of position on the hide (see figure 3.2)

A similar plot for samples cut perpendicular to the backbone is shown in figure 4.3. It can be seen that the tensile strength for samples cut perpendicular to the backbone is lower than the tensile strength for samples cut parallel to the backbone at most locations.

Figures. 4.2 and 4.3, together with the findings others [Osaki, (1999) and Maeser, (1960)] indicate that the tensile strength of leather made from bovine hides vary from one location to another according to a definite natural pattern dictated by the underlying fibre structure or pattern. These fibre patterns in the skin, cause variation at different locations on the hides of all physical properties and in particular that of strength.

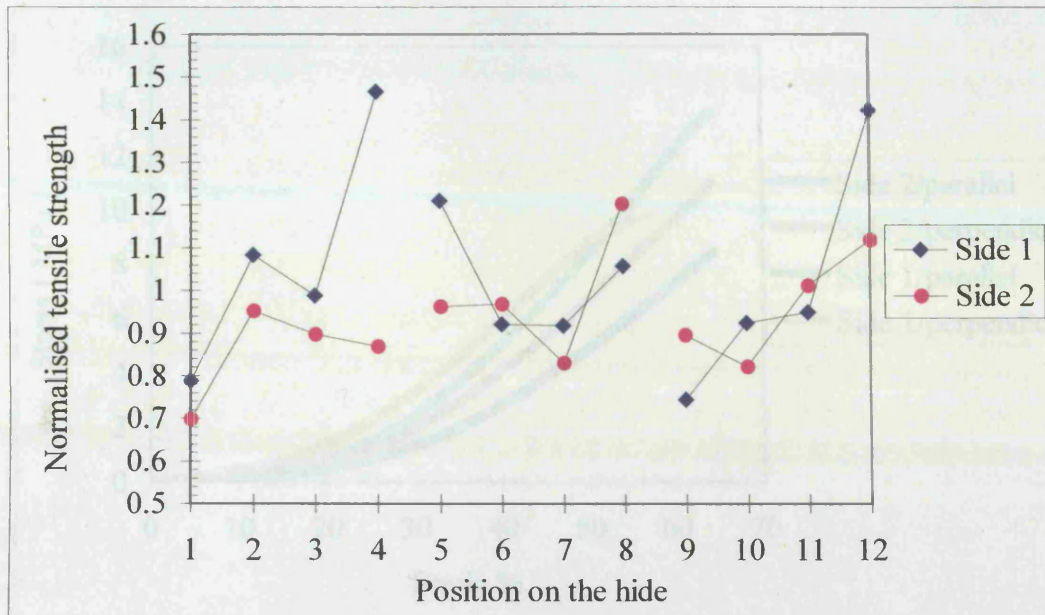


**Figure 4.3:** Normalised tensile strength for samples cut perpendicular to the backbone for the two sides of the same hide as a function of position on the hide (see figure 3.2)

#### 4.7.2 Stress-strain curves for wet blue leather

Figure 4.4 shows typical stress-strain curves for wet blue chrome tanned leather samples cut parallel and perpendicular to the backbone. This figure indicates that although the stress strain curves for samples cut in any direction on the hide look similar, the ultimate stress at break depends on the direction of cutting the sample on the hide. This can be easily explained by assuming that the tensile strength of leather is a function of the number of fibres in the woven fibre network that are oriented in the direction of the applied load. The review presented in section 4.4 demonstrates that most fibres are oriented parallel to the backbone which correlates well with the high strength observed in this direction. As the load is applied to the specimen, the narrow section elongates thus becoming narrower and thinner. The fibres oriented in the direction of the applied load approach each other so that the extent to which the cross section narrows is inversely proportional to the number of fibres oriented in that direction [Kanagy, (1952)].

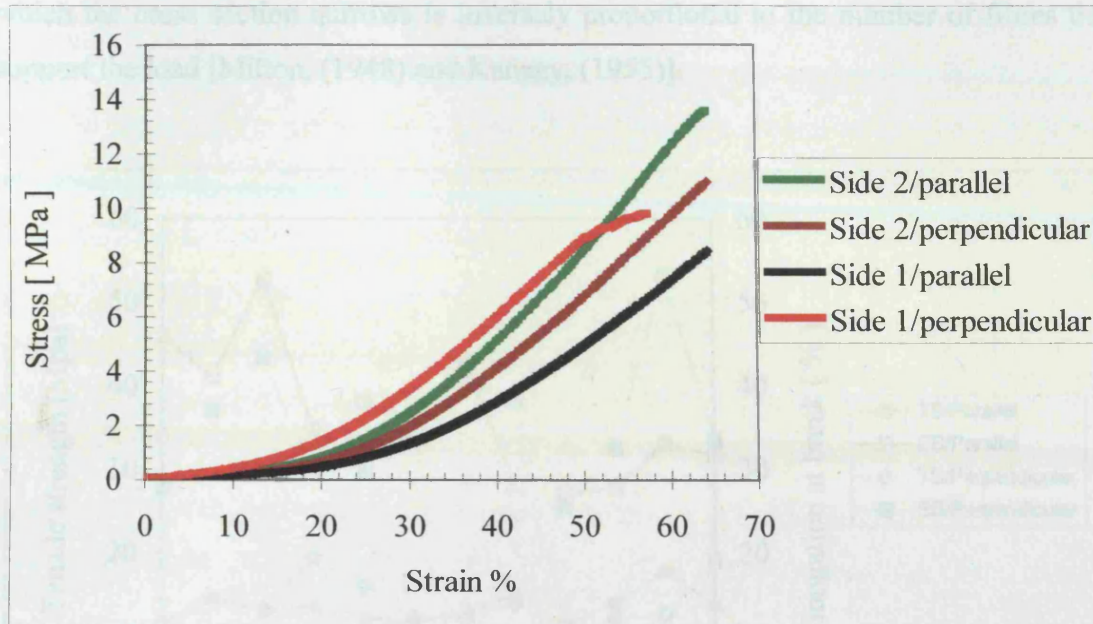


**Figure 4.4:** Stress versus strain curves for leather samples cut parallel and perpendicular to the backbone.

It is well known in the shoe industry that the three dimensional fibre bundle arrangements are not random; they follow certain lines (lines of tightness) along which a majority of the fibre bundles are aligned. Lines of tightness in cattle hide run longitudinally and almost parallel to the backbone [Miller, (1976)]. On the other hand the lines of easy stretch run directly at right angles to the lines of tightness. Since a majority of the fibres are aligned parallel to the backbone, they carry most of the applied load resulting in the observed high strength.

### 4.7.3 Relationship between elongation and strength

Fig 4.5 shows absolute values of tensile strength and elongation to break obtained from strength tests performed in two directions, parallel and perpendicular to the backbone over the entire area of a side. It is clear from this figure that strength and elongation are approximately inversely proportional and that high strength usually indicates low elongation whereas low strength indicates high elongation. Most of the elongation observed in tensile strength test is not caused by elongation of the fibres, but the distortion in the fibre network. [Lin and Hayhurst, (1993)]. The fibres oriented in the direction of the applied load approach each other when stressed so that the extent to

which the cross section narrows is inversely proportional to the number of fibres that support the load [Mitton, (1948) and Kanagy, (1955)].

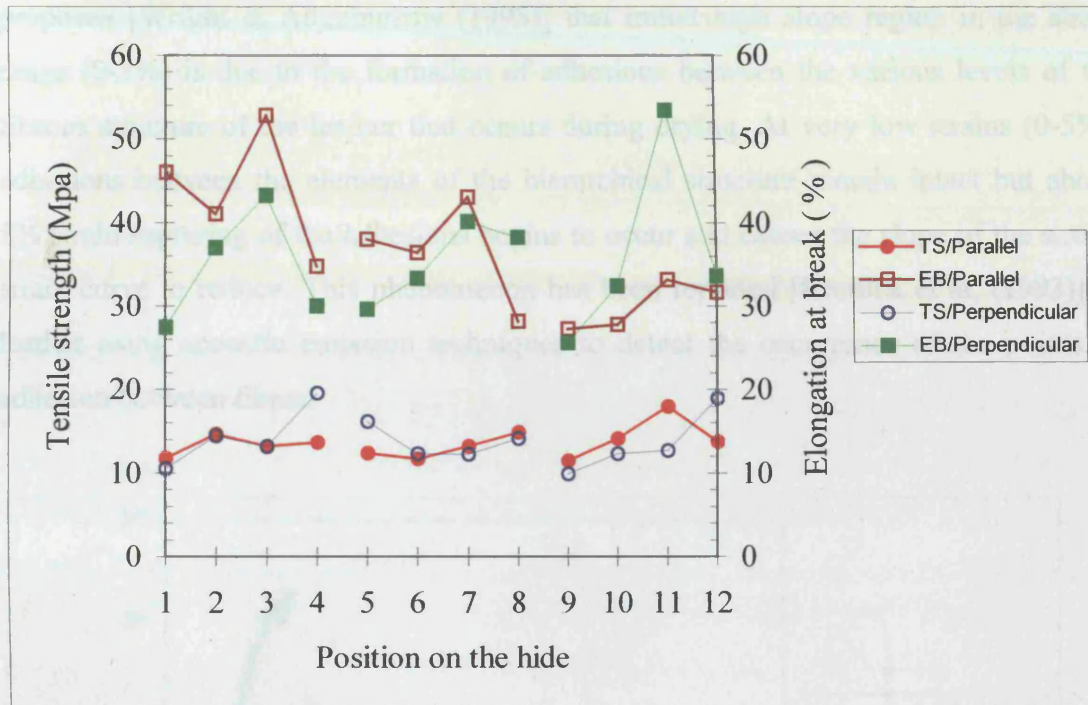


**Figure 4.5:** The average tensile strength (TS) and elongation at break (EB) with position on the hide in directions parallel and perpendicular to the backbone (see figure 3.2).

#### 4.7.4 Effect of drying on stress-Strain curves

Figure 4.6 shows stress strain curves for wet blue samples, control samples dried freely and experimental specimens dried at 30% strain. This figure shows that before drying wet-blue leather like most biological materials exhibits a J-shaped stress-strain curve that plays a crucial role in its fracture behaviour. The initial part of the J-shaped stress-strain curve is almost horizontal indicating very low shear connectivity in the material thereby making it difficult to feed energy into potential crack sites. Clearly the response of the elements of the hierarchical structure of the collagen fibre network is reflected in the shape of the stress-strain curve. As the samples become dry, there is a qualitative change in the shape of the stress-strain curve.

For control samples dried freely, the stress strain curve comprises of three regions. In the first region (0-5% strain) the slope is high, in the second region (3-20% strain) the slope is considerably reduced and in the third region the slope increases again. It was proposed [Wright & Attenburrow (1995)] that initial high slope region in the strain range (0-3%) is due to the formation of adhesions between the various levels of the fibrous structure of the leather that occurs during drying. At very low strains (0-5%), adhesions between the elements of the hierarchical structure remain intact but above 5% strain rupturing of the adhesions begins to occur and causes the slope of the stress-strain curve to reduce. This phenomenon has been reported [Kronick et al, (1993)] in leather using acoustic emission techniques to detect the occurrence of the points of adhesion between fibres.

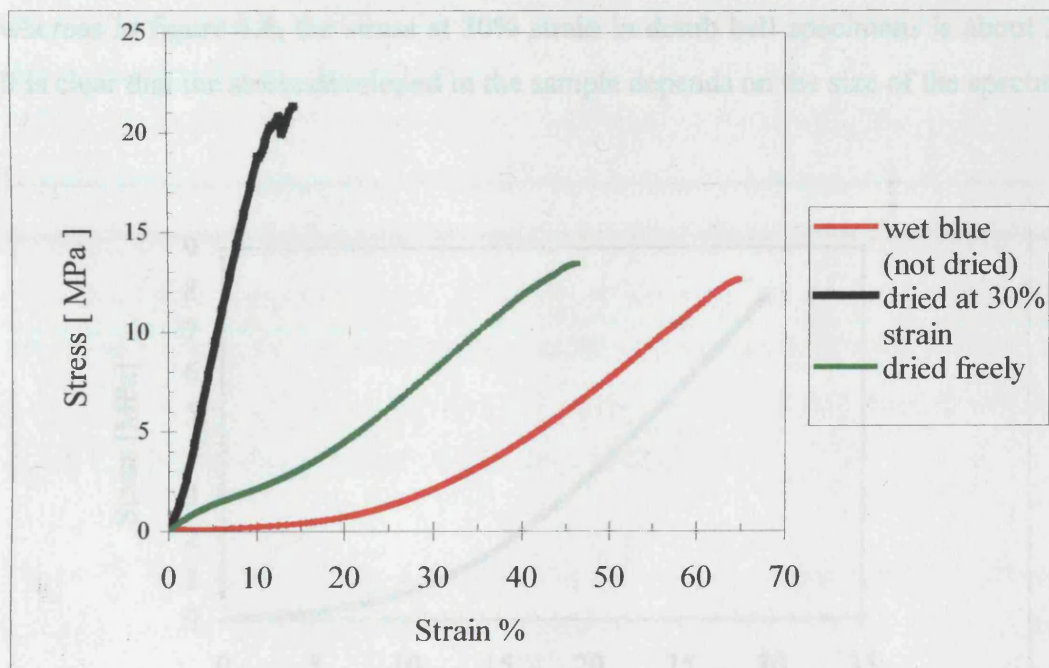


**Figure 4.6:** Typical stress-strain curves for wet blue leather, wet blue dried freely and wet blue dried at 30% uniaxial strain and tested parallel to the strain axis.

Samples dried at 30% uni-axial strain showed a marked departure from the J-shaped curve. This can be explained in terms of fibre orientation and the formation of adhesions between the various levels of the collagen fibre network structure. The first part of the stress strain curve therefore depicts the deformation of a leather specimen as whole entity until most of the inter-fibre adhesions have been broken, in which case a change in the slope of the stress strain curve is inevitable. In the second stage of

deformation, the fibres which tend to stick to each other, slide or move apart or are torn from fillers and excess solidified tanning agent in spaces in the leather and at the same time there is little scope for them to turn in the direction of the applied stress. After the reorientation that takes place during the second stage of deformation, the fibres themselves come under direct strain with a consequential increase in the slope of the stress strain curve typical of the third stage of deformation.

#### 4.7.5 Effect of specimen size

The characteristic J shaped curve was observed for all wet samples irrespective of their size. Figure 4.7 shows the stress-strain curve for the large wet blue sample (150x300mm). In figure 4.7 the stress at 30% strain in the large sample is about 8 MPa whereas in figure 4.6, the stress at 30% strain in dumb bell specimens is about 2MPa. It is clear that the stress developed in the sample depends on the size of the specimen.

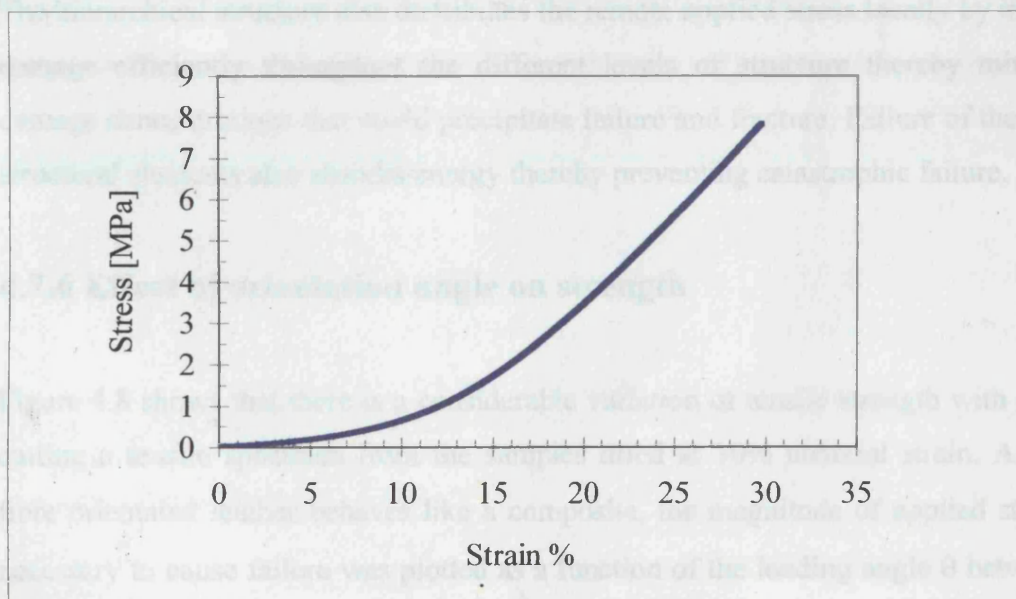


**Figure 4.7:** Stress strain curve for the large rectangular samples (wet blue) prior to drying.

Leather is composed of a complex cross-linked network of collagen fibres. This network can be envisaged as a bio-composite system organised into a complex hierarchical structure. Interfacial interactions between the various components of this

network structure play a predominant role in the mechanisms of fracture of leather. Unlike artificial composites, it is not a case of just one fibre-matrix interface, but rather the interactions at a multiplicity of interfaces between the different structural levels of micro-fibril, fibril, fibril bundle, fibre and fibre bundles. The mechanical properties of leather will therefore depend upon the response of the individual collagen fibrils to the applied stresses and the interaction between them.

X-ray diffraction studies show that randomly oriented collagen fibres in the wall of pig aorta progressively line up with increasing deformation [Atkins and Mai (1985)] suggesting that progressive orientation of fibres is the cause of J-shaped curve in biological materials. At low strains there is progressive straightening of collagen fibres as they become oriented in the direction of stress and the only resistance to deformation may originate from interfacial effects. It is only after all the fibres are straight, that the entire fibre network is pulled elastically.

The hierarchical structure also distributes the remote applied stress locally by imparting damage efficiently throughout the different levels of structure thereby minimising damage concentrations that could precipitate failure and fracture. Failure of these small structural elements also absorbs energy thereby preventing catastrophic failure.

#### **4.7.6 Effect of orientation angle on strength**

Figure 4.8 shows that there is a considerable variation of tensile strength with angle of cutting a tensile specimen from the samples dried at 30% uniaxial strain. Assuming fibre orientated leather behaves like a composite, the magnitude of applied stress  $\sigma_{\theta u}$  necessary to cause failure was plotted as a function of the loading angle  $\theta$  between the stress axis and the pre-strain fibre axis for each of the three failure modes given by equations 4.1 to 4.3. The three curves are plotted in figure 4.8 using the values of  $\sigma_{1u}$ ,  $\sigma_{2u}$  and  $\tau_{12u}$  shown in table 4.1 for both the long and short pre-stretched samples.

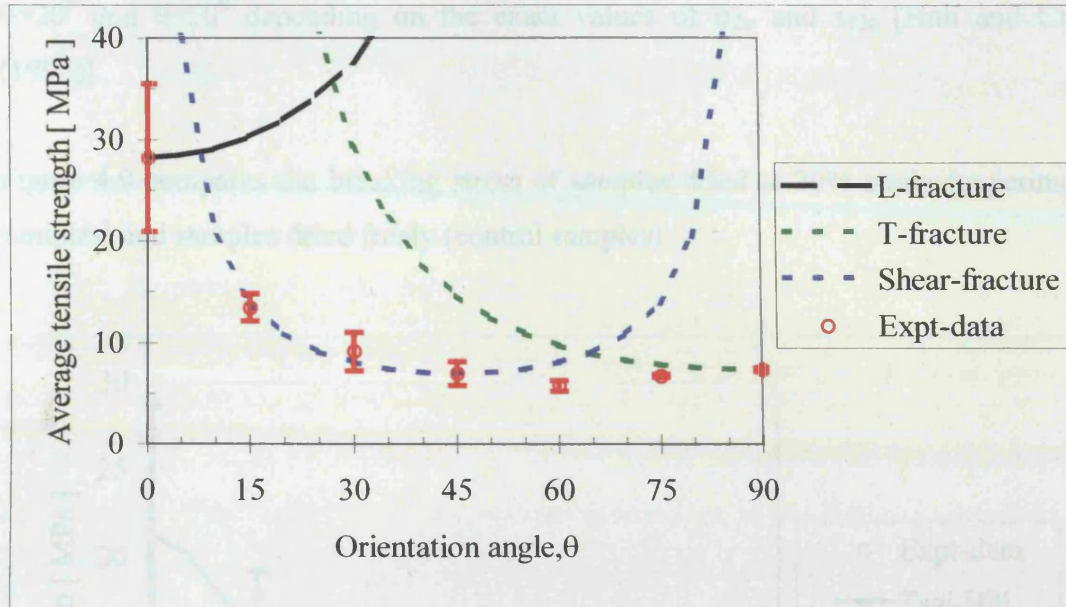


**Figure 4.8:** The dependence of tensile strength on sample orientation with respect to the axis of strain applied during drying. Also shown is the predicted dependence on loading angle  $\theta$ , of the applied stress for the onset of different failure modes according to the maximum stress criterion. (L-longitudinal, T-transverse)

**Table 4.1:** Experimentally determined tensile strength and the shear strength (obtained by curve fitting) values for leather used in the Tsai-Hill model

	Specimens obtained from the long sample [300mm x 150mm]	Specimens obtained from the short sample [100mm x 150mm]
Longitudinal tensile strength [ $\sigma_{1u}$ ] MPa	21.33	15.00
Transverse tensile strength [ $\sigma_{2u}$ ] MPa.	7.88	8.05
Shear strength [ $\tau_{12u}$ ] MPa	5.05	8.23

According to figure 4.8, axial failure is expected only for very small loading angles, but the predicted transition from shear to transverse failure may occur anywhere between

$\theta=20^\circ$  and  $\theta=50^\circ$  depending on the exact values of  $\sigma_{2u}$  and  $\tau_{12u}$  [Hull and Clyne, (1996)].

Figure 4.9 compares the breaking stress of samples dried at 30% strain (experimental samples) and samples dried freely (control samples).

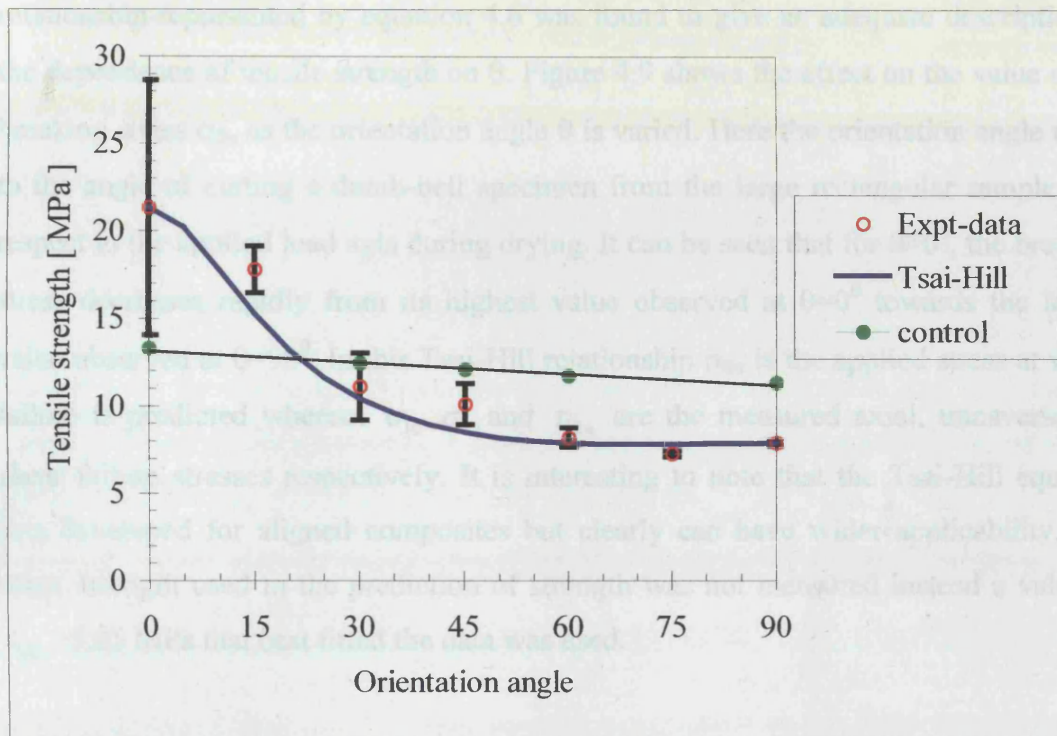


**Figure 4.9:** Dependence of average tensile strength on the angle between the stress axis and the direction of alignment of the fibres in specimens cut from long samples dried at 30% strain and control samples that were dried freely. Also shown is the Tsai-Hill relationship of given by equation 4.6.

For  $\theta=0$ , it is quite clear that the breaking stress of the experimental samples is 50% higher than the breaking stress of the control samples. This figure also shows that for  $\theta \geq 30$ , the tensile strength of experimental samples is lower than the tensile strength of the control samples. It is apparent that the initial 30% stretching along a single axis has caused the subsequent tensile strength to display a marked anisotropy (i.e. a strong dependence on the angle  $\theta$ ). These results are from a separate experiment in which the samples used for drying were mirrored across the backbone line of the wet blue hide. The agreement in tensile strength between two sides of the same hide is generally much

better than that between two adjacent blocks cut from the same side of the hide [Maeser, (1960)].

The ability to mathematically model the behaviour of leather is an important goal that will allow users of leather to achieve a greater degree of confidence in their use of the material. In seeking to model the behaviour of the pre-stretched leather, the Tsai-Hill relationship represented by equation 4.6 was found to give an adequate description of the dependence of tensile strength on  $\theta$ . Figure 4.9 shows the effect on the value of the breaking stress  $\sigma_{\theta u}$  as the orientation angle  $\theta$  is varied. Here the orientation angle refers to the angle of cutting a dumb-bell specimen from the large rectangular sample with respect to the applied load axis during drying. It can be seen that for  $\theta > 0^\circ$ , the breaking stress decreases rapidly from its highest value observed at  $\theta = 0^\circ$  towards the lowest value observed at  $\theta = 90^\circ$ . In this Tsai-Hill relationship  $\sigma_{\theta u}$  is the applied stress at which failure is predicted whereas  $\sigma_{1u}$ ,  $\sigma_{2u}$  and  $\tau_{12u}$  are the measured axial, transverse and shear failure stresses respectively. It is interesting to note that the Tsai-Hill equation was developed for aligned composites but clearly can have wider applicability. The shear strength used in the prediction of strength was not measured instead a value of  $\tau_{12u} = 5.05$  MPa that best fitted the data was used.

Fig.4.10 shows variation of tensile strength with the angle of cutting the specimen from the short sample dried at 30% strain. The dependence of strength on the angle of loading is not as pronounced as in the longer samples. However the Tsai Hill equation still gives a good account of the variation of tensile strength with the loading angle for tensile specimens obtained from the short sample. It appears that the tensile strength of stretched leather depends on specimen size. There is also the effect of through thickness stresses as the shorter samples had higher thickness as compared to the longer samples after drying under the same conditions. Through thickness stresses act so as to transfer load between the fibres and may give rise to inter-fibre failure. The efficiency of load transfer is expected to depend on the how close the fibres are at a given point in the network structure.

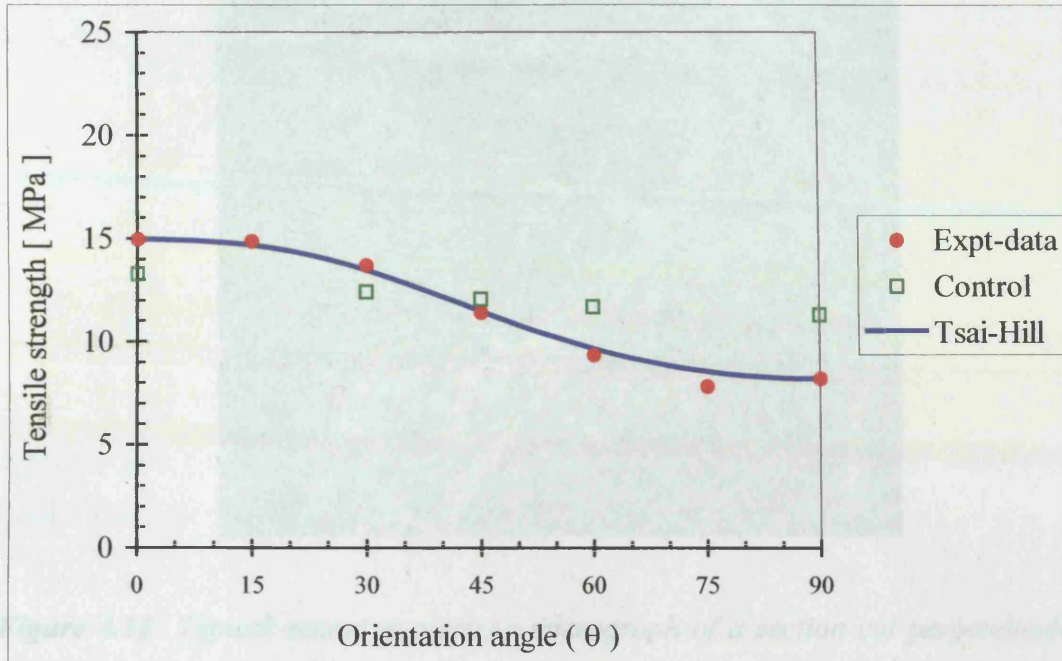


**Figure 4.10** Tensile strength versus orientation angle for control and experimental samples (dried at 30% strain) cut from the short pre-stretch sample. The solid line represents Tsai-Hill relationship given by equation 4.6

#### 4.7.7 Failure mechanisms

Essentially two failure mechanisms have been identified in the leather tested in this study namely, fibre pull-out and fibre fracture. Figure 4.11 is a scanning electron microscope micrograph of a section of a chrome tanned leather sample showing a cavity, which previously must have been occupied by a fibre bundle. Surrounding this cavity is a light coloured binding material (matrix) that was observed around all fibre bundles. In order for fibre pull-out to occur, both fibre fracture and de-bonding between the binding material and the fibre bundles must occur. The sequence of events depends on the strength of the interfacial bond between the binding material and the fibre bundles.

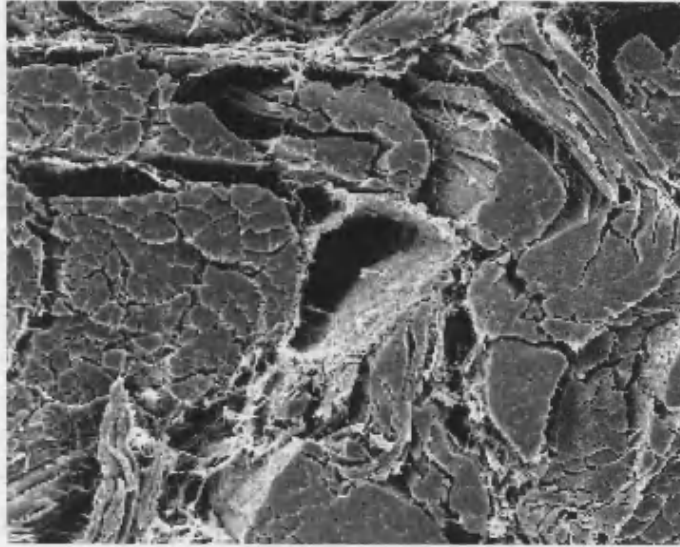


**Figure 4.11:** Typical scanning electron micrograph of a section cut perpendicular to the load axis of strain dried wet blue leather showing a cavity where a fibre has pulled-out (magnification x 1000)

In polymeric composite materials [Hull and Clyne, (1996)] the mechanism of failure depends on whether matrix or fibres has the lower strain to failure. If the matrix is the lower failure strain, then when the strain of the matrix is reached, the matrix fails and the load is transferred progressively to the fibres. On the other hand if the fibres have lower failure strain, when fibre strain is reached, the fibres break into progressively shorter lengths and all the load is transferred to the matrix.

Since fibre pull-out was observed instead of fibre fragmentation, it appears that the interfacial bond is the weakest link in the collagen fibre network. Clearly stronger interfacial bond strength would cause a high stress concentration in network and cracks would tend to pass through large bundles of fibres without much deviation resulting in a flat fracture surface. On the other hand if interfacial bond is weak, cracks tend to form at the interface and link up through highly stressed regions of the fibre network. This causes fibre sliding to occur leading to extensive fibre pullout as shown in figure 4.12

G

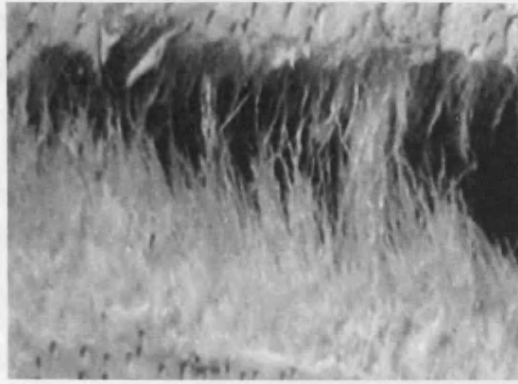


**Figure 4.12:** *Optical microscope image showing fibre pull-out of the collagen fibre network and the binding material surrounding the cavity, x10*

In addition to fibre fracture, de-bonding and pull-out, collagen fibre bundles dissociate into smaller units at high strains as shown in figure 4.13.

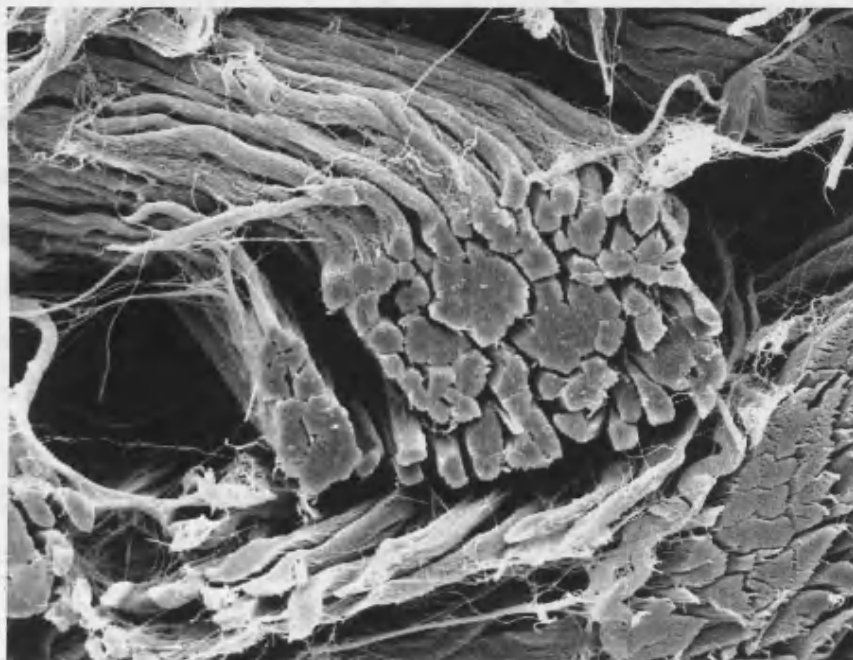


**Figure 4.13:** *Scanning electron micrograph of a section perpendicular to the load axis of a leather sample just before fracture (magnification x 1000) showing debonding between fibres.*

In uniaxial tension, it appears the initial mode of failure, is the dissociation of fibre bundles from the binding material and then subsequently into smaller units of its hierarchical structure. Similar observations [Torp et al, (1975)] were reported in a

tendon. It was concluded that dissociation of the hierarchical structure into smaller units was the primary fracture mechanism in the tendon.

If debonding occurs at each hierarchical level within the fibre as well as the fibre debonding from the binding material then energy required in the process of debonding will definitely increase. Therefore at strains of 30% and higher, a number of fracture mechanisms may take place. The collagen fibrils may dissociate into, sub-fibrils and micro-fibrils resulting in localised slippage and voiding between hierarchical levels and thus accounting for the yielding observed at macroscopic level. Thus once yielding takes place, the structure cannot fully recover to its initial state. In fibre reinforced composites fibre pull out occurs in fibres that are too short to allow sufficient build up of stress in the fibre to cause fibre fracture. In this case the efficiency of the fibres decreases as the strain on the composite increases. At low strains all fibres contribute to load carrying but the contribution from the shorter fibres decreases with a given strain increment and as the strain increases only the longer fibres continue to contribute fully.

The stress strain curve can be explained in terms of the observed fracture mechanisms. When tensile stresses are applied parallel to the fibre direction all the components of the network structure experience the same axial stresses up to strains of about 15%. Above this strain, the network structure starts to disintegrate and this corresponds with the appearance of a knee in the stress strain curve. After the onset of damage at the knee, there is a change in the slope of the stress strain curve, but it does not reduce to zero. This is because the load is transferred across the interface even after the fracture of some of the fibres in the network structure. The network extends with little further increase in the applied stress. As the damage grows in the network structure, the load is progressively transferred to the fibres. If the applied strain at this stage does not reach the ultimate strain of the fibres, further extension causes the axial stress to rise, and the load is now carried entirely by the axial fibres. Fracture occurs when the applied strain reaches the ultimate strain of the fibres.

#### 4.7.8 X-ray diffraction studies

Figure 4.14(a) shows typical X-ray diffraction patterns for chromium tanned bovine leather dried freely (control) and for samples dried under 30% uniaxial strain. The intensity at any point on the ring is proportional to the number of fibres inclined at a particular angle. It can be seen that the intensity of the peaks on the ring is more pronounced for samples dried at 30% uniaxial strain compared to samples dried freely under no constraint.

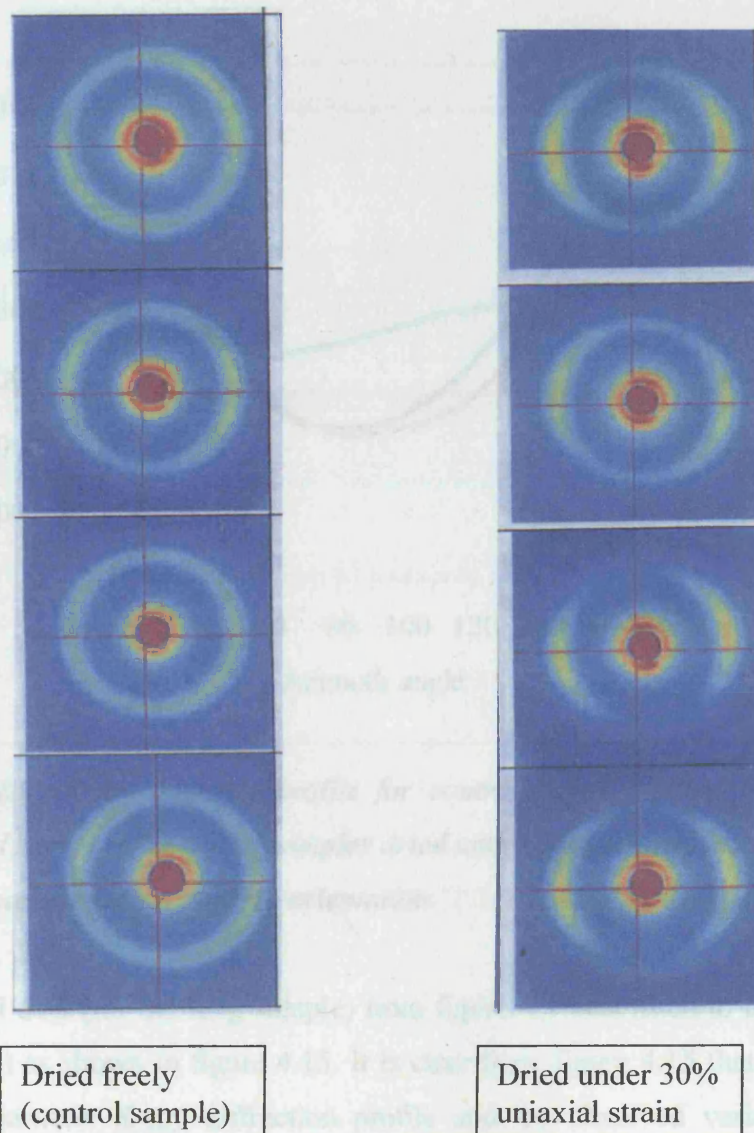


**Figure 4.14(a):** Typical X-ray diffraction patterns of leather strips dried freely and leather strips dried under 30% uniaxial strains.

This provides evidence that fibre orientation occurs when leather is stretched during tensile testing. The tensile strength of leather is therefore expected to be a function of the number of fibres in the woven fibre network that are oriented in the direction of the applied load.

Figure 4.14(b) shows the variation of X-ray intensity with angle for both control samples dried freely and samples dried under 30% uniaxial strain. It seems from figure 4.14(b) that along the stretch axis, there is more orientation in the longer samples compared to the shorter samples.

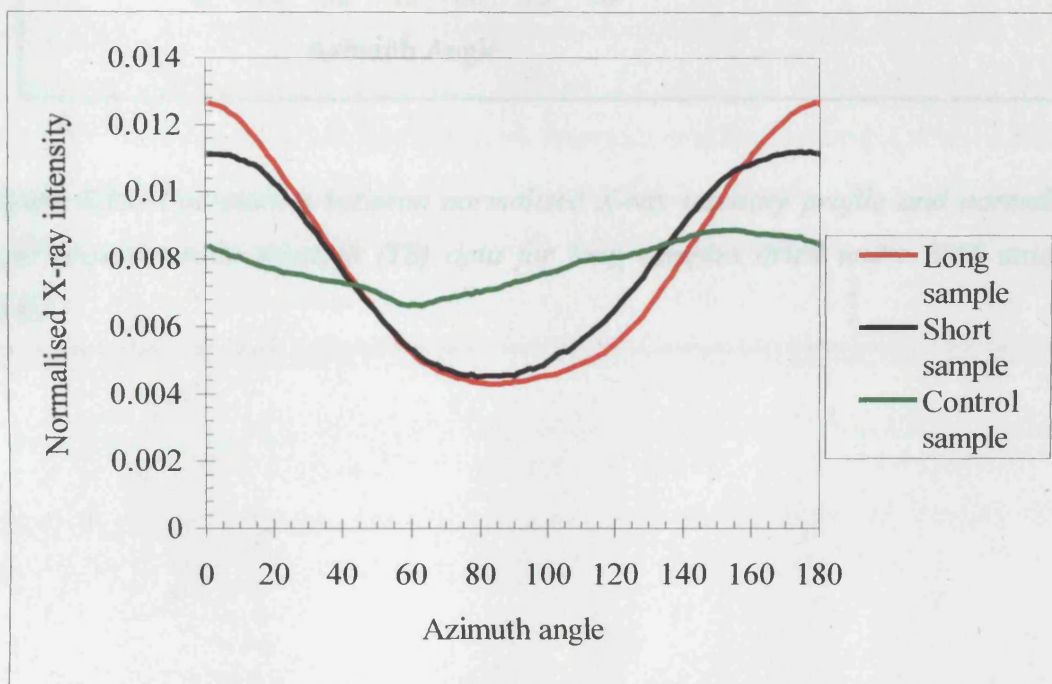


**Figure 4.14(b):** X-ray intensity profile for control samples dried freely, long pre-stretched and short pre-stretched samples dried under 30% uniaxial strain, showing the influence of sample length on fibre orientation.

Experimental data (for the long sample) from figure 4.9 was fitted to the x-ray data of figure 4.14(b) as shown in figure 4.15. It is clear from figure 4.15 that there is a good correlation between X-ray diffraction profile and the observed variation of tensile strength with the orientation angle. The X-ray intensity was normalised by dividing the intensity at each location with the sum of all the intensities over the whole distribution.

### 4.3 CONCLUDING REMARKS

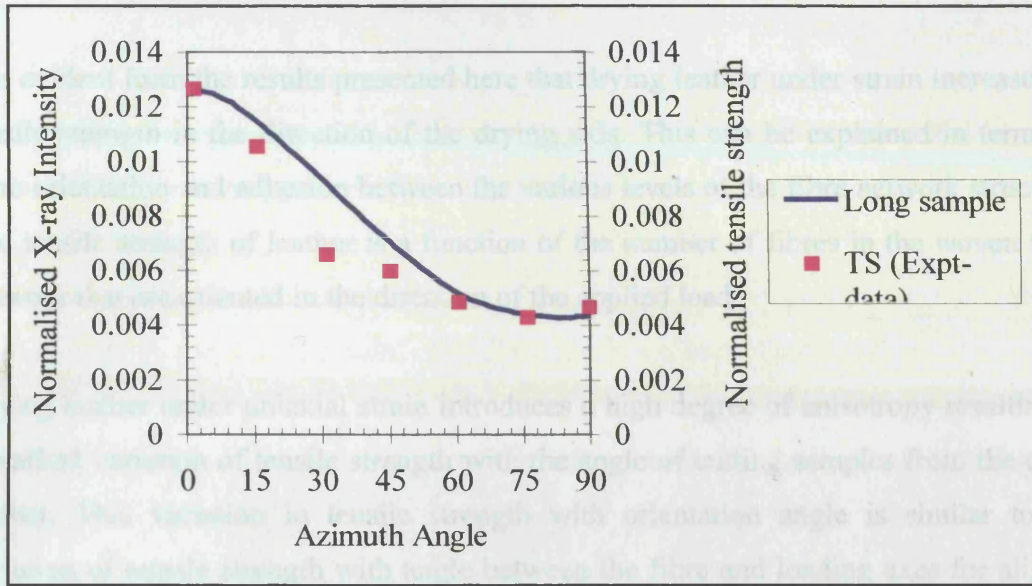


**Figure 4.15:** Correlation between normalised X-ray intensity profile and normalised experimental tensile strength (TS) data for long samples dried under 30% uniaxial strain.

## 4.8 CONCLUDING REMARKS

It is evident from the results presented here that drying leather under strain increases its tensile strength in the direction of the drying axis. This can be explained in terms of fibre orientation and adhesion between the various levels of the fibre network structure. The tensile strength of leather is a function of the number of fibres in the woven fibre network that are oriented in the direction of the applied load

Drying leather under uniaxial strain introduces a high degree of anisotropy resulting in a marked variation of tensile strength with the angle of cutting samples from the dried leather. This variation in tensile strength with orientation angle is similar to the variation of tensile strength with angle between the fibre and loading axes for aligned and discontinuous fibre composites and continuous fibre materials. The Tsai-Hill equation that is normally used to model the variation in strength with orientation angle of fibre composite materials can be used to describe the variation in strength with orientation angle for leather.

## References

Alexander, K.T.W., Covington, A.D., Garwood, R.J. and Stanley, A.M., "The Examination of Collagen Ultra-Structure by Cryo-scanning Electron Microscopy", *XXII IULTCS Congress Proceedings*, Brazil, (1993)

Atkins, A.G. and Mai, Y.W., "Elastic and Plastic Fracture-Metals, Polymers, Ceramics, Composites, Biological Materials", John Wiley & sons, New York, (1985).

Atkins, A.G. and Mai, Y.W., "Elastic and Plastic Fracture", Chichester: Ellis Horwood, (1985), pp 55

Attenburrow, G.E., "The Rheology of leather-A Review", *Journal of the Society of Leather Technologists and Chemists*, (1992), vol 77, pp. 107-113

Azzi, V.D. and Tsai, S.W., "Anisotropic Strength of Composites", *Experimental Mechanics*, (1965), 5, pp283-288

Bailey, J.E., " Mechanical Properties of Composites-Micromechanics" Handbook of Polymer Fibre Composites, Longman Scientific and Technical (UK), (1994), pp 212-230

Haines, B.M., "The Skin before Tannage-Procter's View and Now", *Journal of the Society of Leather Technologists and Chemists*, (1983), vol. 68(3), pp 57-70

Haines, B.M. "Fibre Structure and the Physical Properties of Leather", *Journal of American Leather Chemists Association*, (1974), vol 69, pp 96-109

Heidemann, E. "Fundamentals of Leather Manufacturing", Eduard Roether, K.G., Darmstadt, (1993), page 30.

Hill, R., "A theory of Yielding and Plastic Flow of an Isotropic Metals.", *Proc. R. Soc. Series A*, (1948), 193, pp. 281,

Hill, R., "The Mechanical Theory of Plasticity", Oxford University Press, London, (1950)

Hull, D. and Clyne, T.W., "Strength of Composites", An Introduction to Composite Materials (2<sup>nd</sup> edition), (1996), Cambridge University press, pp 159-207

Jarret, R.M., and Sykes R.J., "Analysis of Video Recordings to Investigate Mechanical Operations", *Journal of Leather Technologists and Chemists*, (1988), **72**, pp 94-96

Kanagy, J.R., Randall, E.B., Carter, T.J., Kinmonth, R.H., and Mann, C.W., "Variations of Physical Properties Within and Between Vegetable Retanned Cow and Steer Hides.", *Journal of the American Leather Chemists Association*, (1952), **47**, pp. 726-748

Kanagy, J.R., "Physical and Performance Properties of Leather", *Chemistry and Technology of Leather*, (1948), pp368-416

Kanagy J.R., "Significance of the Results of Some Physical Tests on Upper Leather", *Journal of the American Leather Chemists Association*, (1955), **50**, pp 112-148

Kendall, K and Fuller, K.N.G. "J-Shaped Stress/Strain Curves and Crack Resistance in Biological Materials", *Journal of Physics D., Applied Physics*, (1987), **20**, pp. 1596-1600.

Kronick, P., Page, A. and Komanowsky, M., "An Acoustic Emission Study of Staking and Fatliqour", *Journal of American Leather Chemists Association*, (1993), **88**, pp 178

Kronick, P and Maleef, B "Non-Destructive Failure Testing of Bovine Leather by Acoustic Emission", *Journal of the American Leather Chemists Association*, (1992), **87**, pp 259-265

Lin, J. and Hayhurst, D.R., "The Development of a Biaxial Tension Test Facility and its Use to Establish Constitutive Equations of Leather", *European Journal of Mechanics A/Solids*, (1993), volume 12, No 4, pp 493-507

Lin, J. and Hayhurst, D.R., "Constitutive Equations for Multi-Axial Straining of Leather under Uniaxial Stress", *European Journal of Mechanics A/Solids*, (1993), volume 12, No 4, pp 471-492,

Maeser, M., "The Effect of Hide Location and Cutting Direction on Tensile Properties of Upper Leathers", *Journal of American Leather Chemists Association*, (1960) Vol55, pp501-522

Mai, Y.W. and Atkins, A.G., "Further Comments on J-Shaped Stress Strain Curves and the Crack Resistance of Biological Materials", *Journal of Physics D, Applied Physics*, (1988), 22, pp. 48-54.

Mathews, F.L. and Rawlings, R.D., "Short Fibre Composites", Handbook of polymer fibre composites, F.R. Jones (editor), Longman Scientific and Technological (UK), (1994), pp 287-325,

Miller, R.G., "Manual of Shoemaking" Published by C.J. Clarks Ltd, (1976), pp 91-99

Mitton, R.G., "Mechanical Properties of Leather Fibres" *Journal of Society of Leather Trades Chemists*, (1945), 29, pp. 169-194

Mitton, R.G. and Price, C. "Low Strain Characteristics of Leather", *Journal of the Society of Leather Trades Chemists*", (1970), 54, pp 44-53

Mitton, R.G., "Tensile Properties and their Variability in Chrome Tanned Calfskins", *Journal of the Society of Leather Trades' Chem.*, (1948), 32, pp 310-323

Mitton, R.G., "Mechanical Properties of Leather Fibres", *Journal of the Society of Leather Trades' Chemists*, (1945), 29, pp 169-194

O'Leary, D.N. and Attenburrow, G.E. "Differences in Strength Between the Grain and Corium Layers of Leather", *Journal of Materials Science*, (1996), **31**, pp. 5677-5682

Osaki, S., "Dielectric Anisotropy of Nonwoven Fabrics by Using the Microwave Method", *Tappi* 72, (1989), pp. 171-174

Osaki, S. " Distribution Map of Collagen Fibre Orientation in a whole Calf Skin", *The Anatomical Record*, (1999), 254, pp 147-152

Osaki, S. "Microwaves Quickly Determine the Fibre Orientation of Paper", *Pappi*, (1987a), 70, pp 105-108

Osaki, S. " A new Method for the Quick Determination of Molecular Orientation in Poly(ethylene terephthalate) Films by use of Polarized Microwaves.", *Polymer Journal*, (1987b), **19**, pp 821-828

Osaki, S., Yamada, M., Takasusu, A. and Murakami, K., "A new Approach to Collagen Fibre Orientation in Cow Skin by the Microwave Method", *Cellular and Molecular Biology*, (1993), **39(6)**, pp 673-680

Pan, N. and Yoon, M., "Structural Anisotropy, Failure Criterion and Shear Strength of Woven Fabrics", *Textiles Research Journal*, (1996), **66(4)**, pp 238-244

Rawlings, R.D. and Mathews, F.R., "Short Fibre Composites", *Handbook of Polymer Fibre Composites*, Longman Scientific and Technical (UK), (1994), pp 287-325

Rowlands, R.E., "Strength (failure) Theories and their Experimental Correlation", in *Handbook of Composites*, vol3-Failure Mechanics of Composites, G.C Sih and A.M. Skudra, (editors), Elsevier: Amsterdam, (1985), pp 71-125,

Torp, S, Baer, E and Friedman, B, "Effects of Age and Mechanical Deformations on the Ultra Structure of Tendon", *Structure of Fibrous Biopolymers*, Sythoff and Noordhoff, Netherlands, (1975), pp 223

Tsai, S.W., and Wu, E.M., "A general Theory of Strength of Anisotropic Materials", *Journal of Composite Materials*, (1971), **5**, pp 58-80

Von Mises R., "Mechanik der Plastischen Formänderung von Kristallen, Z., *Angewandte Mathematik und Mechanik*, (1928), **8**, pp 161-185

Vos, A. and Vlimmeren, P.J., "Topographic Differences in Physical Properties", *Journal of the Society of Leather Technologists and Chemists*, (1973), vol 57, pp 93-98

Ward, A.G. and Chinn, S.J., "The Two Dimensional Deformation of Shoe Upper Materials", *Journal of the Society of Leather Trades Chemists*, (1971), vol 55, pp 221-231.

Wright, D.M. and Attenburrow, G.E., "The Deformation and Set of Partially Processed Leather", *Proceedings of the XXII Congress of the International Union of Leather Chemists and Technologists*, Friedrichshafen, Germany, (1995)

Wright, D.M. and Attenburrow, G.E., "The Deformation and Set of Partially Processed Leather", *Proceedings of the XXII Congress of the International Union of Leather Chemists and Technologists*, Friedrichshafen Germany, part 1, paper 34, (1995b)

Wright, D.M. and Attenburrow, G.E., "The Set and Mechanical Behaviour of Partially Processed Leather Dried under Strain", *Congress Proceedings of the International Union of Leather Chemists and Technologists (IULTCS)*, London, 1997, pp 686-702

Yamamoto, K., Osaki, S., Yamashita, S. and Yamada, M.O., "Age Related Anisotropic Changes in the Fibre Orientation of Human Blood Vessel", *Cellular and Molecular Biology*, (1988), **34**, pp 571-579

## **CHAPTER FIVE**

### **MODELLING ELONGATION AT BREAK**

5.1 INTRODUCTION	88
5.2 ELONGATION AFTER STRAIN DRYING	89
5.3 MECHANICAL PROPERTIES OF COLLAGEN FIBRE AGGREGATES.	89
5.4 DEFORMATION MECHANISMS	89
5.5 POISSON'S RATIO	90
5.6 ELONGATION TO BREAK MODEL	91
5.7 RESULTS AND DISCUSSION	95
References	100

## 5.1 INTRODUCTION

Elongation at break is an important leather quality, particularly in the shoe industry where leather is further stretched upon the last during shoe manufacture and yet will still need to stretch and contract in response to stresses imposed during wear.

The properties of shoe upper leather are mainly dependent on the composition and structure of skins. Shoe upper leather when tested uniaxially has a non-linear stress-elongation relationship [Marriott, (1978)]. During a typical tensile test the stress was observed to increase with elongation up to strains of about 20%. Above 20% strain, the relationship between stress and elongation is non-linear with the stress reaching a plateau at failure when elongation is in the region of 30-60%. For elongations up to 20% the mechanism of deformation is believed to be due to fibre rotation. Above these elongation levels deformation takes place by the combined mechanism of fibre rotation and of slippage between adjacent fibres.

In untanned animal skin, the fibres are set in a matrix of natural binding agents known as ground substance. This is removed during the tanning process to create an open structure of fibres that are held together by the interwoven arrangement of the fibres. During the later stages of the tanning process, the pores between the fibres are partially filled with oils and greases, which determine the subsequent behaviour of the leather. The partial filling of the zones between adjacent fibres produces a porous matrix structure. Under applied uniaxial loading this type of structure enables the fibres to rotate and to slide relatively to each other. The fibres are known to be oriented more or less parallel to the backbone to different degrees depending upon the location on the skin. It is reasonable to assume that the stress at break measured in any strength test is directly related to the number of fibres that become involved in the test prior to rupture. The tensile strength is in general higher in a direction parallel to the backbone than that in a direction perpendicular to it, but the strains at failure have directional dependence which is inverse to the strength [Roddy, (1956)]

## **5.2 ELONGATION AFTER STRAIN DRYING**

When leather is stretched as in shoe lasting, forces must be applied to cause its change of dimensions. In the absence of any forces, leather fibres are seldom completely straight and the straightening that accompanies drying under strain is likely to affect its subsequent elongation or change in dimensions during the shoe lasting process. In this study samples were dried at either 30% uniaxial strain or 30% biaxial strains and are referred to as pre-stretched samples. The load axis during drying is referred to as the pre-stretch axis.

## **5.3 MECHANICAL PROPERTIES OF COLLAGEN FIBRE AGGREGATES**

Studies of the viscoelastic properties of leather [Mitton, (1945); Conabere & Hall, (1946)] indicate that the extension of a fibre under constant load increases sharply with increased humidity but the load extension curve of leather fibres is however independent of temperature. When these fibres were subsequently dried, they contracted but complete recovery to their original dimension was never attained.

## **5.4 DEFORMATION MECHANISMS**

Leather like most collagenous tissues, exhibits a J-shaped stress-strain curve. The J-shaped curve has been explained in two ways. First is the fibre orientation model [Viidik, (1973)], which assumes that at low strains the network structure elongates and as this happens, the fibres turn to align along the strain axis. At higher strains, the network structure has elongated as far as it can and most of the fibres have aligned along the strain axis, further deformation can only occur by straining the fibres themselves. In the fibre recruitment model [Kronick & Buechler, (1986)], the fibres are assumed to have varying degrees of tautness and so as the feltwork is extended, more and more fibres become taut and the stress increases. Both these models assume that the high slope region of the J-curve is due to the stretching of the collagen fibres.

Previous studies on wet blue shoe leather [Wright & Attenburrow, (1996)] indicate that the turning point from low to high strain occurs at strains of about 20%, implying that

the fibres come under direct strain at strains above 20%. It is therefore reasonable to assume that if a piece of leather is strain dried at strains above 20%, and then stretched again along the pre-stretch axis the subsequent elongation is likely to be as a result of the direct elongation of its constituent fibres.

Indeed the dominant straining mechanisms in leather were identified [Mitton, (1948)] as being fibre rotation and fibre network distortion and not fibre elongation. This behaviour was likened to a sheet of wire mesh with the difference that the fibre meshwork is three dimensional instead of two. When a tensile stress is applied to the wire mesh netting, an extension is produced which, is partly due to the elongation of the wires that form the mesh, but which is mainly due to the change of shape.

## **5.5 POISSON'S RATIO**

Poisson's ratio is the absolute value of the ratio of transverse strain to the corresponding axial strain resulting from uniformly distributed axial stress below the proportional limit of the material. Poisson's ratio will have more than one value if the material is not isotropic. In this study Poisson's ratio for the large pre-stretch samples, was determined by stretching the sample up to 30% longitudinal strain and measuring the corresponding transverse strain calculated from the change in width. The ratio of transverse strain to longitudinal strain for the long pre-stretch samples was then calculated to be 0.6. Therefore Poisson's ratio was then taken to be  $\mu=0.6$ . It must however be noted that the gripping system is likely to have an influence on the Poisson's ratio as the material close to the grips does not move freely in response to the applied stresses. This effect is likely to be more pronounced in short pre-stretch samples than in the long pre-stretch samples. Therefore for the short pre-stretch samples, an apparent Poisson's ratio of  $\mu=0.4$  was used.

## 5.6 ELONGATION TO BREAK MODEL

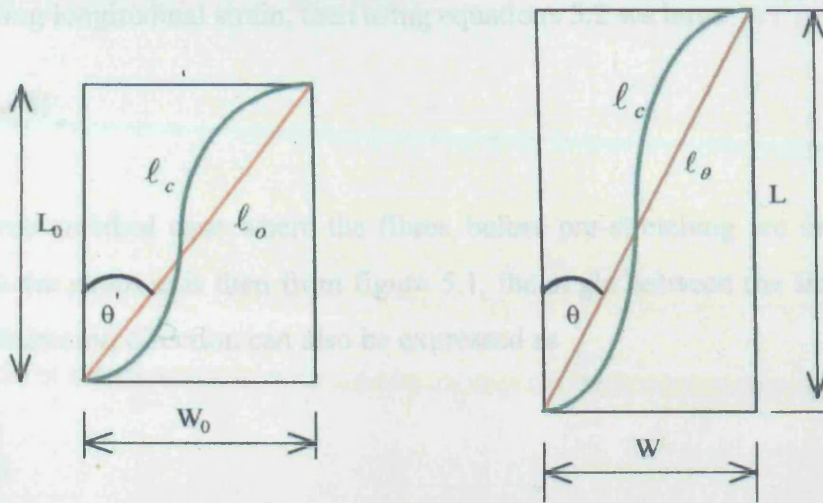


**Figure 5.1:** Schematic diagram showing a pre-stretch sample and the corresponding sample stretched further after the initial pre-stretching and drying.

Consider a leather sample of initial length  $L_0$  and width  $W_0$  before the pre-stretching operation and having a wavy fibre with end-to-end distance of  $\lambda_0$  as shown in figure 5.1. During the pre-stretching operation, this sample is stretched until it attains a length  $L$  and width  $W$  and then left to dry in this state. The longitudinal drying strain  $e_l$  can then be expressed as

$$e_l = \frac{L - L_0}{L_0} \quad (5.1)$$

$$L = (1 + e_l)L_0 \quad (5.2)$$

Likewise the transverse strain  $e_t$ , during drying can also be expressed as

$$e_t = \frac{W - W_0}{W_0} = - \left[ \frac{W_0 - W}{W_0} \right] \quad (5.3)$$

If we define Poisson's ratio  $\mu$ , as  $\mu = -e_t/e_l$  i.e. the ratio of transverse strain to the corresponding longitudinal strain, then using equations 5.2 we have

$$W = (1 - \mu e_l)W_o \quad (5.4)$$

If we assume an ideal case where the fibres, before pre-stretching are oriented at an angle  $\theta'$ , to the strain axis then from figure 5.1, the angle between the strain axis and the fibre orientation direction can also be expressed as

$$\tan \theta' = \frac{W_o}{L_o} \quad (5.5)$$

In terms of the specimen length and width, the end-to-end length  $\lambda_o$  of the fibre can be expressed as

$$\lambda_o = \sqrt{L_o^2 + W_o^2} \quad (5.6)$$

The total strain at break  $e_{bu}$ , in un-stretched leather may be assumed to be made up of two components; one from the straightening of the fibres and the second from the elongation of the fibres themselves after becoming taut. Previous studies indicate that isolated chrome tanned collagen fibres (from the corium) fracture at strains of about 20% [Morgan, (1960)]. However compared to the corium, the grain layer has thinner fibres that tend to have a lower strain (as low as 15%) at break [Dillon et al, (1962)]. Consequently, it has been assumed that fibres in the grain have an ultimate strain of about 15%. Therefore the total longitudinal strain at break  $e_{bu}$ , can be expressed as

$$e_{bu} = \frac{\lambda_c - \lambda_o}{\lambda_o} + 0.15 = \frac{\lambda_c}{\lambda_o} - 0.85 \quad (5.7)$$

When the leather is pre-stained, the wavy fibres become oriented to the stretch direction and at the same time the angle with respect to the stretch axis decreases from

$\theta'$  to  $\theta$ . This process causes the end-to-end fibre distance to increase from  $\lambda_o$  to  $\lambda_\theta$ . In terms of the corresponding specimen dimensions this phenomenon can be quantified as

$$\text{Tan}(\theta) = \frac{W}{L} \quad (5.8a)$$

$$\lambda_\theta = \sqrt{L^2 + W^2} \quad (5.8b)$$

Dividing equation 5.8b with equation 5.6 we get

$$\frac{\lambda_\theta}{\lambda_o} = \sqrt{\frac{L^2 + W^2}{L_o^2 + W_o^2}} \quad (5.9a)$$

Likewise dividing equation 5.8a by equation 5.5 we obtain

$$\frac{\text{Tan}(\theta)}{\text{Tan}(\theta')} = \frac{L_o W}{W_o L} = \frac{(1 - \mu e_l)}{(e_l + 1)} \quad (5.9b)$$

Equation 5.9b can be rewritten as

$$\text{Tan}(\theta') = \frac{(e_l + 1)}{(1 - \mu e_l)} \text{Tan}(\theta) \quad (5.9c)$$

Fixing equations 5.2 and 5.4 into equation 5.9a we get

$$\frac{\lambda_\theta}{\lambda_o} = \sqrt{\frac{(1 + e_l)^2 L_o^2 + (1 - \mu e_l)^2 W_o^2}{L^2 + W^2}} \quad (5.10)$$

Simplifying equation 5.10 and making use of equation 5.5 we obtain

$$\frac{\lambda_{\theta}}{\lambda_o} = \sqrt{\frac{(1+e_l)^2 + (1-\mu e_l)^2 \frac{W_o^2}{L_o^2}}{\left(1 + \frac{W_o^2}{L_o^2}\right)}} = \sqrt{\frac{(1+e_l)^2 + (1-\mu e_l)^2 \tan^2 \theta'}{(1 + \tan^2 \theta')}} = f(\theta') \quad (5.11a)$$

In order to compare this model with experimental data, equation 5.11 can be written in terms of the orientation angle  $\theta$  measured during experimental work by making use of equation 5.9(b). Therefore at any test angle  $\theta$  the length of the fibre will be given by

$$\frac{\lambda_{\theta}}{\lambda_o} = \sqrt{\frac{1 + \tan^2 \theta}{(1+e_l)^{-2} + (1-\mu e_l)^{-2} \tan^2 \theta}} = f(\theta) \quad (5.11b)$$

which can be simply be expressed as

$$\lambda_{\theta} = \lambda_o f(\theta) \quad (5.12)$$

In equation 5.12,  $f(\theta)$  is given by equation 5.11(b). As explained earlier the total strain at break in strained leather is made of two components; one from the re-orientation of the fibres and the second from the elongation of the fibres themselves after becoming taut. Therefore from equation 5.7, the total longitudinal strain  $e_{b\theta}$  at break at a particular angle  $\theta$ , after pre-stretching can be expressed as

$$e_{b\theta} = \left(\frac{\lambda_c - \lambda_{\theta}}{\lambda_{\theta}}\right) + 0.15 = \left(\frac{\lambda_c}{\lambda_{\theta}} - 1\right) + 0.15 = \frac{\lambda_c}{\lambda_{\theta}} - 0.85 \quad (5.13)$$

In equation 5.13,  $\lambda_c$ , is the contour length of the wavy fibres. Fixing equation 5.12 in equation 5.13 gives strain at break in terms of the orientation angle,  $\theta$ .

$$e_{b\theta} = \frac{\lambda_c}{\lambda_{\theta}} - 0.85 = \frac{\lambda_c}{\lambda_o f(\theta)} - 0.85 \quad (5.14)$$

The value of  $\lambda_c/\lambda_o$  can be estimated by setting  $\theta=0$  in equation 5.11(b). It was found experimentally that for  $\theta = 0$  elongation at break  $e_{b\theta} = 0.18$  and equation 5.11(b) gives  $f(\theta)=1.3$ . When  $\theta=0$ , and the samples pre-stretched by 30%, it can be shown that

$$\frac{\lambda_c}{\lambda_o} = 1.03f(\theta = 0) = (1.03)(1.3) = 1.339 \quad (5.15)$$

Therefore from equation 5.14, elongation at break is given by

$$e_{b\theta} = \frac{1.339}{f(\theta)} - 0.85 \quad (5.16)$$

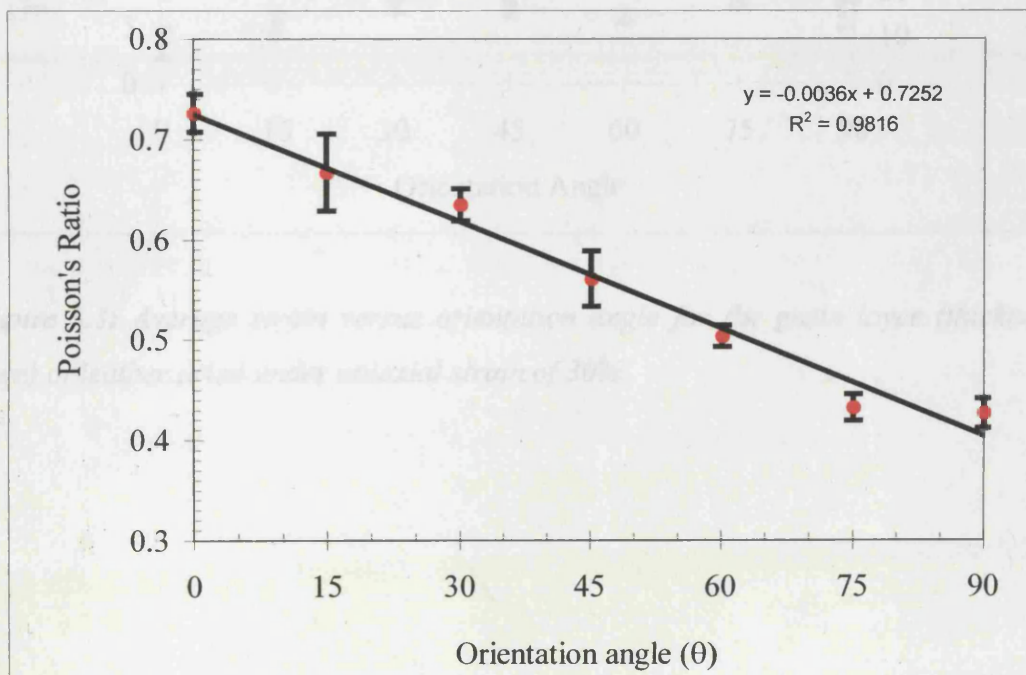
## 5.7 RESULTS AND DISCUSSION

Table 5.1 gives the values of Poisson's ratio for samples cut at various angles from the pre-stretch sample. From this table the average value for Poisson's ratio was calculated to be  $0.564 \approx 0.6$ . This value is higher than the normal upper limit of 0.5 for materials because as the fibres in the leather straighten, they move closer together and so the bulk volume of the material decreases during stretching.

**Table 5.1:** Poisson's ratio values for leather strips cut at various angles from the large pre-stretch sample after drying

Angle, $\theta$	0	15	30	45	60	75	90
Poisson's ratio	0.73	0.67	0.64	0.56	0.50	0.43	0.43

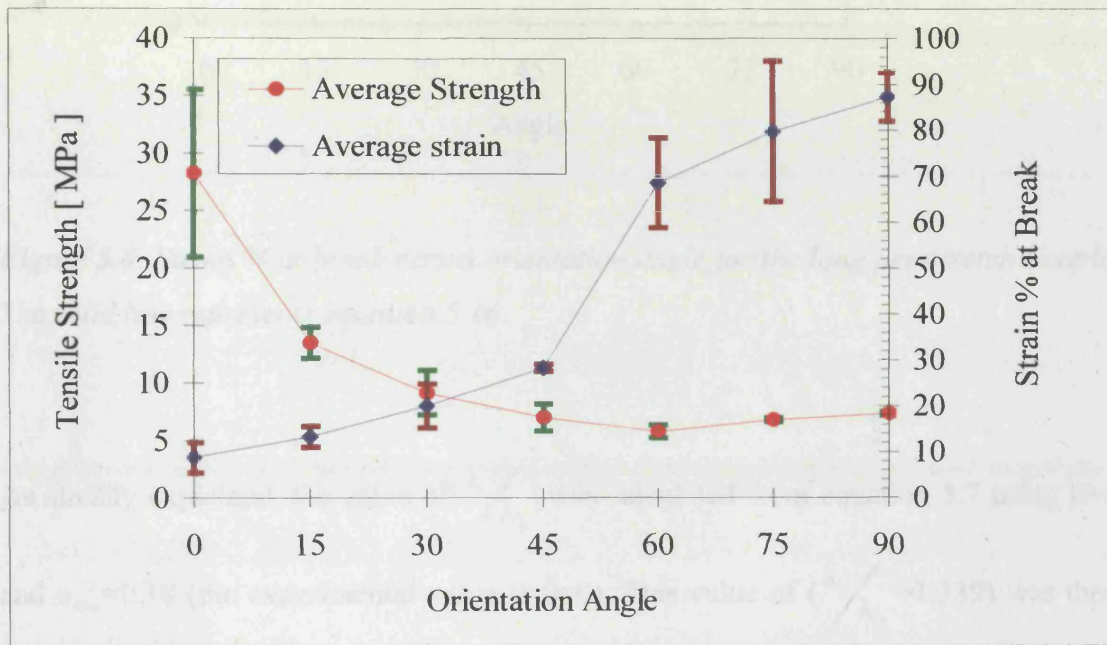
Figure 5.2 shows the values of Poisson's ratio obtained from table 5.1 plotted as a function of the specimen angle with respect to the stretch axis of the large pre-stretch sample. It seems from figure 6.2 that Poisson's ratio depends on the orientation angle of the specimen.



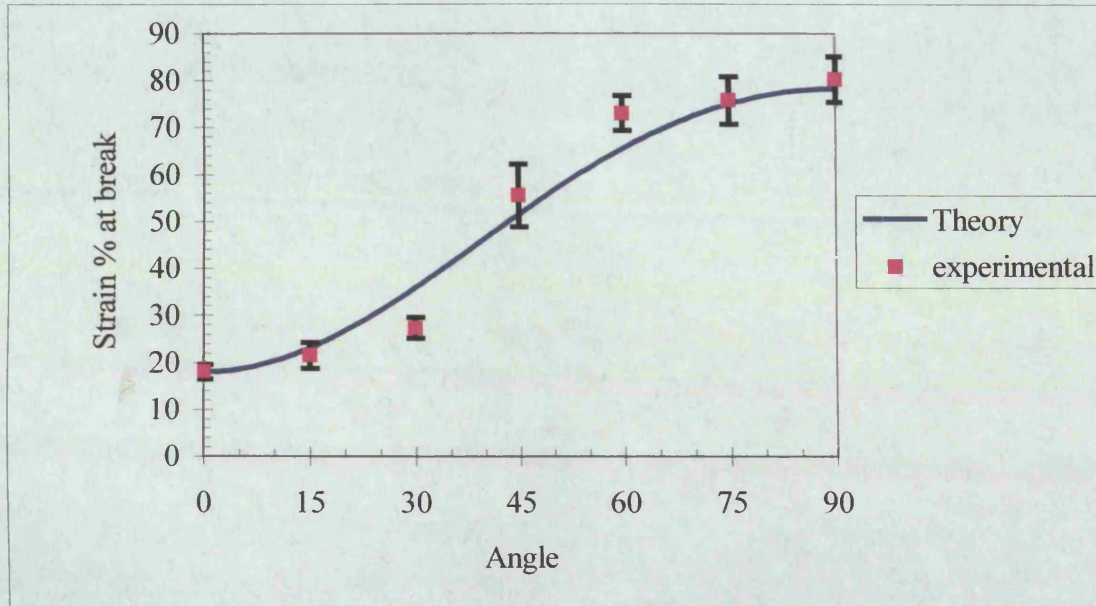
**Figure 5.2:** Poisson's ratio versus the angle of cutting the specimen with respect to the stretch axis

Figure 5.3 shows elongation to break and tensile strength plotted against the angle of cutting the specimen with respect to the stretch axis. This figure indicates that tensile strength and strain at break are inversely proportional and that high strength usually

indicates low elongation and vice versa. This can be explained by assuming that the tensile strength of leather is a function of the number of fibres in the woven fibre matrix of the hide that are oriented in the direction of the applied load. When leather elongates, it also becomes narrower and thinner. The fibres oriented in the direction of the applied load approach each other so that the extent to which the cross section narrows is inversely proportional to the number of fibres oriented in that direction [Kanagy, (1946)].



**Figure 5.3:** Average strain versus orientation angle for the grain layer (thickness < 1mm) of leather dried under uniaxial strain of 30%



**Figure 5.4:** Strain % at break versus orientation angle for the long pre-stretch sample. The solid line represents equation 5.16

As already explained, the value of  $\lambda_c/\lambda_o$  was calculated from equation 5.7 using  $\theta=0$  and  $e_{ibu}=0.18$  (the experimental value at  $\theta=0$ ). This value of ( $\lambda_c/\lambda_o=1.339$ ) was then used in equation 5.14 to allow the calculation of  $e_{b\theta}$  as a function of  $\theta$ . The curve obtained from plotting this relationship is shown in figure 5.4 and conforms well to experimental data of the long pre-stretch samples. The value of Poisson's ratio used was  $\mu=0.6$  for large pre-stretch sample as already discussed.

Figure 5.5 shows equation 5.16 applied to the data of the short pre-stretch samples.

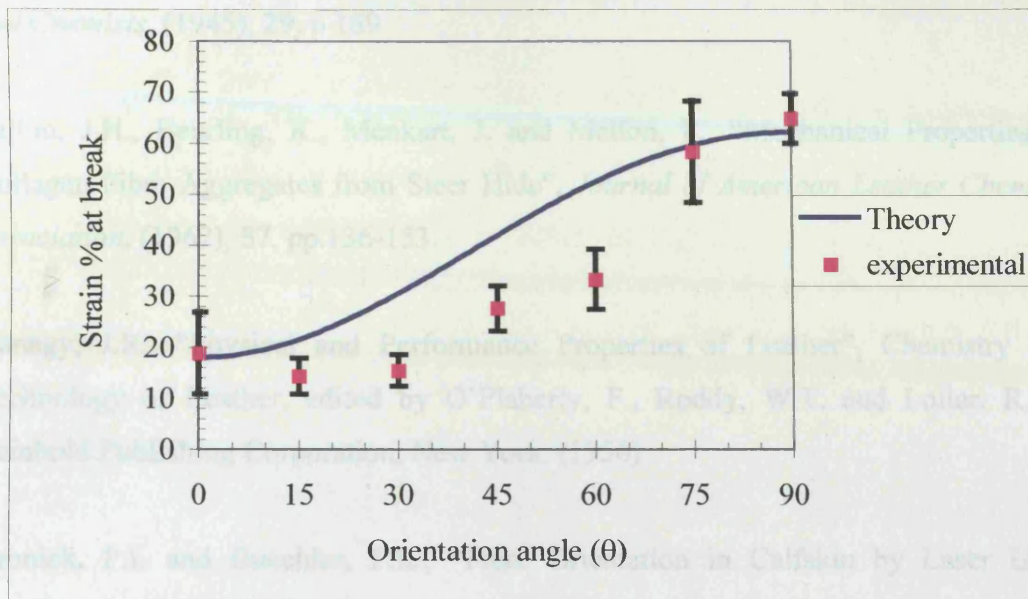


**Figure 5.5:** Elongation at break plotted as a function of the angle of cutting the specimen with respect to the stretch axis for the short pre-stretch samples

It can be seen that equation 5.16 overestimates the strain at break for angles between  $15^\circ$  and  $60^\circ$  for the short pre-stretch samples. It is not clear why this is the case however it could be that the edge effects resulting from the gripping system of the Instron machine prevented the fibres from freely orienting towards the stretch axis because of the close proximity of the grips in the short pre-stretch sample.

## References

- Canabere, G.O. and Hall, R.H., *Journal of the International Society of Leather Trades and Chemists*, (1945), **29**, p 169
- Dillon, J.H., Beurling, K., Menkart, J. and Mellon, F., "Mechanical Properties of Collagen Fibre Aggregates from Steer Hide", *Journal of American Leather Chemists Association*, (1962), **57**, pp.136-153.
- Kanagy, J.R., "Physical and Performance Properties of Leather", Chemistry and Technology of Leather, edited by O'Flaherty, F., Roddy, W.T. and Lollar, R.M., Reinhold Publishing Corporation, New York, (1956)
- Kronick, P.L and Buechler, P.R., "Fibre Orientation in Calfskin by Laser Light Scattering or X-ray Diffraction and Quantitative Relation to Mechanical Properties", *Journal of American Leather Chemists Association*, (1986), **81**, pp 221-230
- Marriott, A.G., "Mechanical Properties of Air Dried Leather Impregnated With Film Forming Polymers", PhD thesis, University of Surrey, (1978).
- Mitton, R.G., "Mechanical Properties of Leather Fibres", *Journal of the Society of Leather Trades' Chemists*, (1945), **29**, pp 169-194
- Mitton, R.G., "Tensile Properties and their Variability in Chrome Tanned Calf Skins", *Journal of the Society of Leather Trades and Chemists*, (1948), **32**, pp 310-323
- Morgan, F.R., "The Mechanical Properties of Chrome Tanned Collagen Fibres", *Journal of the Society of Leather Trades' Chemists*, (1960), **44**, pp121-139
- Morgan, F.R., "The Mechanical Properties of Collagen Fibres: Stress-Strain Curves", *Journal of the Society of Leather Trades' Chemists*, (1960), **44**, pp 170-181

Roddy, W.T., "Chemistry and Technology of Leather", American Chemical Society Monograph, edited by O'Flaherty F., Roddy, W.T. and Lollar, R.M., Renhold Publishing Corp., New York, (1956).

Viidik, A., "Rheology of Skin with Special Reference to Age Related Parameters and their Possible Correlation to Structure", *Front. Matrix. Biol.*, (1973), **1**, pp 157

Wright, D.M. and Attenburrow, G.E., "Factors Influencing the Plastic Deformation of Leather", *Proceedings of the III Asian International Conference of Leather Science and Technology*, Himeji city, Japan, (1996)

## CHAPTER SIX

---

### FRACTURE TOUGHNESS CHARACTERIZATION OF LEATHER

6.1. INTRODUCTION.	104
6.1.1 Fracture mechanics	105
6.1.1.1. Notch sensitivity	106
6.1.1.2 Stress intensity approach	107
6.1.1.3 Energy balance approach	108
6.1.2. Characterization of fracture in ductile materials	109
6.1.2.1. The J-integral	109
6.1.2.2. Essential work of fracture	110
6.1.3. Tear behaviour	114
6.1.3.1. Tear specimen geometry	114
6.1.3.2. Tear test fracture toughness evaluation	115
6.1.3.3. Correlation between fracture toughness tests	116
6.2. EXPERIMENTAL PROCEDURES FOR THIS WORK	117
6.2.1 Materials	117
6.2.2 Crack Propagation tests	118
6.3. RESULTS AND DISCUSSION	118
6.3.1. Effect of uniaxial stretching on EWF	118
6.3.2. Effect of biaxial stretching on EWF	120
6.3.3. Effect of fatliquors on EWF	122
6.3.4. Effect of applied strain on EWF	126
6.3.5. Fracture toughness from tear tests	129
6.3.6. Effect of specimen size and geometry	130
6.3.7. Load displacement curves	132
6.3.8. Notch sensitivity	136
6.3.9. Effect of uniaxial drying on fracture toughness	138
6.3.10. Effect of biaxial drying on fracture toughness	140
6.3.11. Validity of the results	140
6.3.12. Fracture mechanisms	143

6.3.12.1 Frictional sliding and fibre pull-out	144
6.3.12.2 Fibre fracture	144
6.4. CONCLUSION	145
References	146

## 6.1 INTRODUCTION

The prediction of the initiation and subsequent propagation of cracks in many materials is essential for assuring satisfactory performance in the applications for which the material is suitable. Fracture mechanics procedures have been developed to measure parameters such as the stress intensity factor,  $K$  or the  $J$  integral that are used to characterize the fracture resistance of polymers and other engineering materials under specified conditions. However there is currently no single physical parameter that is independent of sampling angle and specimen geometry that can be used to characterize the fracture resistance of leather. An ideal fracture toughness parameter should be independent of the sampling angle and specimen geometry and should also correlate well with other specific strength requirements such as tearing strength.

Cracks in the grain surface of finished leather are undesirable for aesthetic values as well as the durability and service expectancy of leather products. To assess the initiation of cracks in the grain surface of leather, the leather industry uses the Lastometer ball burst test (IUP9), as it is believed to simulate conditions experienced during the lasting operation in footwear manufacture. However the Lastometer test is not a true fracture toughness test as it mainly identifies the strength and distension of the grain and does not address the initiation and subsequent propagation of cracks as is normally the case in fracture toughness tests. On the other hand to assess the tear characteristics of leather, the trouser tear test is normally used. This test is mainly used to determine the force required to tear a given piece of leather. It is very difficult using this test to control the fracture path and as a result mixed mode failure is usually observed.

Clearly a new method is required to characterize the fracture resistance of leather. Such a method will be of great benefit to the leather industry as it may lead to effective optimisation of the leather making process, yielding higher quality leather products. A fracture toughness parameter will without doubt be useful in establishing how much strain can be applied to increase area yield without compromising the quality anticipated for the end use of a given piece of leather.

The applicability of fracture mechanics to conventional isotropic materials has been well demonstrated. For fibre reinforced materials, however, fracture mechanics investigations have met with mixed success. The following section reviews the fundamentals of fracture mechanics for isotropic materials and discusses the applicability of some these parameters to leather.

### **6.1.1 Fracture mechanics**

Fracture mechanics is a theoretical formulation of the conditions of deformation under which a crack will propagate in a continuous medium. Fracture mechanics theory is thus expressed in terms of stresses, strains, elastic moduli, stored energies and geometric factors such as crack length. Fracture mechanics theory assumes that any material has flaws or cracks that are capable of growth or propagation to cause failure. It then considers the conditions of stress, strain etc. under which propagation will occur. This in turn requires the introduction of a criterion for propagation, which can take one of two forms

The crack will propagate when the stress at its tip reaches some critical value, which overcomes the forces of cohesion [Kelly and Macmillan, (1986)]. This is sometimes referred to as the stress intensity factor approach.

The crack will propagate when the energy released from the body by crack growth just exceeds the energy required for the creation of new surfaces of the crack [Griffith, (1920)]. This is sometimes referred to as Griffith's energy balance approach.

Criterion (ii) is a necessary but not a sufficient condition, because it implicitly requires criterion (i) to be satisfied simultaneously. In practice however, this distinction proves to be rather academic and criterion (ii) is often more useful because the detailed stress pattern at the tip of a crack is almost impossible to ascertain [Andrews, (1980)]. However criterion (i) can still be used to determine the influence of a notch on the breaking stress of a given material in terms of notch sensitivity.

### 6.1.1.1 Notch sensitivity

Consider a linear elastic plate loaded at infinity with a single edge notch situated midway down one of its sides as shown in the figure below

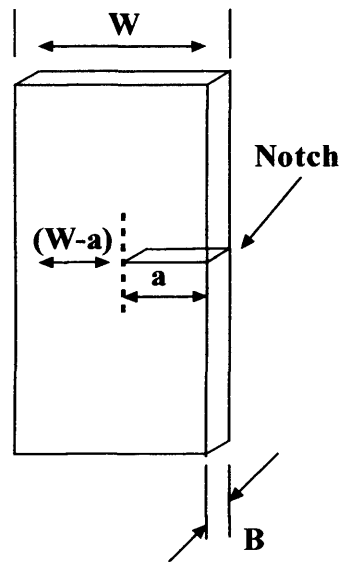


**Figure 6.1:** Schematic drawing of a notched specimen.

The nominal fracture stress,  $\sigma_f$  is normally defined in terms of the original cross sectional area of the specimen and can be expressed as

$$\sigma_f = \frac{F_f}{W.B} \quad (6.1a)$$

where  $F_f$  is the fracture force

The presence of the notch may cause a stress concentration at the tip of the notch. If this stress concentration causes fracture to occur at lower applied stresses compared to the stresses required to fracture a similar un-notched specimen the plate is said to be notch sensitive. On the other hand a notch in a notch-insensitive material reduces the nominal breaking stress only in direct proportion to the reduction in cross-sectional area caused by the presence of the notch [Kelly & Macmillan, (1986)].

The relationship between the nominal fracture stress,  $\sigma_f$ , of a notch insensitive specimen and notch length,  $a$ , is given by

$$\sigma_f = \sigma_{UN} \left[ 1 - \frac{a}{W} \right] \quad (6.1b)$$

where  $\sigma_{UN}$ , is the nominal breaking stress of an un-notched specimen. This means that for a notch insensitive material, if the notch is half way across the width of the specimen, then the strength reduces by a half. On the other hand, for notch sensitive materials, the failure stress,  $\sigma_f$ , falls more steeply with notch length,  $a$ , than is predicted by equation 6.1b. The steeper the fall, the more notch sensitive the material is said to be.

### **6.1.1.2 Stress intensity approach**

The stress intensity factor,  $K$ , is used in fracture mechanics to predict the stress state (“stress intensity”) near the tip of a crack caused by a remote load or residual stresses. When this stress state becomes critical a small crack grows (“extends”) and the material fails. The stress at which this failure occurs is referred to as the fracture strength. The value of the stress intensity factor,  $K$ , is a function of the applied stress, the size and position of the crack as well as the geometry of the solid piece where the cracks are detected. For a crack of length  $2a$  lying perpendicular to the applied stress,  $\sigma$ , in an infinite body, the stress intensity factor is given by

$$K = \sigma \sqrt{\pi a} \quad (6.2)$$

Failure occurs when,  $\sigma = \sigma_c$ , and  $K$  reaches a critical value  $K_{IC}$  (fracture toughness). Apart from a small region at the notch tip, the material is assumed to deform in a linear elastic manner.

### 6.1.1.3 Energy balance approach

A description of the process of fracture in polymers begins with Griffith's theory [Griffith, (1920)], which was originally developed for glasses. The starting point is the need to determine the energy required to form the new surface, which appears as the material cracks. The energy available to form these new surfaces is the difference between the work done on the material and the change in elastically stored energy. Crack extension occurs when the energy available for crack growth is sufficient to overcome the resistance of the material and thus form new crack surfaces. The material resistance may include the surface energy, plastic work, or other type of energy dissipation associated with a propagating crack. In the energy balance approach, the driving force for fracture is normally described in terms of strain energy release rate  $G$ , which is defined as the rate of change in potential energy with crack area for a linear elastic material. For a crack of length  $2a$  lying perpendicular to the applied stress,  $\sigma$ , in an infinite body, the strain energy release rate is given by

$$G = \frac{\pi\sigma^2 a}{E} \quad (6.3)$$

where  $E$  is young's modulus,  $\sigma$  is the remotely applied stress, and  $a$ , is half the crack length. Failure occurs when  $\sigma = \sigma_c$  and  $G$  reaches a critical value  $G_{IC}$  (fracture toughness).

Apart from the results presented later, crack propagation studies in leather had not been done. Fracture toughness characterization for leather is usually reported in terms of the total energy required to break a given leather specimen using a trouser tear test specimen. Total energy to fracture studies [Liu and McClintick, (1997)] performed to model the influence of strain rate, moisture content and sampling angle on fracture energy, indicate that fracture energy at first decreases and then increases with increasing strain rate. The heat generated during high strain rates is believed to have a plastisizing effect on leather fibre bundles thereby increasing the fracture resistance of leather. The sampling angle showed little or no effect on the fracture energy as compared to tensile strength and elongation at break, both of which depend on the

sampling angle. However proper fracture toughness characterization in terms of parameters such as  $K_{IC}$  and  $G_{IC}$  was not done. The fracture parameters  $K_{IC}$  and  $G_{IC}$  are therefore normally used to predict the onset of fracture propagation in engineering materials. Both  $K_{IC}$  and  $G_{IC}$  are independent of size and geometry of the cracked body so that fracture toughness measurement on a laboratory specimen should be applicable to a larger structure.

## **6.1.2 Characterization of fracture in ductile materials**

The theory of LEFM deals with brittle fractures in which very little plastic flow occurs at the tip of the crack. In this case fracture can be characterized in terms of a single parameter such as the critical stress intensity factor,  $K_{IC}$ , or the critical strain energy release rate,  $G_{IC}$ . However, fracture toughness characterization using LEFM becomes difficult when ductile polymers, especially polymer blends with high fracture toughness to yield strength ratios are involved. The formation of a large plastic zone prior to crack initiation violates the limit of small scale yielding which ensures the validity of LEFM. Much of the plastic flow work dissipated in the plastic zone is not directly associated with the fracture process. For ductile materials, two approaches have been used in order to characterize the fracture behaviour, namely the essential work and the J-integral.

### ***6.1.2.1 The J-integral***

In the J-integral approach, elastic-plastic deformation at the crack-tip is normally idealised as non-linear elastic [Rice, (1968)]. This provides the basis for extending fracture mechanics methodology well beyond the validity limits of LEFM. The J-integral has enjoyed great success as a fracture characterizing parameter for many ductile polymers [Williams, (1984)].

Although the theoretical analysis of the J-integral has been well established [Rice (1968), Begley & Landes (1972) and Landes and Begley, (1972)], the size requirements, which guarantee the J-integral to be obtained under plane strain conditions, limit its applicability to fracture toughness characterization of thin

materials. The J integral also has limited validity when a material exhibits rate dependent mechanical properties [Anderson, (1995)]. However a number of researchers [Jones and Bradley (1989), Letton, (1991) and Hashemi and Yuan (1994)] have applied J integral test methods to polymers.

### 6.1.2.2 Essential work of fracture (EWF)

The essential work of fracture concept was originally introduced by Broberg [Broberg, (1968)] and later developed by Cotterell and Mai [Cotterell & Mai, (1984)]. As an alternative to the J-integral analysis, the specific essential work of fracture has been successfully used to determine the fracture toughness of many ductile materials, including many toughened polymer blends [Hashemi, (1993) and Chan & Williams (1994)]. The essential work of fracture (EWF) has since gained widespread acceptance for fracture toughness characterization of materials exhibiting crack tip plastic yielding under plane stress conditions [Hashemi;(1997) and Karger-Kocsis, (1997)]. The EWF approach is described below and the applicability of this approach to leather is also examined. The single edge notch tension (SENT) specimen used in this study is shown in the figure 6.2.

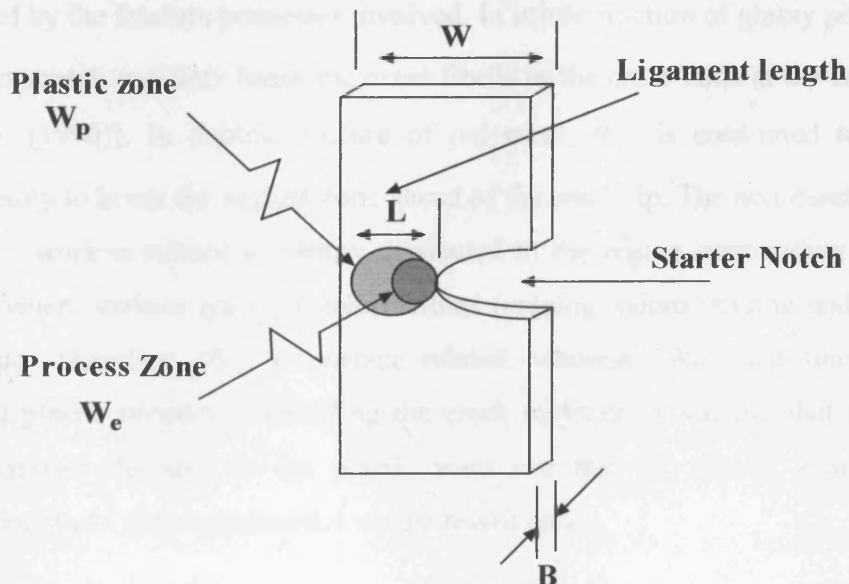


**Figure 6.2:** Schematic drawing of the essential work of fracture SENT specimen showing the process zone and the plastic zone

According to the theory of essential work of fracture, the non-elastic region at the tip of a crack can be divided into two regions [Broberg, (1968)],

- An inner fracture process zone (FPZ)
- An outer plastic deformation zone (PDZ)

During crack propagation, much of the fracture work dissipated in the plastic deformation zone is not directly associated with the fracture process. Only that work which goes directly into the fracture process zone is a material constant and therefore can be considered as a fracture toughness characterization parameter. Hence the total work of fracture  $W_f$ , can be isolated into two terms namely, the essential work of fracture ( $W_e$ ) and the non-essential work of fracture ( $W_p$ ). The essential work of fracture is the energy dissipated in the fracture process zone, whereas the non-essential work of fracture is the energy dissipated in the plastic deformation zone. The total work of fracture can therefore be written as

$$W_f = W_e + W_p \quad (6.4)$$

Physically,  $W_e$ , is the work required to create two new fracture surfaces and is consumed by the fracture processes involved. In brittle fracture of glassy polymers,  $W_e$ , is used to stretch and later break the craze fibrils in the craze zone at the crack tip [Wu and Mai, (1996)]. In ductile fracture of polymers,  $W_e$ , is consumed to form, and subsequently to break the necked zone ahead of the crack tip. The non-essential work or the plastic work is related to energy dissipated in the region surrounding the fracture surfaces where various types of deformations (crazing, micro-voiding and shear) may take place. Therefore ( $W_e$ ) is surface related, whereas ( $W_p$ ) is a function of the deformed plastic volume surrounding the crack surfaces. Assuming that the ligament length controls the size of the plastic zone and that the plastic zone volume is proportional to  $L^2$  then equation 6.4 can be rewritten as

$$W_f = \omega_e LB + \beta \omega_p L^2 B \quad (6.5)$$

in which  $\omega_e$  is the specific essential work of fracture (work done per unit area LB of new fracture surfaces) and  $\omega_p$  is the specific plastic work of fracture, L is the ligament length B is the specimen thickness and  $\beta$  is the shape factor whose value is related to the shape of the plastic zone. Equation 6.5 can be expressed in terms of the specific total work of fracture as

$$\omega_f = \frac{W_f}{LB} = \omega_e + \beta\omega_p L \quad (6.6)$$

Thus if the specific total work of fracture  $\omega_f$  is plotted against the ligament length, a linear relation should be obtained which when extrapolated to zero ligament length should give the specific essential work of fracture  $\omega_e$ . On the other hand the slope ( $\beta\omega_p$ ) of the linear relation gives  $\omega_p$  provided the shape of the plastic zone,  $\beta$  is well defined. The EWF procedure is therefore a simple method that consists of testing different ligament length specimens, registering  $W_f$  for each from the area under the load displacement curve, plotting  $\omega_f$  versus L and then calculating the best fit regression line which gives  $\omega_e$  and  $\beta\omega_p$ . Both single edge notch tension (SENT) and double edge notch tension (DENT) specimens have been successfully used.

As already mentioned, equation 5.6 assumes that the ligament length, L controls the size of the plastic zone and that the volume of this zone is proportional to  $L^2B$  with the shape factor  $\beta$  being the proportionality constant. This proportionality constant may be affected in two ways [Hashemi, (1997)];

Firstly if L is not small compared to the total width of the sample, then the size of the plastic zone can be disturbed by edge effects. To avoid edge effects it is recommended that L should be kept below  $W/3$ . Secondly, if the ligament length were larger than twice the radius of the plastic zone around the crack tip then the ligament area would not yield completely at failure. Under this condition L will not control the size of the plastic zone. In order to avoid this problem it is proposed that L should be smaller than the minimum of the following two criteria:

$$L \leq W/3 \text{ and } L \leq 2r_p \quad (6.7)$$

Where  $r_p$  is the radius of the plastic zone.

Finally the size of test specimen must be chosen such that  $\omega_e$ ,  $\omega_p$  and  $\beta$  are independent of  $L$ . To achieve this, the state of pure stress must always exist in the specimen and this imposes a lower limit on the size of ligament length, which is governed by the specimen thickness,  $B$ . It has been shown [Mai and Cotterell, (1985)] that for ligament lengths smaller than  $3B$ , transition from pure plane stress fracture to mixed mode fracture may be expected, giving rise to a non-linear relationship between  $\omega_f$  and  $L$  due to increasing plastic flow constraint with decreasing ligament length. It is therefore suggested that in order to meet the practical requirements, fracture specimens must satisfy the following size criterion:

$$3B \leq L \leq \min(W/3, 2r_p) \quad (6.8)$$

However there is still some controversy over the conditions under which the essential work of fracture is applicable as imposed by specimen geometry requirements. The restriction imposed on the ratio of  $L/B$  has been found to depend on the material. In toughened polymer blends for example, the relationship between  $\omega_f$  and  $L$  remains unchanged in the entire ligament length. These results indicate that there may not exist a universal ligament length range for which the transition from plane stress to plane strain occurs and the actual ratio  $L/B$  at which the mode transition occurs may depend on the nature of the material being tested, for instance, how sensitive the material is to plastic constraint to which it is subjected [Wu and Mai, (1996)].

The pre-requisite that the essential work of fracture is applicable when the ligament length further satisfies the condition,  $L \leq \min(W/3, 2r_p)$ , relates to the plastic deformation zone surrounding the fracture process zone. Previous studies on polycarbonate films [Hashemi, (2000)] showed no evidence of non-linearity for ligament lengths exceeding  $W/3$  leading to the conclusion that the pre-requisite  $L \leq W/3$  is too restrictive. This was thought to be due to the tendency of the yielded zone to remain localised because of the strain softening in polycarbonate films during the

yielding process. Similar observations have been reported in isotactic polypropylene [MasPOCH et al (1999)].

Essential work of fracture parameters can be determined using SENT specimens. However another interesting approach is one that correlates tear strength with,  $\omega_e$  and  $\omega_p$ . Both these can be deduced from trouser tear tests that have been successfully applied to thin polymer films [Karger, (1996)].

### **6.1.3 Tear behaviour**

The study of tear characteristics of leather is important because a common mode of mechanical failure of footwear and clothing in service is a tearing of some form. It has been generally accepted that the loads required to initiate or propagate a tear or the maximum tearing load are measures of the tear resistance of the material [Guy and Marriott, (1974)]. Since a tearing load of some form has been generally accepted as a measure of tear resistance, most work to date has been concerned with correlating the tearing loads obtained from various tests for the same range of materials.

#### ***6.1.3.1 Tear specimen geometry***

A variety of specimen shapes are used by the leather industry to evaluate the tear characteristics of leather. The trouser tear test whose geometry is shown in the figure 6.3 was however preferred because it is also used to characterize fracture resistance of polymeric materials.

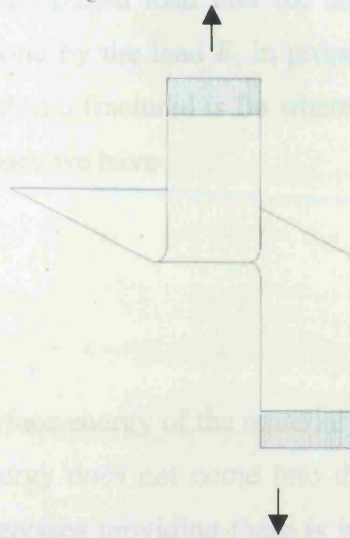


**Figure 6.3:** Schematic drawing of the mode III trouser tear test.

During tearing experiments, the load is applied at a constant rate of specimen extension. The total tearing energy is the sum of the energy required to initiate the tear and the energy required to propagate the tear. The energy required to propagate the tear is dependent on the distance travelled by the tear. However studies from several test specimen shapes have shown that the tearing energy is independent of specimen geometry but markedly dependent on the diameter of the crack tip [Guy and Marriott, (1974)]. The ratio of tearing energy to the diameter of the crack tip is however approximately constant [Rivlin & Thomas (1953)].

### 6.1.3.2 Tear test fracture toughness evaluation

According to Kendall and Fuller [Kendall and Fuller, (1987)], fracture resistance of non-linear materials can be judged on the basis of either of fracture surface energy criterion or energy stored at fracture. If the fracture resistance of biological materials is judged by fracture surface energy criterion then their toughness is not particularly great, with fracture energies only in the range of (1-20kJ/m<sup>2</sup>) [Mai and Atkins, (1989)]. The theory of fracture mechanics suggests that for brittle substances fracture surface energy provides a fundamental measure of the resistance to cracking which is independent of test geometry and shape of the stress-strain curve. However the trouser tear test does

not significantly depend upon the elastic properties of the material, merely converting the potential energy of the applied load into the surface energy of the crack. Thus during tearing the work done by the load  $F$ , in propagating the crack a distance,  $a$ , is  $2Fa$  and the area of the material fractured is  $Ba$  where  $B$  is the thickness. Balancing the potential and surface energies we have

$$F = \frac{BR}{2} \quad (6.9)$$

where  $R$  is the fracture surface energy of the material identical to the fracture toughness of the material. Strain energy does not come into this calculation because it remains constant as the crack progresses providing there is insignificant extension of the legs. This is true whatever the shape of the stress strain curve. Therefore a J-shaped or r-shaped stress-strain curve will not influence the tearing force.

### ***6.1.3.3 Correlation between fracture toughness tests***

Since different tests give different fracture toughness values for a given material, it is essential that the tests correlate well and measure the same fundamental property of the material, if the results are to be used as alternatives. A correlation between various fracture toughness parameters is essential in tailoring tannery processes to produce leather having both good tensile strength and tear strength. Previous studies [Liu & McClintick, (1997)] on the relationship between tensile strength and tear strength, indicate that tear strength shows little variation with change in sampling angle whereas tensile strength shows a maximum for samples cut parallel to the backbone line and then steadily decreases when sampling angle increases from the backbone line. However a qualitative relationship between tear strength and tensile strength was not established in these studies.

In the SENT and DENT specimens used in this study, stresses were applied in the plane of the specimen (mode I) whereas in the trouser tear test, the tearing forces  $F$ , are applied out of the plane of the specimen (mode III). It has been shown [Isherwood & Williams, (1978) and Mai & Cotterell, (1984)] that in the absence of plastic work in the

legs, the relationship between the tearing force,  $F$ , and the thickness of the specimen,  $B$ , may be expressed as

$$F = \omega_p B^2 \quad (6.10)$$

where  $\omega_p$  is the energy to fracture. To obtain  $\omega_p$  a series of trouser tear tests are carried out at a constant rate of testing for specimens of varying thickness. If the tearing force is then plotted against the square of the thickness, a line graph is obtained whose gradient yields the value of  $\omega_p$ . Assuming no stretching or bending of the arms, then for a two-leg trouser-tearing test, mode III fracture toughness  $R$ , is then given by

$$R = \frac{2F}{B} = \omega_{IIIe} \quad (6.11)$$

Equation 6.10 and 6.11 can be combined to give

$$\omega_{IIIe} = \frac{F}{B^2} = 2\omega_p B \quad (6.12)$$

In polycarbonate films, the fracture toughness values obtained from mode I SENT and DENT specimens were observed to be much higher than the fracture toughness values obtained from mode III trouser tear tests [Hashemi, (1993)].

## 6.2 EXPERIMENTAL PROCEDURE FOR THIS WORK

### 6.2.1 Materials

The material used in this work was wet blue chrome tanned bovine hide supplied by a UK tannery. Rectangular pieces of dimensions (150 mm x 300 mm) were cut out as described in section 3.1.1 and then split along the corium grain boundary to a thickness of about 1 mm. The split samples were then clamped in specially constructed plates (150 mm wide) mounted on the jaws of an Instron 1122 testing machine, housed in a room conditioned at 65% RH and 20°C. They were then stretched at a rate of

100mm/min to 15%, 20% and 30% strain along their length and held in this state for 24hrs to dry. On release the material was found to have retained the strain imparted during drying. After drying the samples were conditioned for 48 hrs before performing crack propagation tests. This procedure was repeated at 15%, 20% and 30% biaxial strains for the fatliquored and non-fatliquored samples.

## **6.2.2 Crack propagation tests**

Fracture propagation studies were performed using single edge notched tension (SENT) specimens as shown in Figure 6.1. Rectangular strips of dimensions 16 mm x 80mm were prepared and notched to different ligament lengths,  $L$ . The notches were made using specially prepared rectangular dies having different notch lengths. After notching, specimens were tested to complete failure in the Instron testing machine at room temperature and at a speed of 10mm/min. Load displacement curves were recorded automatically on a chart recorder and the load displacement values logged on a personal computer. Some samples were stamped with a rectangular grid of 1 mm squares and the deformation of the grid in tension examined with the aid of Prior scientific stereo microscope placed on its side.

## **6.3 RESULTS AND DISCUSSION**

### **6.3.1 Effect of uniaxial stretching on (EWF)**

Figure 6.4(a) shows the variation of specific work of fracture  $\omega_f$ , with ligament length  $L$  for both control and experimental (dried at 30% uni-axial strain) SENT specimens tested for cracking normal to pre-stretch axis.

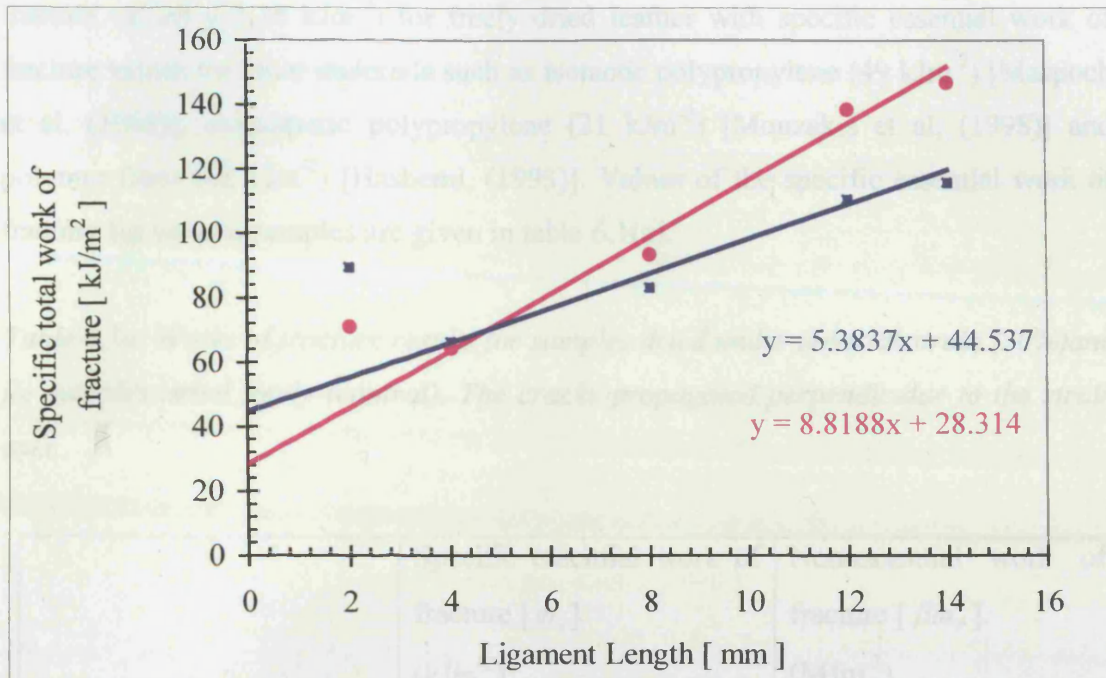


**Figure 6.4(a):** Specific total work of fracture versus ligament length for both unstretched control (circles) and uniaxially stretched (squares) SENT specimens. (tested For crack propagation across the pre-strain axis)

It is evident from this figure that the relationship between specific work of fracture  $\omega_f$  and ligament length  $L$ , is essentially linear with some deviation occurring at small values of  $L$ . Equations of linear regression lines fitted through the linear part of the data for each curve give the specific essential work of fracture  $\omega_e$ , for control and experimental samples as  $28.3 \text{ kJm}^{-2}$  and  $44.5 \text{ kJm}^{-2}$  respectively as determined from the y-intercept of these curves. The specific essential work of fracture and hence the fracture toughness of the experimental samples is higher than the fracture toughness of the control samples. This can be explained in terms of the number of fibres that are involved in the fracture process.

When calculating specific essential work of fracture values, data for the ligament lengths  $L < 4 \text{ mm}$ , were discounted. The justification for this was that at the shortest ligament length of  $2 \text{ mm}$ , the stress field was likely to have been distorted by edge effects thereby giving unreliable results. Apart from these discrepancies the results show excellent conformity to the theoretical expectations thus giving essential work of fracture values that appear reasonable. It is interesting to compare essential work of

fracture values (22-28  $\text{kJm}^{-2}$ ) for freely dried leather with specific essential work of fracture values for other materials such as isotactic polypropylene (49  $\text{kJm}^{-2}$ ) [MasPOCH et al, (1998)], elastomeric polypropylene (21  $\text{kJm}^{-2}$ ) [Mouzakis et al, (1998)] and polymer films (62  $\text{kJm}^{-2}$ ) [Hashemi, (1993)]. Values of the specific essential work of fracture for various samples are given in table 6.1(a).

**Table 6.1a:** Works of fracture results for samples dried under uniaxial strain (30%) and for samples dried freely (control). The cracks propagated perpendicular to the strain axis.

	Specific essential work of fracture [ $\omega_e$ ]. ( $\text{kJm}^{-2}$ )	Non-essential work of fracture [ $\beta\omega_p$ ]. ( $\text{MJm}^{-3}$ )
Uniaxially stretched (30%) during drying	44.5	5.4
Control for uniaxial samples	28.3	8.8

It can be seen that the degree of uniaxial stretching applied during drying increases the essential work of fracture by 57% for crack propagation across the stretch axis.

### 6.3.2 Effect of biaxial stretching on EWF

Figure 6.4(b) is a plot of the specific total work of fracture against ligament length for samples dried under 30% biaxial strains together with the corresponding control samples dried freely. Here all the data (parallel and perpendicular directions) conform to the expected straight line relationship. Thus the specific essential work of fracture can be used to calculate the fracture resistance of leather.

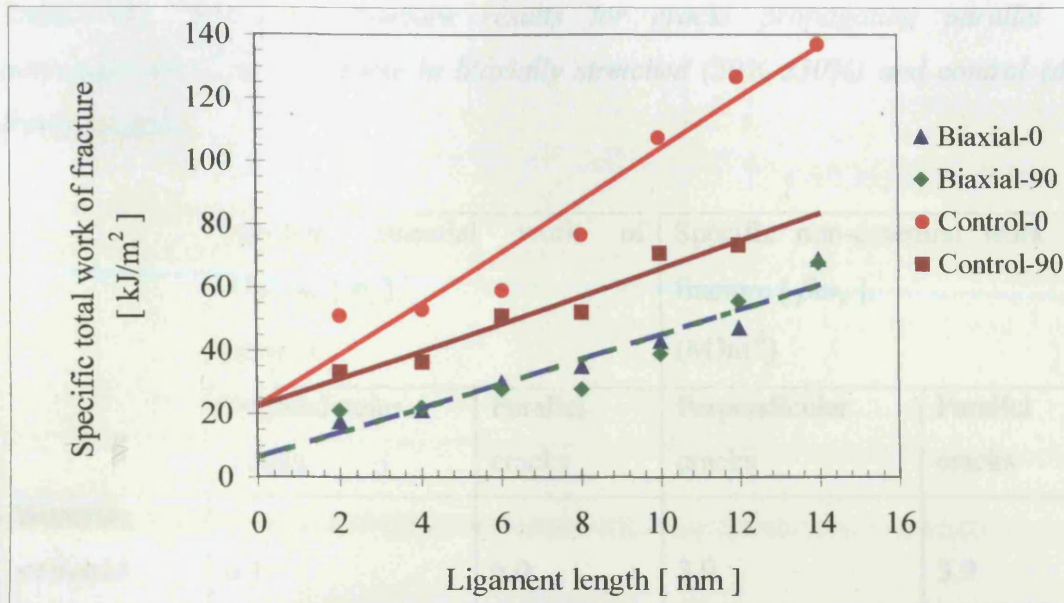


**Figure 6.4(b):** Specific total work of fracture versus ligament length for unstretched control and biaxially stretched SENT specimens. Specimens were tested parallel ( $0^\circ$ ) and perpendicular ( $90^\circ$ ) to the backbone

Table 6.1(b) shows the effect of drying under biaxial strain (30% $\times$ 30%) on the specific works of fracture. It can be seen that the degree of biaxial stretching used in these experiments has acted to reduce the specific essential work of fracture by some 73%.

Figure 6.3(a) shows the specific total work of fracture versus ligament length for both non-ligamented samples and biaxially stretched (30% strain) ligamented SENT samples for cracks propagating perpendicular to the stretch direction applied during drying. The values for specific essential work of fracture and the non-essential work of fracture obtained from Figure 6.3(a) are given in table 6.1(a). It can be seen that the specific essential work of fracture (17 kJ/m<sup>2</sup>) for the ligamented and then stretched samples is greater than the specific essential work of fracture (30 kJ/m<sup>2</sup>) for the unstretched and non-ligamented samples. It is also evident that the non-essential work of fracture (2.5 kJ/m<sup>2</sup>) for the ligamented and stretched samples is greater than the non-essential work of fracture (0.5 kJ/m<sup>2</sup>) for unstretched and non-ligamented samples.

**Table 6.1b:** Works of fracture results for cracks propagating parallel and perpendicular to the backbone in biaxially stretched (30% x30%) and control (dried freely) samples

	Specific essential work of fracture [ $\omega_e$ ]. (kJm <sup>-2</sup> )		Specific non-essential work of fracture [ $\beta\omega_p$ ]. (MJm <sup>-3</sup> )	
	Perpendicular cracks	Parallel cracks	Perpendicular cracks	Parallel cracks
Biaxially stretched during drying	6.1	6.0	3.9	3.9
Control samples dried freely	22.6	22.4	8.1	4.4

### 6.3.3 Effect of fatiguors on EWF

Figure 6.5(a) shows the specific total work of fracture versus ligament length for both non fatliquored samples and uniaxially stretched (30% strain) fatliquored SENT samples for cracks propagating perpendicular to the stretch direction applied during drying. The values for specific essential work of fracture and the non-essential work of fracture obtained from figure 6.5(a) are given in table 6.2(a). It can be seen that the specific essential work of fracture (47 kJm<sup>-2</sup>) for the fatliquored and then stretched samples is greater than the specific essential work of fracture (30 kJm<sup>-2</sup>) for the unstretched and non-fatliquored samples. It is also evident that the non-essential work of fracture (8.5 MJm<sup>-3</sup>) for the fatliquored and stretched samples is greater than the non-essential work of fracture (6.7 MJm<sup>-3</sup>) for unstretched and non-fatliquored samples.

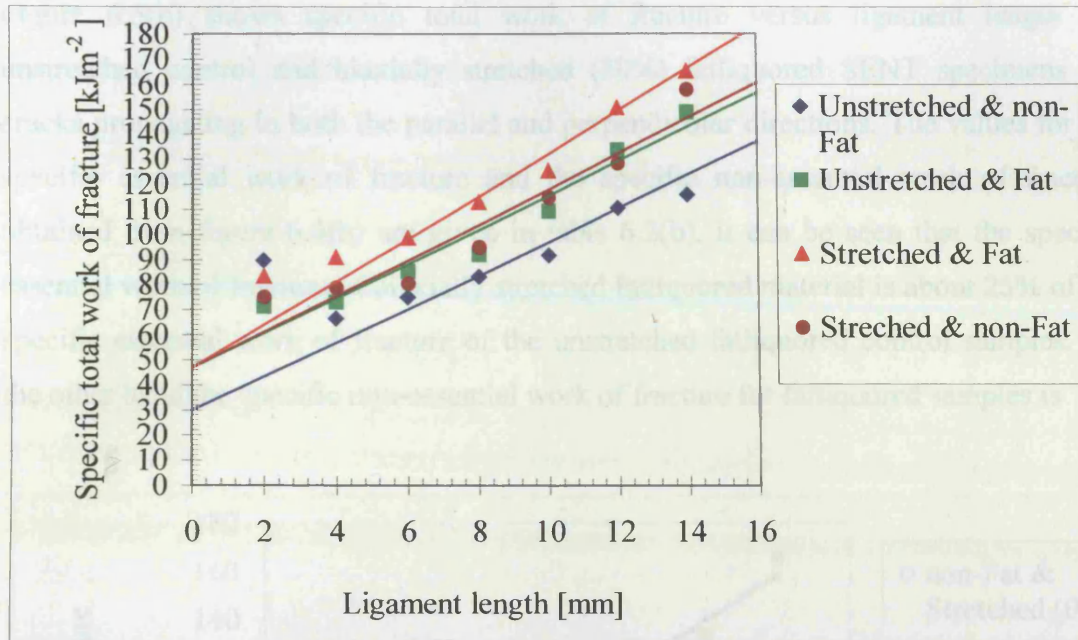


**Figure 6.5a:** Specific total work of fracture versus ligament length for unstretched control and uniaxially stretched (30%) fatlioured SENT specimens for cracks propagating perpendicular to the stretch axis

**Table 6.2(a):** Specific essential work of fracture (EWF) and specific non-essential work of fracture for fatlioured and non-fatlioured samples

	Specific essential work of fracture [ $\omega_e$ ]. (kJm <sup>-2</sup> )	Non-essential work of fracture [ $\beta\omega_p$ ]. (MJm <sup>-3</sup> )
Unstretched and Fatlioured	47	6.8
Fatlioured and then dried Stretched at 30% uniaxial strain	47	8.5
Unstretched and non-Fatlioured	30	6.7
non-Fatlioured and dried Stretched at 30% uniaxial strain	47	7.1

Figure 6.5(b) shows specific total work of fracture versus ligament length for unstretched control and biaxially stretched (30%) fatliquored SENT specimens for cracks propagating in both the parallel and perpendicular directions. The values for the specific essential work of fracture and the specific non-essential work of fracture obtained from figure 6.4(b) are given in table 6.2(b). It can be seen that the specific essential work of fracture of biaxially stretched fatliquored material is about 25% of the specific essential work of fracture of the unstretched fatliquored control samples. On the other hand the specific non-essential work of fracture for fatliquored samples is

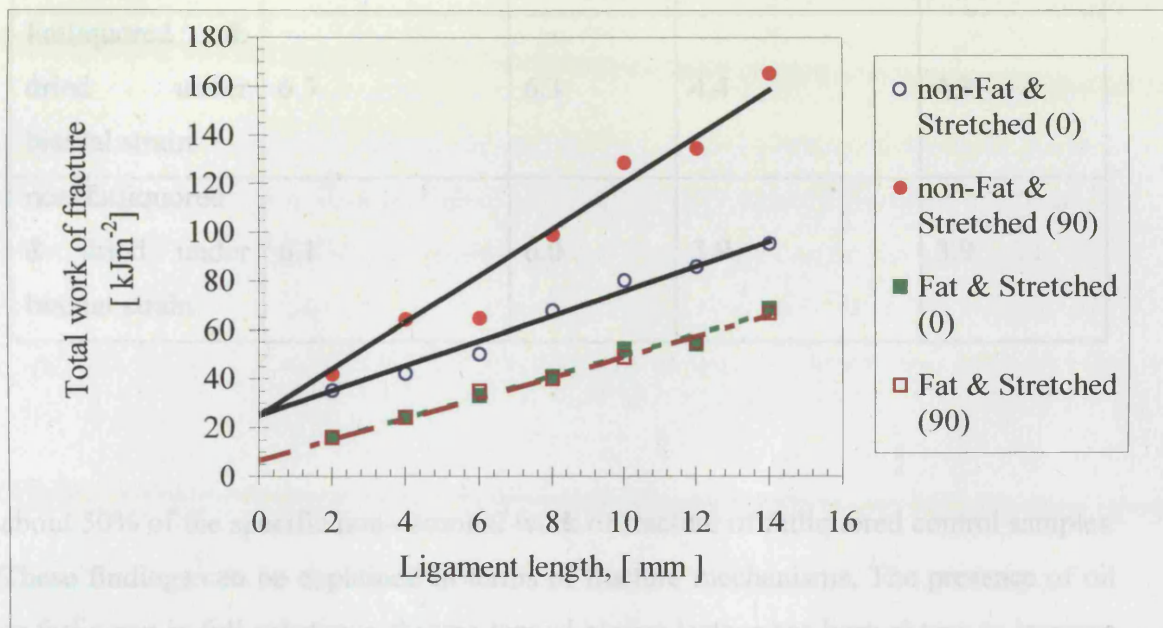


**Figure 6.5b:** Total specific work of fracture versus ligament length for non-fatliquored and biaxially stretched fatliquored SENT specimens for cracks propagating parallel ( $0^\circ$ ) and perpendicular ( $90^\circ$ ) to the backbone

**Table 6.2(b): Specific essential and non-essential work of fracture for fatliquored and non-fatliquored samples with and without biaxial stretching (30% biaxial strains)**

	Specific essential work of fracture [ $\omega_e$ ]. (kJm <sup>-2</sup> )		Specific non-essential work of fracture [ $\beta\omega_p$ ]. (MJm <sup>-3</sup> )	
	Perpendicular	Parallel	Perpendicular	Parallel
Fatliquored & dried freely	25.0	25.0	9.5	5.1
Fatliquored & dried under biaxial strain	6.3	6.3	4.4	4.3
non-fatliquored & dried under biaxial strain	6.1	6.0	3.9	3.9

about 50% of the specific non-essential work of fracture of fatliquored control samples. These findings can be explained in terms of fracture mechanisms. The presence of oil or fatliquors in full substance chrome tanned bovine leather has been shown to increase tensile strength by 42% and elongation at break by 34% [Mattei and Roddy, (1957)]. These effects were attributed to an increase in fibre mobility as a direct consequence of the presence of fatliquors, which are believed to reduce friction between the fibres and thus making it easier for them to slide past each other in response to applied stresses.

In the grain material, the presence of fatliquor was observed to increase [O'Leary and Attenburrow, (1995)] the nominal stress at rupture for specimens parallel to the backbone by 30% and for specimens perpendicular to the backbone by 21%. The nominal strain at rupture was also observed to increase by 27% and by 32% for parallel and perpendicular specimens respectively. Fatliquors are added to leather for similar reasons as the addition of plasticisers to polymers. Plasticisers are added to polymers in order to improve their flow properties [Higgins, (1991)]. Oil increases the flow

characteristics of leather by filling the spaces between the network structure thus preventing fibre adhesions as well as providing some lubrication between adjacent fibrous units, processes which facilitate high levels of fibre mobility.

### 6.3.4 Effect of applied strain on EWF

Figure 6.6(a) shows essential work of fracture versus the strain applied during drying. The essential work of fracture is sensitive to the type of the stresses applied to leather while wet. When tensile uniaxial strains are applied during drying the essential work of fracture remains constant for strains up to 15% and then increases sharply by about 50% when the strain is increased by a further 15%. The reverse happens when leather is dried under the action of biaxial strains. In this case the essential work of fracture remains constant up to 15% and then drops sharply by about 50% when the strain is increased by a further 15%. It therefore appears that leather can be stretched up to 15% by either uniaxial strains or biaxial strains without necessarily affecting quality. Any strains above 15% increases the EWF in the case of uniaxial strains and decreases the EWF in the case of biaxial strains.

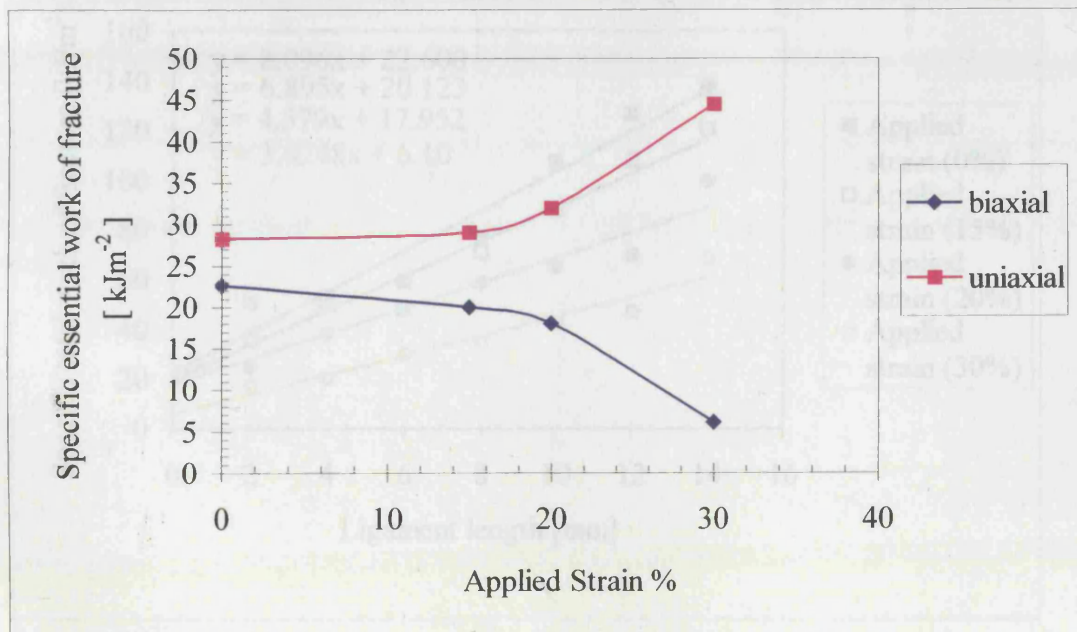


**Figure 6.6(a):** Specific essential work of fracture versus the the strain applied during drying for uniaxially and biaxially stretched leather.

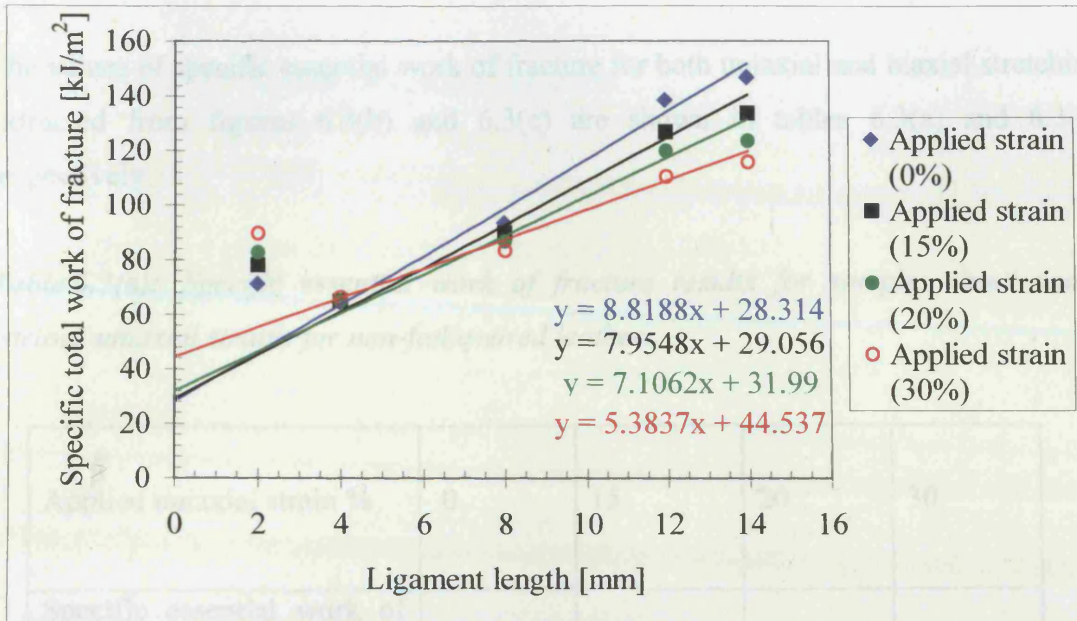


**Figure 6.6(b):** Specific total work of fracture versus ligament length for SENT samples; uniaxially stretched and dried under varying strain levels. Cracks propagated perpendicular to the stretch axis.

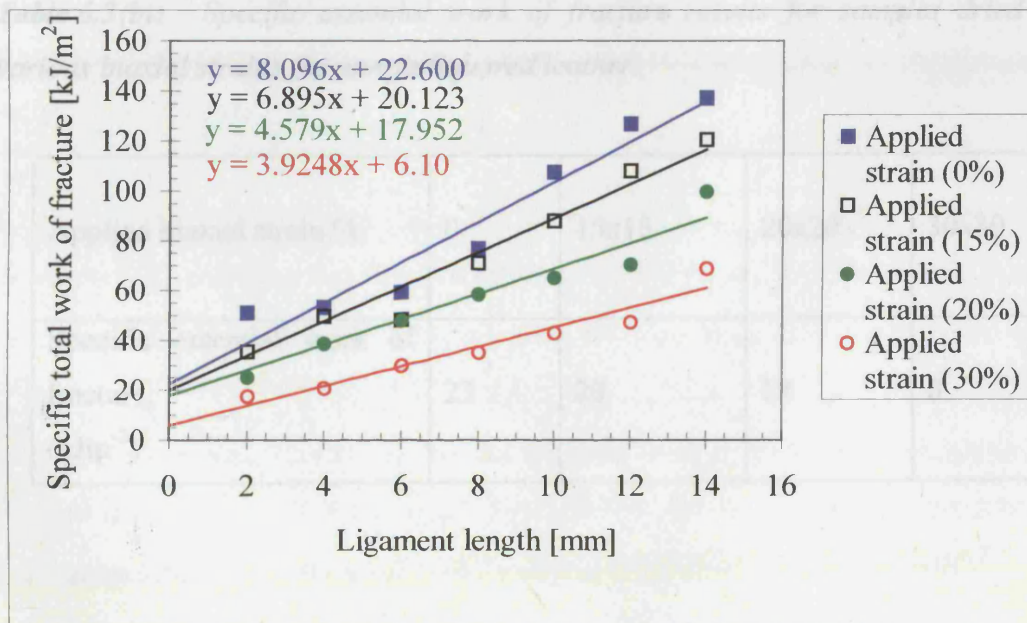


**Figure 6.6(c):** Specific total work of fracture versus ligament length for SENT samples; biaxially stretched and dried under varying strain levels. Specimens were tested parallel (0°) to the backbone

The values of specific essential work of fracture for both uniaxial and biaxial stretching extracted from figures 6.3(b) and 6.3(c) are shown in tables 6.3(a) and 6.3(b) respectively.

**Table 6.3(a):** *Specific essential work of fracture results for samples dried under various uniaxial strains for non-fatliquored leather.*

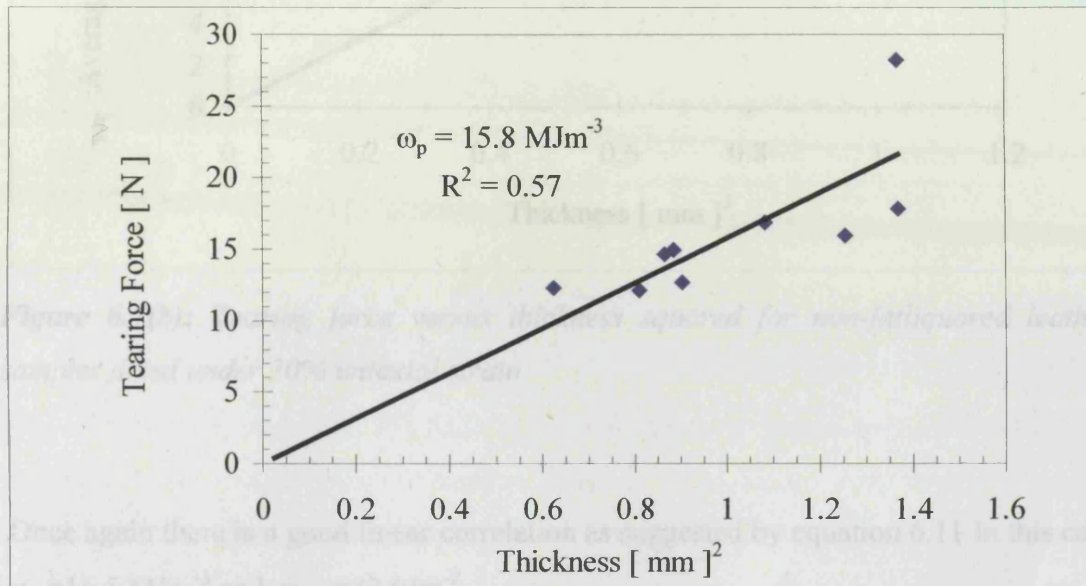
Applied uniaxial strain %	0	15	20	30
Specific essential work of fracture. (kJm <sup>-2</sup> )	28	29	32	45

**Table 6.3(b):** *Specific essential work of fracture results for samples dried under various biaxial strains for non-fatliquored leather.*

Applied biaxial strain %	0	15x15	20x20	30x30
Specific essential work of fracture. (kJm <sup>-2</sup> )	23	20	18	6

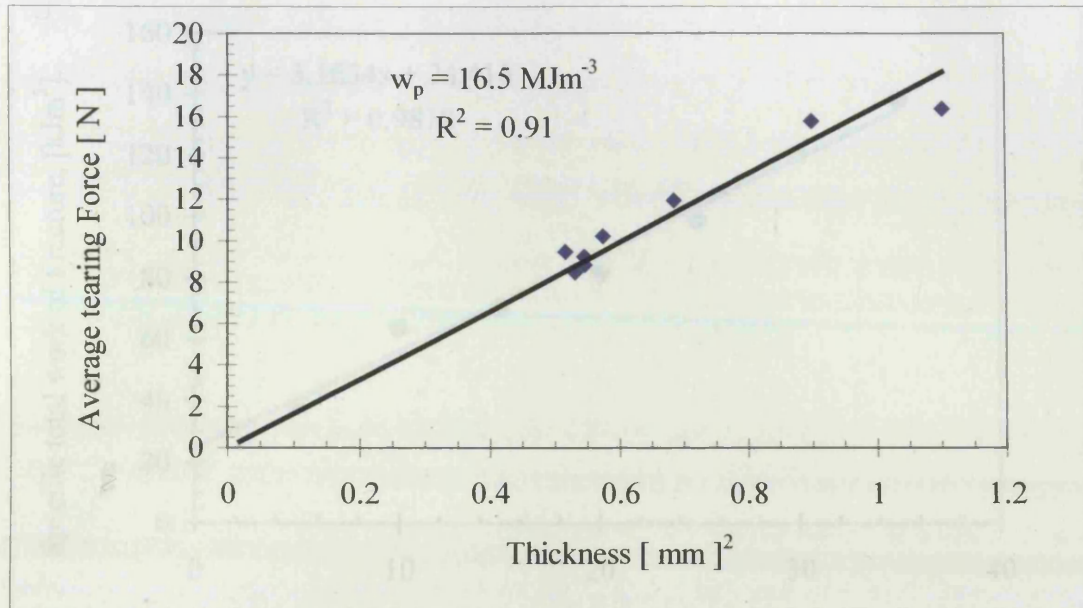
### 6.3.5 Fracture toughness from tear tests

Figure 6.7(a) shows the dependence of tearing force on thickness squared for trouser tear specimens obtained from control samples (dried freely).



**Figure 6.7(a):** Tearing force versus ligament thickness squared for control trouser tear samples dried freely.

Clearly the results show that there is a fairly good linear correlation as suggested by equation 6.12 and from the slope of this line we obtain  $\omega_p = 15.8 \text{ MJ m}^{-3}$ . Assuming no stretching, or bending of the arms, then from equation 6.12 we find the work of fracture  $\omega_{IIIe} = 31.6 \text{ B}$ . Most of the samples used in these investigations had an average thickness of  $\sim 1 \text{ mm}$ . This means that the essential work of fracture for leather using this method is given by  $\omega_{IIIe} = 31.6 \text{ kJm}^{-2}$ . Figure 6.7(b) shows a similar plot for trouser tear specimens obtained from experimental samples dried at 30% uniaxial strain.



**Figure 6.7(b):** Tearing force versus thickness squared for non-fatigued leather samples dried under 30% uniaxial strain

*Fig. 6.7(b): Specific work of fracture versus ligament length of SENT specimens obtained from non-fatigued leather samples dried under 30% uniaxial strain*

Once again there is a good linear correlation as suggested by equation 6.11 In this case  $\omega_p = 16.5 \text{ MJm}^{-3}$  and  $\omega_{lle} = 33 \text{ kJm}^{-2}$ .

### 6.3.6 Effect of specimen size and geometry

Figures 6.8(a) and 6.8(b) shows plots of the specific work of fracture,  $\omega_f$  versus ligament length, L for both SENT and DENT specimens respectively tested at  $10 \text{ mm}(\text{min})^{-1}$ . These plots show that the relationship between  $\omega_f$  and L is essentially linear. Equations of linear regression lines fitted to the data give  $\omega_e = 24.4 \text{ kJm}^{-2}$  for SENT specimens and  $\omega_e = 22.5 \text{ kJm}^{-2}$  for DENT specimens.

*Ligament Length [mm]*

*Figure 6.8(b): Specific work of fracture versus ligament length of DENT specimens obtained from non-fatigued leather samples dried under 30% uniaxial strain (B=1.45mm, W=50mm, H=70mm)*

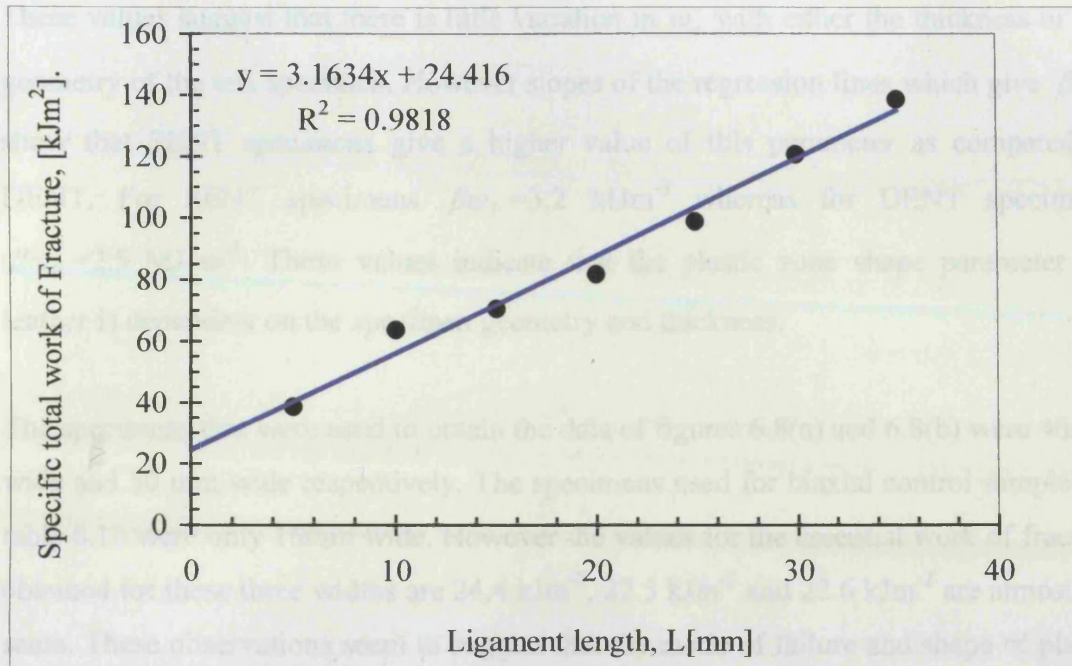


**Fig. 6.8(a):** Specific work of fracture versus ligament length of SENT specimens obtained from non-fatigued leather samples dried under 30% uniaxial strains [B=1.5mm, W=40mm, H=70mm].

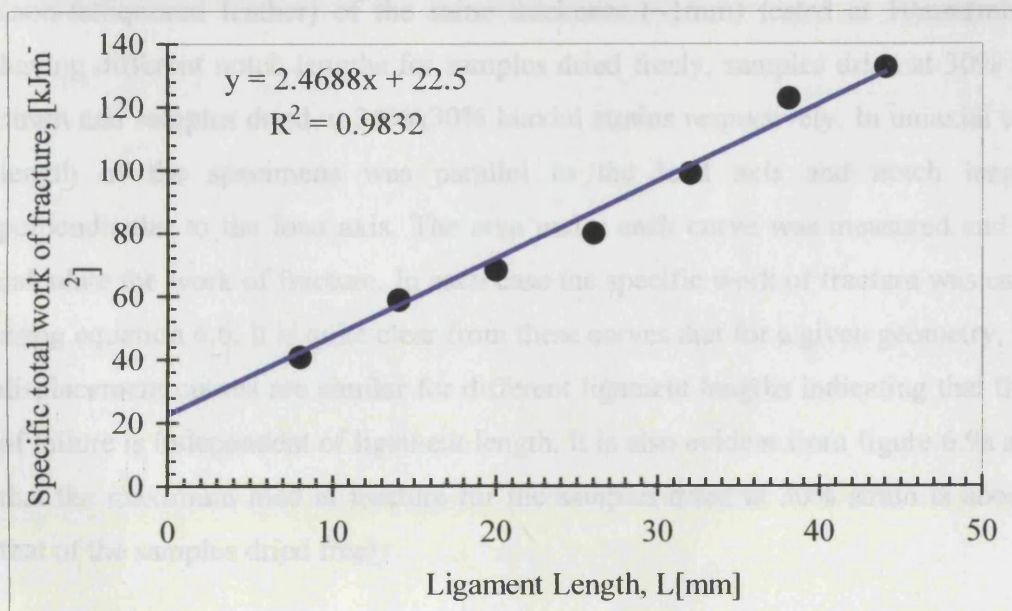


**Figure 6.8(b):** Specific work of fracture versus ligament length of DENT specimens obtained from non fatigued leather samples dried under 30% uniaxial strains [ B=1.45mm, W=50mm, H=70mm].

These values suggest that there is little variation in  $\omega_e$  with either the thickness or the geometry of the test specimen. However slopes of the regression lines which give  $\beta\omega_p$  show that SENT specimens give a higher value of this parameter as compared to DENT. For SENT specimens  $\beta\omega_p=3.2 \text{ MJm}^{-3}$  whereas for DENT specimens  $\beta\omega_p=2.5 \text{ MJ m}^{-3}$ . These values indicate that the plastic zone shape parameter for leather is dependent on the specimen geometry and thickness.

The specimens that were used to obtain the data of figures 6.8(a) and 6.8(b) were 40mm wide and 50 mm wide respectively. The specimens used for biaxial control samples of table 6.1b were only 16mm wide. However the values for the essential work of fracture obtained for these three widths are  $24.4 \text{ kJm}^{-2}$ ,  $22.5 \text{ kJm}^{-2}$  and  $22.6 \text{ kJm}^{-2}$  are almost the same. These observations seem to suggest that the mode of failure and shape of plastic zone surrounding the crack tip are not influenced by the width of the test specimen.

### **6.3.7 Load displacement curves**

Figures 6.9a to 6.9c are typical load versus displacement curves for SENT specimens (non-fatigued leather) of the same thickness ( $\sim 1\text{mm}$ ) tested at  $10\text{mm}(\text{min})^{-1}$  and having different notch lengths for samples dried freely, samples dried at 30% uniaxial strain and samples dried at 30% $\times$ 30% biaxial strains respectively. In uniaxial tests, the length of the specimens was parallel to the load axis and notch length was perpendicular to the load axis. The area under each curve was measured and used to calculate the work of fracture. In each case the specific work of fracture was calculated using equation 6.6. It is quite clear from these curves that for a given geometry, the load displacement curves are similar for different ligament lengths indicating that the mode of failure is independent of ligament length. It is also evident from figure 6.9a and 6.9b that the maximum load at fracture for the samples dried at 30% strain is about twice that of the samples dried freely.

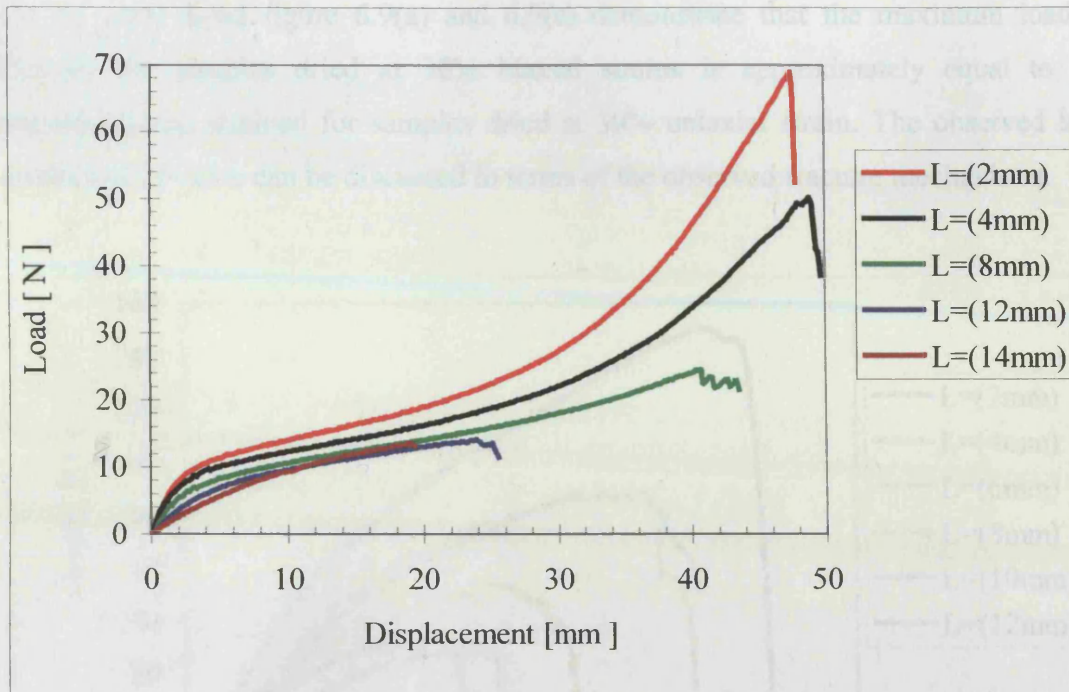


**Figure 6.9(a):** Load displacement curves for control SENT specimens dried without constraint for various ligament lengths,  $L$

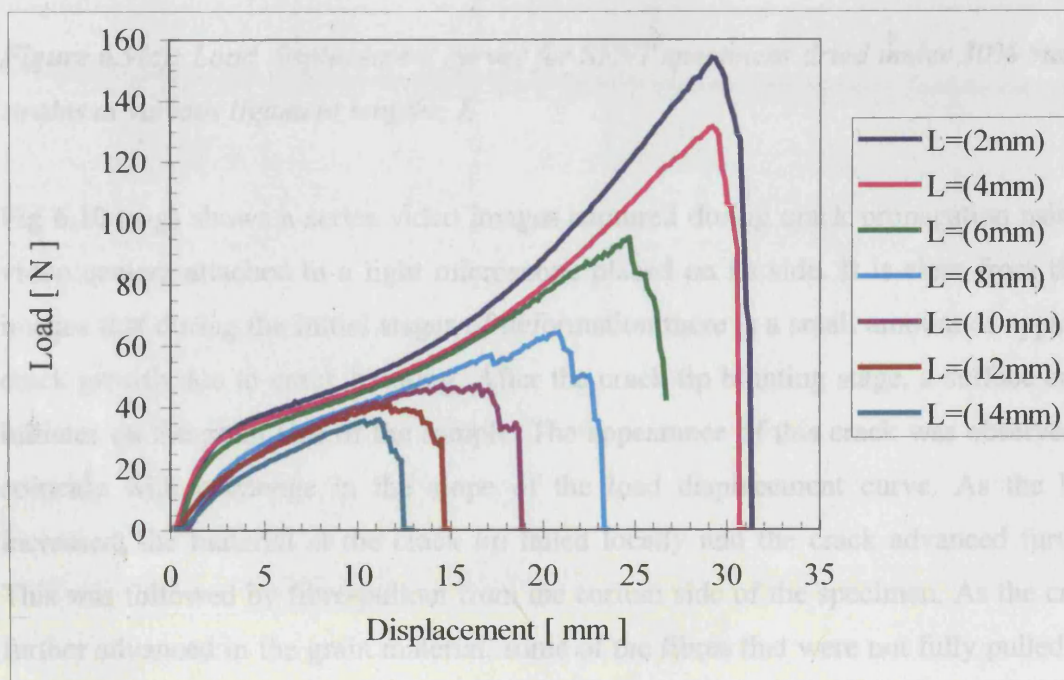


**Figure 6.9 (b):** Typical load displacement curves for SENT specimens dried at 30% uniaxial strain at various ligament lengths,  $L$ .

On the other hand figure 6.9(a) and 6.9(c) demonstrate that the maximum load at fracture for samples dried at 30% biaxial strains is approximately equal to the maximum load attained for samples dried at 30% uniaxial strain. The observed load displacement curve can be discussed in terms of the observed fracture mechanisms.

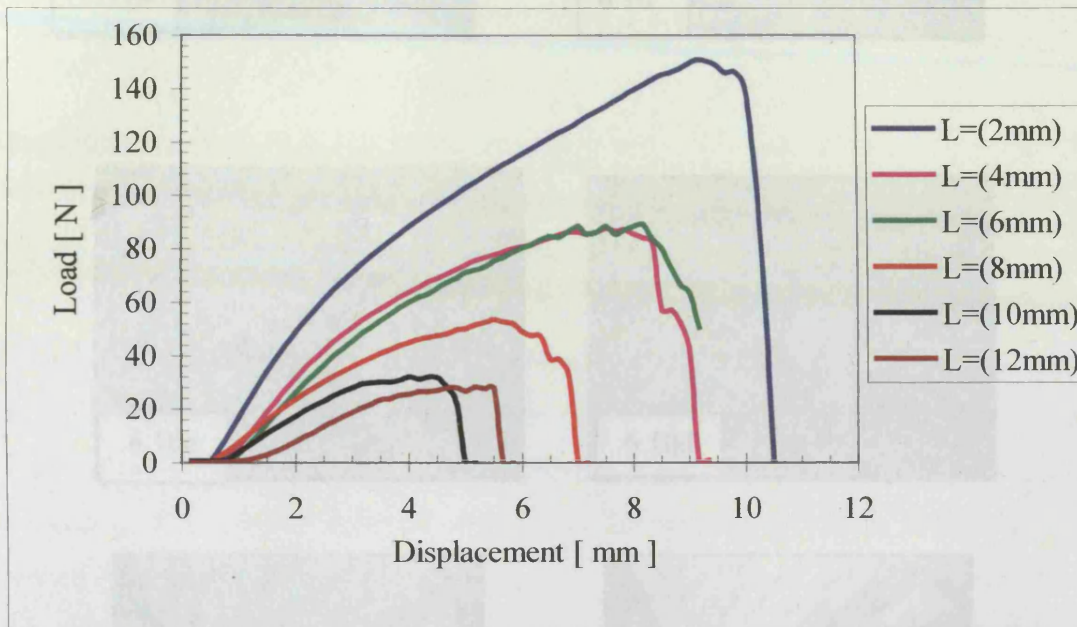


**Figure 6.9(c):** Load displacement curves for SENT specimens dried under 30% biaxial strains at various ligament lengths,  $L$

Fig 6.10 (a-g) shows a series video images captured during crack propagation using a video camera attached to a light microscope placed on its side. It is clear from these images that during the initial stages of deformation there is a small amount of apparent crack growth due to crack blunting. After the crack tip blunting stage, a surface crack initiates on the grain side of the sample. The appearance of this crack was observed to coincide with a change in the slope of the load displacement curve. As the load increased, the material at the crack tip failed locally and the crack advanced further. This was followed by fibre-pullout from the corium side of the specimen. As the crack further advanced in the grain material, some of the fibres that were not fully pulled out of the two sides of the crack surfaces were observed to bridge up the crack.

*Crack propagation in fracture is a direction perpendicular to the direction of the initial strain (30% applied during drying. In all cases magnification is X10.*

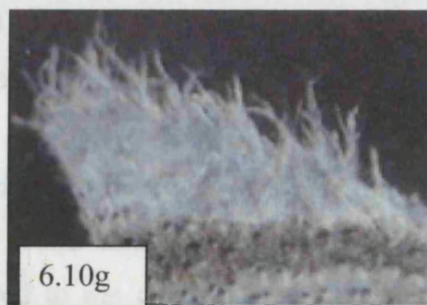
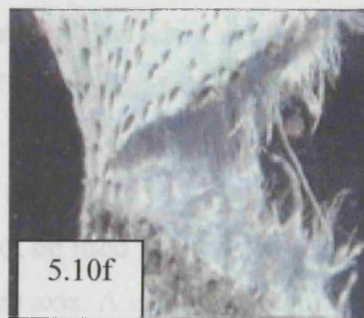
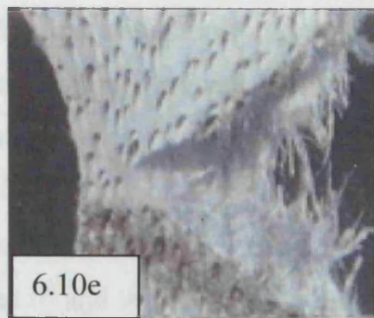
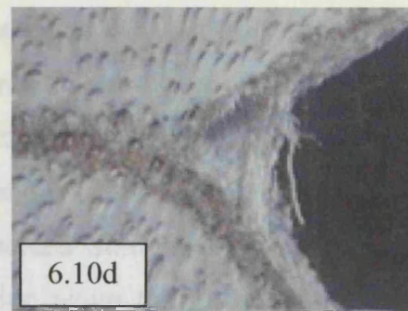
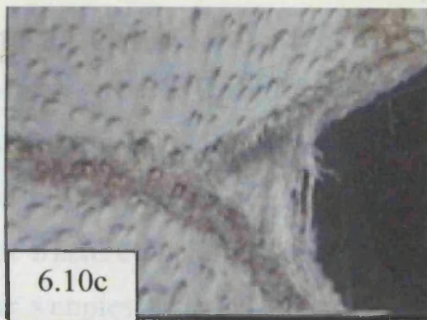
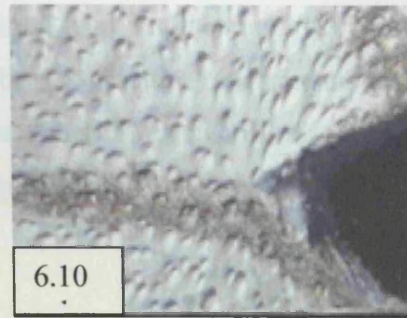
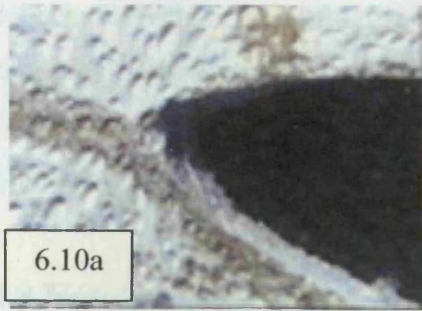


**Figure 6.10 (a-g):** A series of consecutive video images showing a crack initiating and then propagating to fracture in a direction perpendicular to the direction of the uniaxial strain (30%) applied during drying. In all cases magnification is X10.

It is because of this crack bridging that a rising load displacement curve was observed during crack propagation. It is also likely that the fracture mechanisms taking place at the crack tip may result in temperature rise and therefore causing fibre reorientation that has a marked effect on notch sensitivity of the material.

### **6.3.8 Notch sensitivity**

The measurement of notch sensitivity is clearly of value in assessing the crack resistance of leather. However it is not possible to derive a truly scientific parameter, which can be used to quantify crack resistance in non-linear materials such as leather. The essential work of fracture theory offers this possibility. With one exception, all leathers examined conformed to the expectations of the theory in that plots of specific work of fracture against ligament length yielded Straight line graphs. The exception was the samples tested for crack propagation along the initial stretch axis for 30% uniaxially pre-stretched material where data did not conform to a straight line. The reason for this was almost certainly due to the fact that when stretched along this axis the whole sample showed a high degree of plastic stretch before and during crack propagation

The essential work of fracture approach cannot be used to compare resistance to crack growth at  $0^{\circ}$  and  $90^{\circ}$  to the 30% uniaxial stretch axis. A useful comparison can however be made by examining the notch sensitivity in these two directions. Figure 6.11 shows marked differences in notch sensitivity depending on the direction of crack propagation in leather that has been stretched 30% in a single direction during drying. Previous studies on the notch sensitivity of leather [O'Leary & Attenburrow, (1996)] were concerned with fracture resistance differences between the grain and the corium layers. It was found that the grain layer was more sensitive to the presence of a notch compared to the corium layer. It was concluded that this difference was due to the ability of the corium fibre structure to deform in such a way as to blunt the propagating crack whereas the grain layer sustained a sharp crack allowing a significant stress concentration at its tip. In the present case crack tips appear to be equally sharp as shown in figure 6.12.

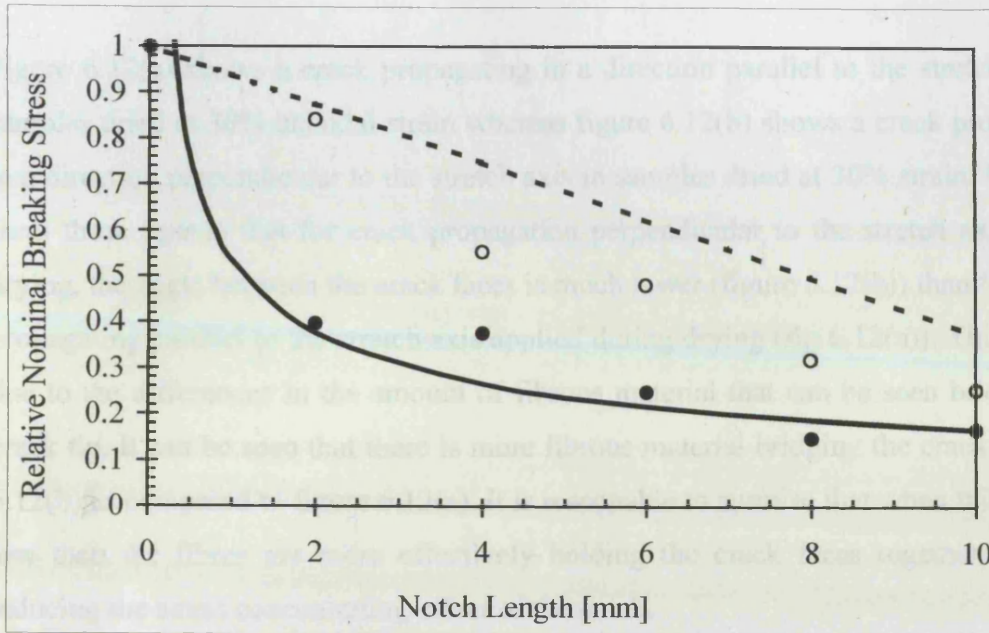


**Figure.6.11:** Relative nominal breaking stress plotted against Notch length. Closed and open circles represent samples tested perpendicular and parallel to the pre-strain axis respectively. The dashed line represents  $\sigma_n = [1 - (a/W)]\sigma_0$  whereas the solid line represents  $\sigma_n = 0.535a^{-0.5}\sigma_0$

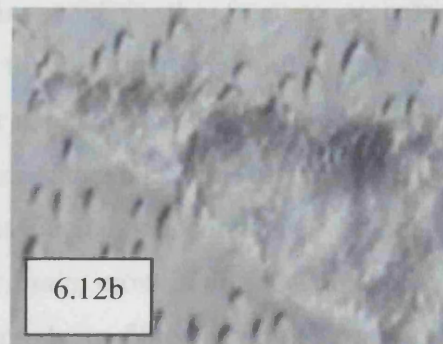


**Figure 6.12:** Cracks propagating in a direction (a) parallel to the stretch axis and (b) perpendicular to the stretch axis in samples dried at 30% strain. In both cases magnification is X10

Figure 6.12(a) shows a crack propagating in a direction parallel to the stretch axis in samples dried at 30% uniaxial strain whereas figure 6.12(b) shows a crack propagating in a direction perpendicular to the stretch axis in samples dried at 30% strain. It is clear from these figures that for crack propagation perpendicular to the stretch axis during drying, the angle between the crack faces is much lower (figure 6.12(b)) than for cracks propagating parallel to the stretch axis applied during drying (fig 6.12(a)). This may be due to the differences in the amount of fibrous material that can be seen bridging the crack tip. It can be seen that there is more fibrous material bridging the crack in figure 6.12(b) as compared to figure 6.12(a). It is reasonable to surmise that when this angle is low then the fibres are more effectively holding the crack faces together and thus reducing the stress concentrating effect of the crack.

### **6.3.9 Influence of uniaxial stretching on fracture toughness**

Figure 6.13(a) shows a crack propagating in a control leather sample dried freely and 6.13(b) shows the corresponding fracture surface. Similarly figure 6.13(c) shows a crack propagating perpendicular to the stretch axis samples dried under 30% uniaxial strain and the corresponding fracture surface is shown in figure 6.13(d). It is clear from these figures that there are more fibres involved in the fracture process for the uniaxially stretched samples as compared to the unstretched control samples. A greater number of bridging fibres were observed for uniaxially stretched samples as compared to the control samples. For samples dried under uniaxial strain the fibres are very close together as a result of lateral contraction that inevitably accompanies uniaxial loading. When samples are stretched and dried under strain, crosslinking reactions take place at regions where the fibres make contact. This produces fibres having intermittent regions of low interfacial shear strength. It appears that a crack seeks the low strength regions that debond (separation of points of adhesion between the fibres) ahead of it. This phenomenon increases fracture toughness by temporarily arresting the crack.

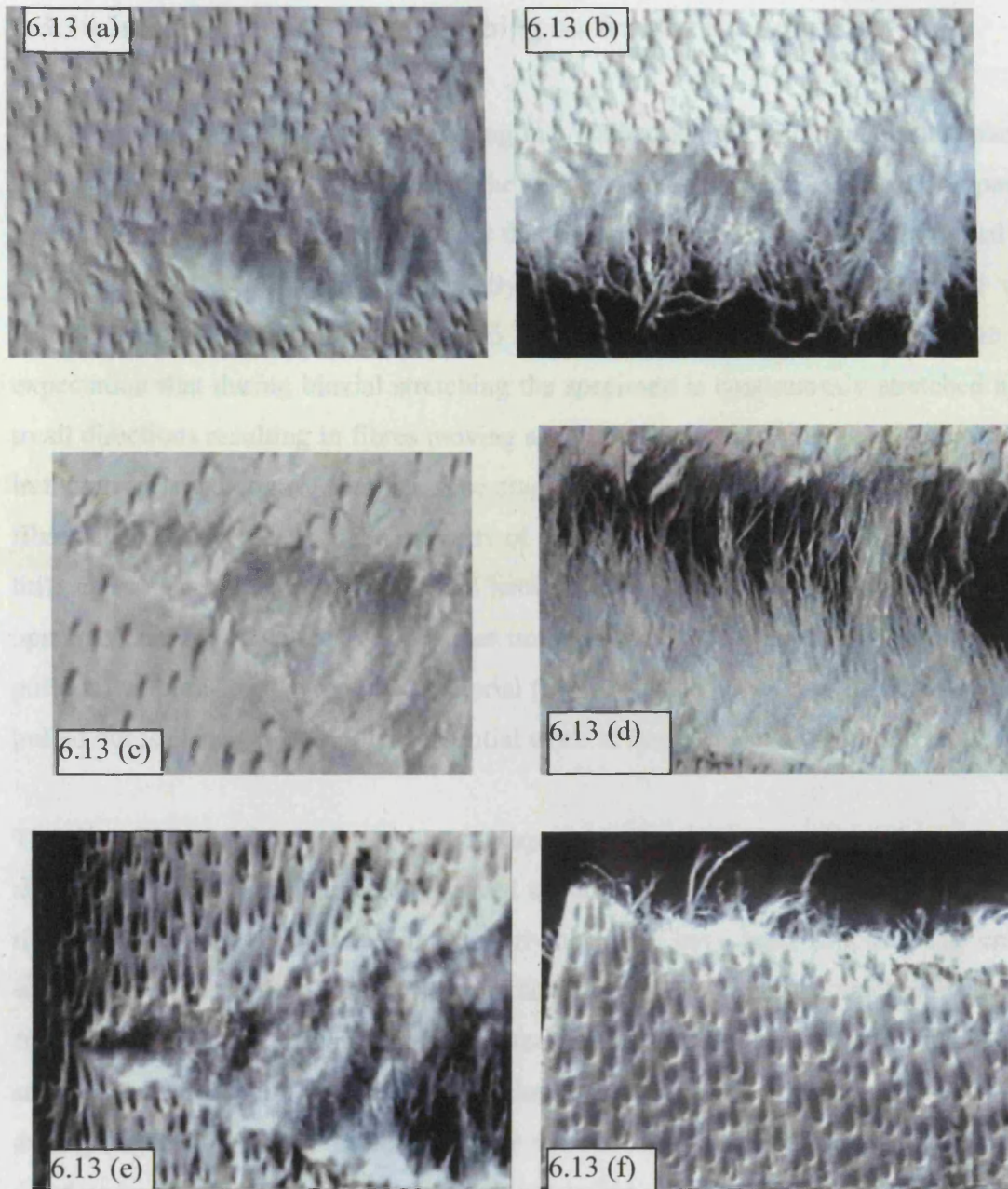


**Figure 6.13:** Cracks propagating in leather together with the associated fracture surfaces for control samples dried freely [(a & b)], uniaxially stretched samples dried under 30% strain [(c & d)] and biaxially stretched samples dried at 30x30% strain [(e & f)]. In all cases magnification is X10.

### **6.3.10 Influence of biaxial stretching on fracture toughness**

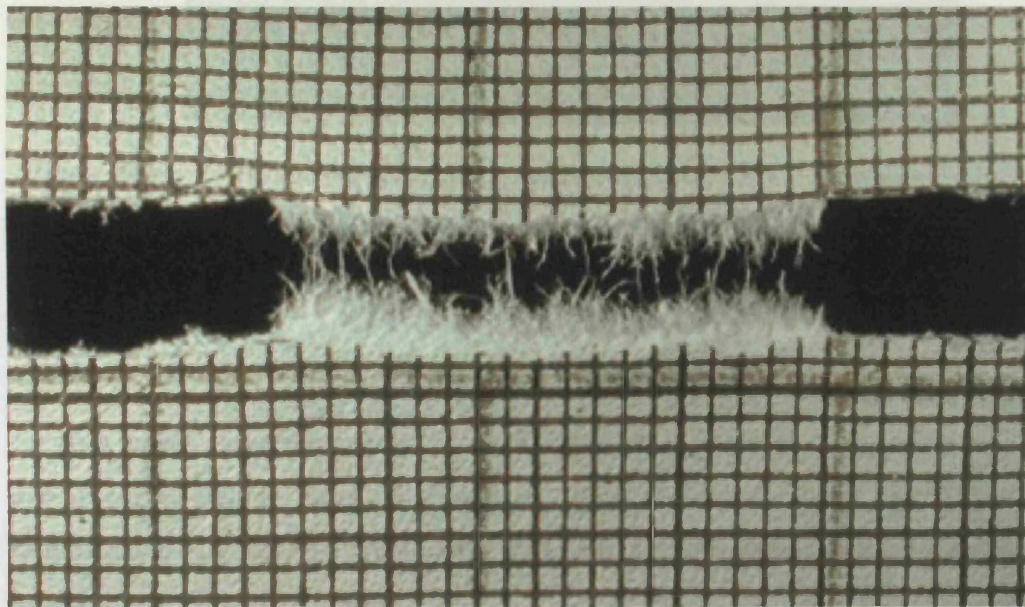
Figure 6.13(e) shows a crack propagating in a leather sample dried under 30% biaxial strains whereas figure 6.13(f) shows the corresponding fracture surface. Comparing figures 6.13b, 6.13d and 6.13f it is clear that relatively few fibres have been pulled out in the case of leather stretched biaxially during drying (fig 6.13(f)) compared with leather dried with no constraint (fig 6.13(b)). This would seem to be due to the expectation that during biaxial stretching the specimen is continuously stretched apart in all directions resulting in fibres moving apart as compared to their relative proximity in the unstretched control samples. The crack therefore propagates in a medium of low fibre density. This means that a majority of the fibres in the path of the crack have very little capacity to deviate the crack and hence they fracture instead of pulling out. The opposite occurs in samples dried under uniaxial strain and hence there is more fibre pullout from uni-axially stretched material (fig 6.13(d)). The relative numbers of fibres pulled out is clearly related to the essential work of fracture as shown in table 6.1.

The tips of the cracks were relatively sharp and had a crack tip radius of curvature of about 1/10mm. The cracks were observed to run round hair follicles. Behind the crack tip can be seen a region where the underlying fibres have been exposed. The cracks were observed to initiate first in the grain side of the sample. As the crack moves away from the notch tip the corium side fibres start pulling out of the fibre network and at the same time bridging the crack. It is clear that for leather that was unconstrained during drying (fig 6.13b), many more fibres are visible on the surface compared to leather dried under bi-axial stretch (fig, 6.13f). Most pulled out fibres were however found for uniaxially stretched material.

### **6.3.11 Validity of the results**

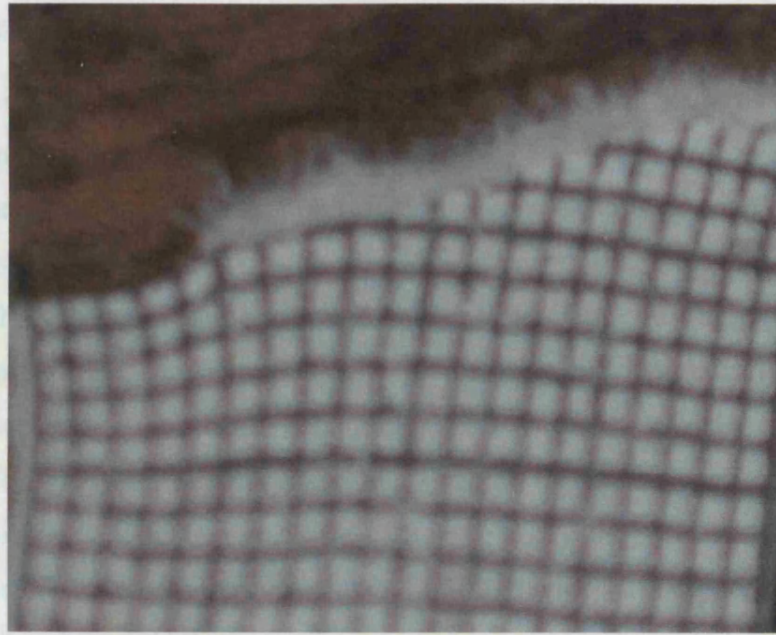
As already mentioned, the EWF method is valid if there is complete yielding of the ligament before crack initiation. To ensure that the ligament length has completely yielded, thus controlling the size of the plastic zone, it has been suggested that the ligament length should be less than twice the plastic zone radius and that the size of the

plastic zone should be free of specimen edge effects. A grid printed on the specimen gave an indication of the stress state just before crack initiation and subsequent propagation. Figure 6.14(a) shows a typical fractured specimen with a crack propagating perpendicular to the stretch direction. It can be seen from this figure that there is little or no evidence of gross yielding even after fracture. Indeed yielding was observed in a very small region ahead of the crack tip. Except for small ligament lengths ( $L < 4$  mm) the essential work of fracture approach was found to be applicable to these samples.



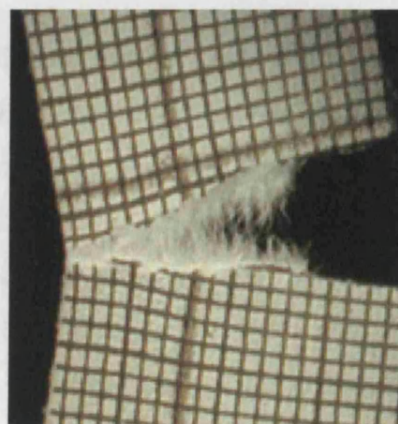
*Figure 6.14 (a) Optical microscope video image of DENT specimens obtained from samples dried under 30% uniaxial strain showing the strain distribution after fracture. This figure clearly shows that there is no gross yielding for specimens in which cracks propagated perpendicular to the strain direction during drying.*

Figure 6.14(b) shows a fractured specimen in which a crack was propagated parallel to the stretch direction applied during drying. As can be seen from the grid, global yielding is apparent and therefore the essential work of fracture approach could not be used to determine the fracture resistance. In fact cracks initiated in these samples after considerable necking followed by catastrophic failure.



**Figure 6.14 (b)** Optical microscope video image of SENT specimen showing gross yielding as indicated by the marked elongation of the original squares to give rectangles well away from the crack surface. The cracks propagated parallel to the strain direction during drying.

In both cases however when the crack was very close to the specimen edge, the specimens tended to bend as shown in figure 6.14(c) resulting in both tensile and compressive stresses. To avoid this problem, all tests were stopped just before the beginning of this phenomenon.



**Figure 6.14 (c):** Optical microscope video image of SENT specimen showing the strain distribution after fracture. Note the specimen bending that occurs as the crack approaches the specimen edges.

### **6.3.12 Fracture mechanisms**

Based on the results presented in this chapter and knowledge of fracture mechanisms in fibrous composites a generalised approach to fracture mechanisms on leather is proposed below. The initiation and propagation of a crack in any material is preceded by the creation of a deformation zone ahead of the macro-crack tip. This deformation zone is usually referred to as the process zone (damage zone). In fibrous composites, a number of fracture mechanisms operate in the process zone. These may include, fibre fracture, fibre elongation, fibre debonding, fibre bridging of the crack and the subsequent fibre pull-out. The unbroken fibres behind the macro crack tip contribute to two major micro-mechanisms; crack face bridging and fibre pull-out of unbroken but debonded fibres. The total energy dissipated in this region is therefore the summation of the pull-out and the bridging energies.

Leather is made up of a complex network of collagen fibre bundles. These bundles have a hierarchical structure composed of collagen fibres that are themselves composite materials. The various units of this hierarchical structure are held together by highly specific interactions between surfaces. The mechanical behaviour of leather will therefore depend on the response of individual constituents and the interaction between them as a result of applied stresses. The response of the hierarchical structure to applied stresses is reflected in the shape of the stress strain curve.

The initial response of leather to tensile loads is the progressive straightening of the wavy collagen fibres, while further response to stress corresponds to elastic deformation of the straight fibres. At high strains, yielding occurs and irreversible damage is imparted to the structure since the hierarchical structure begins to dissociate into individual units. Localized slippage and voiding between hierarchical levels accounts for the observed yielding at macroscopic level. Thus once leather has yielded, it cannot fully recover to its initial state. The hierarchical structure distributes the remote stress locally by imparting damage efficiently throughout the different levels of structure thereby minimizing damage concentrations that could precipitate failure and fracture. This allows the damaged leather to continue to function almost normally. The failure of these small structural elements also absorbs a tremendous amount of energy thereby preventing catastrophic failure. In the process zone, a number of damage

mechanisms operate including, frictional sliding of the fibres, fibre fracture and fibre bridging (in notched samples).

#### ***6.3.12.1. Frictional sliding and fibre pull-out.***

Potentially the most significant source of fracture work for most fibre composites is interfacial frictional sliding. Depending on the interfacial roughness, contact pressure and sliding distance, this process can absorb large quantities of energy. The potential for contribution to the toughness from fibre pull out of the collagen fibre network is substantial. However, the mechanism can apparently only operate with relatively short fibres. Continuous fibres are expected to break in the crack plane, since there will always be embedded lengths on either side of the crack plane which are long enough for the stress in the fibre to build up sufficiently to break it. The mechanisms of frictional sliding and the subsequent fibre pull out of the collagen fibre network is likely to depend on the closeness of the fibres of a give network structure.

#### ***6.3.12.2 Fibre fracture***

Depending on the fibre architecture and loading configuration, final fracture of the sample usually involves the fracture of the fibres. The fracture strain of collagen fibres is higher than the strain at which interfacial debonding between the fibres occurs. During crack propagation, interfacial debonding between the fibres takes place before disassociation of the fibre bundles into their respective constituents. The fibres can therefore still stretch without immediate failure. The added strain energy in the fibres causes disassociation of the fibres along the interface into their respective units. This continues until when the fibres themselves fracture. The contribution this makes to the fracture energy of the material is small for most fibres.

## **6.4 CONCLUSIONS**

In most situations the essential work of fracture approach is applicable to leather and therefore offers a simple and practical way of measuring the plane stress fracture toughness of leather. The results presented here also seem to indicate that the essential work of fracture is independent of the specimen size and geometry of the test specimen. Drying under strain markedly affects the grain crack resistance. When large amounts of bi-axial strain (30% $\times$ 30%) are applied during drying then specific essential work of fracture falls by 73%. The large fall in specific essential of fracture which occurs after biaxial stretching implies that for material dried under biaxial strain less energy is consumed in the so called process zone. In stretching the fibres across the growing crack work is done as individual fibres pull out of the entangled network of fibres that comprise leather. The relative numbers of fibres pulled out is related to the essential work of fracture. However 30% uniaxial strain applied during drying can give a substantial increase in essential work of fracture for cracks propagating across the stretch axis. Essential work of fracture is related to the magnitude and nature of the fibrous material pulled from the leather in the wake of the crack.

## References

- Anderson, T.L., "Fracture Mechanics-Fundamentals and Applications", second edition, CRC press LLC, (1995)
- Andrews, E.H., "The Mechanical Properties of Biological Materials-Fracture", *Symposia of the Society for Experimental Biology*, (1980), **34**, p 13
- Atkins, A.G. and Mai, Y.W., "Elastic and Plastic Fracture-Metals, Polymers, Ceramics, Composites, Biological Materials", John Wiley & sons, New York, (1985).
- Begley, J.A. and Landes, J.D., " The J-integral as a Failure Criterion", *ASTM STP 514*, (1972), pp. 1-20
- Broberg, K.B., "Critical Review of Some Theories in Fracture Mechanics", *International Journal of Fracture Mechanics*, (1968), **4**, pp 11-19
- Chan, W.Y.F. and Williams, J.G., "Determination of the Fracture Toughness of Polymeric Films by the Essential Work Method", *Polymer*, (1994), **35**, pp 1666-1672
- Griffith, A.A., "The Phenomenon of Rupture and Flow in Solids", *Philosophical Transactions of the Royal Society London*, (1920), **A221**, pp 163-198
- Guy, R. and Marriott, "The Measurement of Elongation at Break in Leather Testing", *Journal of the Society of Leather Technologists and Chemists*, (1974), vol. 58, pp137-144
- Hashemi, S., "Ductile Fracture of Polymer Films", *Plastics, Rubber and Composites Processing and Applications*, (1993), Vol. 20, No. 4, pp229-237
- Hashemi, S., "Work of Fracture of PBT/PC Blend: Effect of Specimen Size, Geometry, and Rate of Testing", *Polymer Engineering and Science*, (1997), vol. 35, No. 5, pp 912-921

Hashemi, S. and Yuan, Z., "Fracture of Poly(ether-ether ketone) Films", *Plastics, Rubber and Composites Processing and Applications*, (1994), vol. 21, No. 3, pp151-161

Hashemi, S., "Temperature and Deformation Rate Dependence of the Work of Fracture in Polycarbonate (PC) Film." *Journal of Materials Sciences*, (2000), **35**, pp 5851-5856

Higgins, R.A., "Properties of Engineering Materials", Edward Arnold, London, (1991)

Isherwood, D.P and Williams, J.G., *Engineering Fracture Mechanics*, (1978), **10**, p 887

Jones, R.E. and Bradley, W.L., "Fracture Toughness Testing of Polyethylene Pipe Materials." *ASTM STP 995*, vol. 1, (1989), pp. 447-456.

Karger-Kocsis, J., "Relationships Between Molecular and Plane-Stress Essential Work of Fracture Parameters in Amorphous Copolyesters", *Polymer Bulletin*, (1997), **39**, pp 503-510

Karger-Kocsis, J., "For What Kind of Polymer is the Toughness Assessment by the Essential Work Concept Straight Forward?" *Polymer Bulletin*, (1996), **37**, pp 119-126

Kelly, A and Macmillan, N.H., "Strong Solids", (1986), Clarendon press, Oxford

Kendall, K and Fuller, K.N.G. "J-shaped Stress/Strain Curves and Crack Resistance in Biological Materials", *Journal of Physics D., Applied Physics*, (1987), **20**, pp. 1596-1600.

Landes, J.D. and Begley, J.A., " The Effect of Specimen Geometry on  $J_{IC}$ .", *ASTM STP 514*, (1972), pp. 24-29

Letton, A., "The use of Specimen Compliance in Predicting Crack Growth", *Polymer Science and Engineering*, (1991)

- Liu, C.K., and McClintick, A.D., "An Energy Approach to the Characterization of the Fracture Resistance of Leather", *Journal of the American Leather Chemists Association*, (1997), **92**, pp103-118
- Mai, Y.W. and Atkins, A.G., "Further Comments on J-shaped Stress-Strain Curves and Crack Resistance of Biological Materials", *Journal of Physics D-Applied Physics*, (1989), **22**, pp 48-54
- Mai, Y.W. and Cotterell, B., *International Journal of Fracture*, (1984), **24**, p 229
- Mai, Y.W. and Cotterell, B., *Engineering Fracture Mechanics*, (1985), **21**, p 123
- Maspoch, M.L., Ferrer, D., Gordillo, A., Santana, O.O. and Martinez, A.B., "Effect of Specimen Dimensions and the Test Speed on the Fracture Toughness of iPP by the Essential Work of Fracture (EWF) Method", *Journal of Applied Polymer Science*, (1999), vol. 73, pp 177-187
- Mattei, V. and Roddy, W.T., "Physical Properties of Leather Fatliquored at Different Oil Levels", *Journal of American Leather Chemists Association*, (1957), **52**, p 110
- Mouzakis, D.E., Gahleitner, M. and Karger-Kocsis, J., "Toughness Assessment of Elastomeric Polypropylene (ELPP) by Essential Work of Fracture Method", *Journal of Applied Polymer Science*, (1998), vol. 70, pp 873-881
- O'Leary, D.N. and Attenburrow, G.E. "Differences in Strength Between the Grain and Corium Layers of Leather", *Journal of Materials Science*, (1996), **31**, pp. 5677-5682
- O'Leary, D., "Differences in Strength Between the Grain and the Corium Layers of Leather", *PHD Thesis*, Leicester University, (1995)
- Rice, J.R., "A Path Independent Integral and the Approximate Analysis of Strain Concentration by Notches and Cracks", *Journal of Applied Mechanics*, (1968), vol. 35, pp. 379-386

Rivlin, R.S., Thomas, A.G. "Rupture of Rubber 1-Characteristic Energy of Tearing"  
*Journal of Polymer Science*, (1953), **10**, pp 291-318

Williams, J.G., "Fracture Mechanics of Polymers", John Wiley & sons, New York,  
(1984)

Wu, J. and Mai, Y.W., "The Essential Fracture Work Concept for Toughness  
Measurement of Ductile Polymers", *Polymer Engineering and Science*, (1996), vol. 36,  
No. **18**, pp 2275-2288

# CHAPTER SEVEN

---

## CONCLUDING REMARKS AND FUTURE WORK

7.1 CHARACTERIZATION OF LEATHER QUALITY	151
7.1.1 Area Yield	151
7.1.2 Freely dried leather	152
7.1.3 Leather dried under uniaxial strain	152
7.1.4 Leather dried under biaxial strain	153
7.1.5 Leather quality from trouser tear test	153
7.1.6 Leather strength	153
7.1.7 Elongation to break	154
7.1.8 Influence of fatliqours	154
7.1.9 Fracture mechanisms	155
7.2 FURTHER RESEARCH	157

## **7.1 CHARACTERIZATION OF LEATHER QUALITY**

The main objective of this study was to establish how stretching leather could increase area yield without affecting its quality. The energy required to fracture a given piece of leather was the physical quantity used to characterise leather quality. Since toughness is an important criterion in most leather products such as upholstery and garments, fracture energy was used to determine the fracture toughness of leather using the essential work of fracture approach. The fracture toughness so determined was found to correlate well with other specific strength requirements, such as tensile strength and tear strength. If developed further this approach could provide essential knowledge to the leather industry regarding how to improve the toughness, tearing strength and softness of leather. Based on this findings discussed in chapter six, applicability of essential work of fracture method to leather has been demonstrated. Tests using SENT and DENT specimens yield a linear relationship between the specific total work of fracture and ligament length under plane stress conditions. The results derived from the tests show that the specific essential work of fracture is a material constant that is independent of geometry but is influenced by strains imposed on leather during processing, in particular the drying operation. The strain imposed on leather while wet, if sustained throughout the drying period, alters the angle of weave and fibre run which are known to influence the mechanical properties of leather.

### **7.1.1 Area Yield**

Area yield can be increased by either stretching wet blue leather uniaxially or biaxially and then allowing it to dry under strain. Uniaxial stretching introduces a high degree of anisotropy resulting in an increase not only in tensile strength parallel to the stretch direction but also in the essential work of fracture for cracks propagating perpendicular to the stretch direction. The increase in tensile strength in the parallel direction is accompanied with a corresponding reduction in strength in the perpendicular direction. This can be made use of in drive belts where high tensile strength is required mainly along the length of the belt. On the other hand biaxial stretching gives much higher area yield but there is a reduction in the essential work of fracture in both directions of

stretching. In both cases however drying at upto 15% tensile strains can be done without necessarily degrading quality as characterised by the essential work of fracture (see figure5.6). This means area gains up to 32% are feasible.

### **7.1.2 Freely dried leather**

For leather dried freely, the essential work of fracture was observed to be independent of sampling angle (angle of cutting the specimen with respect to the backbone) and therefore can be used to represent the fracture resistance of leather as compared to elongation at break and tensile strength which depend on the sampling angle. The essential work of fracture for cracks propagating both parallel and perpendicular to the backbone was found to be about  $22.6 \text{ kJ/m}^2$  for the 1 mm grain split of chrome tanned leather studied.

### **7.1.3 Leather dried under uniaxial strain**

Uniaxial stretching of leather during drying introduces a degree of anisotropy that affects its fracture toughness. For samples in which the cracks propagated perpendicular to the stretch direction, tests using SENT and DENT specimens yielded a linear relationship between the specific total work of fracture and ligament length under plane stress conditions as expected from the EWF method. In this case the essential work of fracture was found to be  $44 \text{ kJ/m}^2$ , which is about twice that of samples dried freely. However for cracks propagating parallel to the stretch direction, the essential work of fracture approach was not applicable because of the gross yielding that accompanied crack propagation for samples cut in this direction. However the most important finding was that samples with high tensile strength were also observed to have high fracture toughness values indicating a positive correlation between tensile strength and essential work of fracture.

#### **7.1.4 Leather dried under biaxial strain**

The essential work of fracture for samples dried under biaxial strains was found to be same for cracks propagating both parallel and perpendicular to the backbone. This indicates that for samples dried under biaxial strains, the essential work of fracture is independent of the sampling and orientation angles. The essential work of fracture in the case of samples dried at 30% biaxial strains was found to be about  $6\text{kJ/m}^2$  which is considerably lower than the essential work of fracture of control samples. This implies that drying leather at 30% biaxial strains degrades its quality and therefore should be avoided. However biaxial strains of upto 15% are feasible.

#### **7.1.5 Leather quality from trouser tear test**

Embedded in the main objective was the need to develop experimental techniques and the relevant equipment needed to collect data so as to compare the results with those of other sheet materials. The trouser tear test (ASTM D 1938) and split tear test (ASTM D 460) are frequently used by the leather industry to determine resistance to crack propagation of leather. In both tests, force is applied to the specimen in the same direction as the separating jaws of the test equipment. This configuration results in an out-of-plane shear mode of crack propagation (Mode III fracture) in which it is very difficult to control the fracture path. If the sample breaks across one of the legs of the specimen, rather than between the legs, the test is no longer measuring the resistance to tear propagation. The essential work of fracture offers an alternative simple method of evaluating leather quality without concern for the sampling angle.

#### **7.1.6 Leather strength**

Leather quality depends on the arrangement and strength of its fibres. The tensile strength of leather depends on the number of fibres in the woven fibre network that are oriented in the direction of the applied load. Stretching leather while wet and then drying it under strain influences fibre orientation because the fibres have a tendency of rotating and turning in the direction of applied strain. When dried freely, the orientation of the fibres is expected to be the same as that of the sample before drying. Drying

leather under uniaxial strain introduces a high degree of anisotropy resulting in a marked variation of tensile strength with the angle of cutting samples from the dried leather. This variation in tensile strength with orientation angle is similar to the variation of tensile strength with angle between the fibre and loading axes for aligned fibre composites and continuous fibre materials. The Tsai-Hill equation that is normally used to model the variation of strength with orientation of fibre composite materials can be used to describe the variation of strength with orientation angle for leather.

### **7.1.7 Elongation to break**

When leather is stretched, the observed elongation is the sum of the elongation of the constituent fibres and the distortion of the collagen fibre network. Leather dried under strain has a lower elongation to break due to the prior deformation of the fibre network. Elongation to break can therefore be modelled by assuming that subsequent elongation to be mainly due to the straightening and elongation of the fibres themselves. This model predicts well the elongation to break of samples obtained from the long rectangular samples dried under strain but overestimates the elongation to break for short samples dried under strain. This is thought to be due the fact that short samples are very close to jaws of the testing machine and therefore the fibres have limited mobility as compared to those in a longer sample.

### **7.1.8 Influence of fatliquors**

The presence of fatliquors in leather increases tensile strength, elongation to break and the essential work of fracture. These effects can be attributed to an increase in fibre mobility as a direct consequence of the presence of fatliquors, which are believed to reduce friction between the fibres and thus making it easier for them to slide past each other in response to applied stresses.

### 7.1.9 Fracture mechanisms

Leather is made up of collagen fibre bundles that have a hierarchical structure made of collagen fibres that are themselves composite materials. The mechanical behaviour of leather depends on the response to applied stresses of individual constituents and the interaction between them. It was observed that tensile loading of leather causes damage in the form of frictional sliding and fibre pullout, fibre fracture and interfacial peeling. The number of fibres pulled out is related to both tensile strength and essential work of fracture.

## 7.2 FURTHER RESEARCH

Equation 6.6 assumes that the ligament length controls the size of the plastic zone and that the plastic zone volume is proportional to  $L^2$ . It has been suggested that if the ligament length is not large compared to the thickness of the specimen, the state of stress in the ligament region becomes one of mixed mode at short ligament lengths, rather than the required state of pure plane stress. As a consequence,  $\omega_e$  and  $\omega_p$  both become dependent upon  $L$  giving rise to non-linear relationship between  $\omega_f$  and  $L$  at short ligament lengths. This is avoided by ensuring that the ligament length satisfies three requirements. Firstly, the ligament length should be greater than three times the specimen thickness. The area yield achieved during biaxial stretching of leather is accompanied by a reduction in its thickness. If the fracture toughness of leather is to be characterised by the essential work of fracture, further research is needed to determine the influence of thickness on the essential work of fracture for leather. This should be done at a constant ratio of specimen length to width

Secondly it is recommended that  $L$  should be less than twice the plastic zone size to ensure that final fracture occurs after full yielding of the ligament region in which case the size of the plastic zone is controlled by the ligament length. Work is needed to evaluate the plastic zone size for leather by mapping out the strain distribution at the crack tip from which the plastic zone size can be evaluated. This should be done at a constant ratio of specimen length to width.

Thirdly, it has been suggested that the ligament length should be less than a third of the sample width so that the size of the process zone is not disturbed by the lateral boundaries of the test specimen. However, given that the plots of  $\omega_f$  versus  $L$  showed no evidence of non-linearity for ligament lengths exceeding  $W/3$ , one may conclude that the pre-requisite  $L \leq W/3$  is too restrictive for leather. For uniaxially dried samples in which cracks were propagating perpendicular to the stretch axis, this may be due to the fact that yielding was localised at the crack tip.

However confidence in the use of essential work of fracture can be achieved by carrying out further research on a large scale on different types of leather of varying thickness. In all cases tests in the scanning electron microscope will help to identify the underlying fracture mechanisms.

#### **APPENDIX: DATA FOR SOME OF THE FIGURES**

**Data for figure 4.2**

Position	Normalised Tensile Strength Side 1	Normalised Tensile Strength Side 2
1	0.886	0.877
2	1.101	0.943
3	0.989	0.797
4	1.028	0.875
5	0.932	1.058
6	0.880	0.983
7	0.993	1.00976
8	1.117	0.814
9	0.860	1.042
10	1.057	1.134
11	1.346	1.168
12	1.031	1.364

**Data for figure 4.3**

Position	Normalised Strength Side 1	Normalised Strength Side 2
1	0.788	0.698
2	1.082	0.953
3	0.989	0.898
4	1.466	0.869
5	1.212	0.963
6	0.922	0.969
7	0.918	0.832
8	1.058	1.204
9	0.745	0.896
10	0.924	0.823
11	0.950	1.012
12	1.423	1.119

**Data for figure 4.5**

Position on the hide	Tensile Strength [MPa] Parallel to the Backbone	Elongation to Break [%] Parallel to the Backbone	Tensile Strength [MPa] Perpendicular to the Backbone	Elongation to Break [%] Perpendicular to the Backbone
1	11.809	46.015	10.510	27.416
2	14.680	41.032	14.437	36.982
3	13.188	52.8	13.179	43.25
4	13.710	34.75	19.545	30
5	12.427	37.982	16.156	29.616
6	11.739	36.416	12.287	33.349
7	13.236	43.05	12.239	40.15
8	14.8881	28.15	14.107	38.2
9	11.466	27.283	9.931	25.599
10	14.097	27.816	12.324	32.399
11	17.952	33.2	12.668	53.4
12	13.744	31.7	18.974	33.6

**Data for figure 4.8**

Angle	Average Tensile Strength [MPa] Predicted using the Maximum Stress Criterion (L-fracture)	Average Tensile Strength [MPa] Predicted using the Maximum Stress Criterion (T-fracture)	Average Tensile Strength [MPa] Predicted using the Maximum Stress Criterion (Shear-fracture)	Average Tensile Strength [MPa] (Experimental data for Uniaxially Dried Long Samples)
0	28.227			28.227
5	28.443	966.677	40.260	
10	29.105	243.519	20.440	
15	30.253	109.618	13.982	13.485
20	31.966	62.772	10.876	
25	34.364	41.113	9.126	
30	37.636	29.372	8.073	9.139
35	42.066	22.319	7.439	
40	48.101	17.772	7.099	
45	56.454	14.686	6.991	6.991
50	68.317	12.513	7.099	
55	85.799	10.943	7.440	
60	112.908	9.791	8.073	5.768
65	158.040	8.939	9.126	
70	241.302	8.316	10.876	
75	421.378	7.870	13.982	6.754
80	936.104	7.571	20.440	
85	3715.974	7.399	40.259	
90	7.52E+33	7.343	5.706E+16	7.343

**Data for figure 4.9**

Angle	Tensile Strength [MPa] Experimental data for Long Samples	Tensile Strength [MPa] Predicted Using Tsai-Hill Theory (Long Samples)	Tensile Strength [MPa] Experimental data for Control Samples
0	21.333	21.333	13.27
5		20.229	
10		17.781	
15	17.802	15.257	
20		13.184	
25		11.608	
30	11.109	10.439	12.44
35		9.580	
40		8.954	
45	10.105	8.506	12.07
50		8.195	
55		7.991	
60	8.196	7.872	11.73
65		7.816	
70		7.805	
75	7.267	7.820	
80		7.846	
85		7.868	
90	7.877	7.877	11.32

**Data for figure 4.10**

Angle	Tensile Strength [MPa] Experimental data for Short Samples	Tensile Strength [MPa] Experimental data for Control Samples	Tensile Strength [MPa] Predicted Using Tsai-Hill Theory (Short Samples)
0	14.955	13.2698	14.975
5			14.948
10			14.861
15	14.891		14.692
20			14.418
25			14.021
30	13.704	12.4384	13.502
35			12.883
40			12.204
45	11.455	12.072	11.510
50			10.843
55			10.231
60	9.386	11.7256	9.692
65			9.237
70			8.868
75	7.85		8.585
80			8.385
85			8.265
90	8.226	11.3176	8.226

**Data for figure 4.15**

Azimuth angle	Normalised X-RAY Intensity for Long sample	Normalised Tensile Strength {TS (Expt-data)}
1.4063	0.0126	0.0127
2.8125	0.012588	
4.2187	0.012551	
5.625	0.012487	
7.0312	0.012369	
8.4375	0.012272	
9.8437	0.012159	
11.25	0.011988	
12.656	0.011827	
14.063	0.01166	
15.469	0.011462	0.0106
16.875	0.011279	
18.281	0.011085	
19.688	0.01091	
21.094	0.010692	
22.5	0.010458	
23.906	0.010263	
25.312	0.010074	
26.719	0.00987	
28.125	0.0096612	
29.531	0.0094333	
30.937	0.0092163	0.00660
32.344	0.008988	
33.75	0.0087545	
35.156	0.0085357	
36.562	0.0083312	
37.969	0.0081176	
39.375	0.0078823	
40.781	0.0076613	
42.187	0.0074741	
43.594	0.0072688	
45	0.0070648	0.0060
46.406	0.0068656	
47.812	0.0066869	
49.219	0.0064815	
50.625	0.0062958	
52.031	0.0061251	
53.437	0.0059559	
54.844	0.0057719	
56.25	0.0055929	
57.656	0.0054485	
59.062	0.0053141	
60.469	0.0051782	0.00487
61.875	0.0050482	
63.281	0.0049392	

64.687	0.0048695	
66.094	0.0047865	
67.5	0.0047099	
68.906	0.004645	
70.312	0.0045885	
71.719	0.0045386	
73.125	0.0044841	
74.531	0.0044522	
75.937	0.00442	0.00432
77.344	0.0043683	
78.75	0.0043461	
80.156	0.0043234	
81.562	0.0043111	
82.969	0.0042927	
84.375	0.0042897	
85.781	0.0042939	
87.187	0.0043232	
88.594	0.0043372	
90	0.0043619	0.00468

**Data for figure 5.3**

Orientation Angle	Average % Strain	Average Strength [MPa]
0	8.75	28.227
15	13.25	13.485
30	20.041	9.139
45	28.292	6.991
60	68.582	5.768
75	79.79	6.754
90	87.289	7.343

**Data for figure 5.4**

Orientation Angle	Predicted Strain % at Break for Long samples	Experimental Strain % at Break for Long Samples
0	18	18
1	18.02374	
2	18.09488	
3	18.21326	
4	18.37855	
5	18.59034	
6	18.84809	
7	19.15113	
8	19.49871	
9	19.88997	
10	20.32394	
11	20.79957	
12	21.31573	
13	21.87121	
14	22.46473	
15	23.09493	21.499
16	23.76043	
17	24.45978	
18	25.19149	
19	25.95403	
20	26.74586	
21	27.5654	
22	28.41107	
23	29.28126	
24	30.17438	
25	31.08881	
26	32.02296	
27	32.97524	
28	33.94406	
29	34.92786	
30	35.92508	27.416
31	36.9342	
32	37.95372	
33	38.98214	
34	40.01801	
35	41.0599	
36	42.10641	
37	43.15616	
38	44.20782	
39	45.26007	
40	46.31164	
41	47.36126	
42	48.40773	
43	49.44985	
44	50.48648	

45	51.51648	55.582
46	52.53877	
47	53.55229	
48	54.55601	
49	55.54891	
50	56.53005	
51	57.49847	
52	58.45326	
53	59.39355	
54	60.31848	
55	61.22723	
56	62.11899	
57	62.99301	
58	63.84853	
59	64.68484	
60	65.50125	73.081
61	66.29709	
62	67.07173	
63	67.82455	
64	68.55496	
65	69.2624	
66	69.94632	
67	70.60621	
68	71.24158	
69	71.85194	
70	72.43686	
71	72.9959	
72	73.52866	
73	74.03477	
74	74.51385	
75	74.96558	75.831
76	75.38963	
77	75.78571	
78	76.15354	
79	76.49288	
80	76.80348	
81	77.08515	
82	77.33767	
83	77.56089	
84	77.75465	
85	77.91882	
86	78.05329	
87	78.15797	
88	78.23279	
89	78.27771	
90	78.29268	80.248

**Data for figure 5.5**

Angle	Predicted Strain % at Break for Short Samples	Experimental Strain % at Break for Short Samples
0	18	18.833
1	18.01633	
2	18.06527	
3	18.14671	
4	18.2605	
5	18.40637	
6	18.58401	
7	18.79305	
8	19.03305	
9	19.30349	
10	19.60381	
11	19.9334	
12	20.29158	
13	20.67762	
14	21.09075	
15	21.53016	14.333
16	21.99499	
17	22.48435	
18	22.99731	
19	23.53292	
20	24.0902	
21	24.66814	
22	25.26571	
23	25.88189	
24	26.51562	
25	27.16583	
26	27.83145	
27	28.51142	
28	29.20464	
29	29.91005	
30	30.62658	15.5
31	31.35314	
32	32.08868	
33	32.83214	
34	33.58248	
35	34.33865	
36	35.09964	
37	35.86444	
38	36.63206	
39	37.4015	
40	38.17182	
41	38.94206	
42	39.7113	
43	40.47862	
44	41.24314	

45	42.00398	27.666
46	42.76029	
47	43.51123	
48	44.256	
49	44.99379	
50	45.72384	
51	46.4454	
52	47.15772	
53	47.8601	
54	48.55185	
55	49.23229	
56	49.90077	
57	50.55666	
58	51.19935	
59	51.82824	
60	52.44277	33.332
61	53.04238	
62	53.62655	
63	54.19475	
64	54.7465	
65	55.28131	
66	55.79875	
67	56.29836	
68	56.77973	
69	57.24247	
70	57.68619	
71	58.11054	
72	58.51516	
73	58.89974	
74	59.26397	
75	59.60756	58.332
76	59.93023	
77	60.23175	
78	60.51187	
79	60.77037	
80	61.00706	
81	61.22176	
82	61.4143	
83	61.58452	
84	61.73232	
85	61.85756	
86	61.96017	
87	62.04005	
88	62.09715	
89	62.13143	
90	62.14286	64.831

**Data for figure 6.4(a)**

Ligament Length [mm]	SWOF [kJ/m <sup>2</sup> ] for (exp) Samples	SWOF [kJ/m <sup>2</sup> ] for (control) Samples
2	89.671	71.197
4	66.413	64.401
6		
8	83.47	93.74
10		
12	110.678	138.71
14	115.947	146.95

**Data for figure 6.4(b)**

Ligament Length [mm]	SWOF [kJ/m <sup>2</sup> ] Biaxial-0	SWOF [kJ/m <sup>2</sup> ] Biaxial-90	SWOF [kJ/m <sup>2</sup> ] Control-0	SWOF [kJ/m <sup>2</sup> ] Control-90
2	17.485	21.003	51.074	33.241
4	20.919	21.946	53.168	36.525
6	29.929	27.871	59.213	51.085
8	35.14	27.933	76.864	52.215
10				
10	43.041	38.964	107.428	70.935
12				
12	47.178	55.683	126.728	73.408
14				
14	68.829	67.879	137.101	

**Data for figure 6.5(a)**

Ligament length [mm]	SWOF [kJ/m <sup>2</sup> ] Unstretched & non-Fat	SWOF [kJ/m <sup>2</sup> ] Unstretched & Fat	SWOF [kJ/m <sup>2</sup> ] Stretched & Fat	SWOF [kJ/m <sup>2</sup> ] Stretched & non-Fat
2	89.671	71.197	83.23	75
4	66.413	72.98	90.76	78.8
6	75	85.48	98.65	80.54
8	83.47	92.11	113	95.163
10	92	109.56	125.43	115
12	110.678	133.71	150.71	128.44
14	115.947	148.95	165.21	158

**Data for table 6.5(b)**

Ligament length [mm]	SWOF [kJ/m <sup>2</sup> ] for non-Fat & Stretched (0)	SWOF [kJ/m <sup>2</sup> ] for non-Fat & Stretched (90)	SWOF [kJ/m <sup>2</sup> ] For Fat & Stretched (0)	SWOF [kJ/m <sup>2</sup> ] for Fat & Stretched (90)
2	35.123	42.021	16	15.978
4	42.173	64.371	24.195	24.217
6	50.165	64.876	33.21	35
8	67.791	98.987	40.875	40.11
10				
10	80.112	128.57	52.073	48.783
12				
12	85.782	134.428	54.377	55.023
14				
14	95.443	165.317	68.717	66.732

**Data for figure 6.6 (a)**

Applied Strain %	SWOF [kJ/m <sup>2</sup> ] of Biaxially Stretched Samples	SWOF [kJ/m <sup>2</sup> ] of Uniaxially Stretched Samples
0	22.6	28.3
15	20	29
20	18	32
30	6.1	44.5

**Data for figure 6.6 (b)**

Ligament Length [mm]	SWOF [kJ/m <sup>2</sup> ] for (0%) Uniaxially Applied Strain	SWOF [kJ/m <sup>2</sup> ] for (15%) Uniaxially Applied Strain	SWOF [kJ/m <sup>2</sup> ] for (20%) Uniaxially Applied Strain	SWOF [kJ/m <sup>2</sup> ] for (30%) Uniaxially Applied Strain
2	71.197	78.124	82.707	89.671
4	64.401	65	65	66.413
6				
8	93.74	90	87	83.47
10				
12	138.71	127	120	110.678
14	146.95	133.916	123.659	115.947

**Data for figure 6.6(c)**

Ligament Length [mm]	SWOF [kJ/m <sup>2</sup> ] for (0%) Biaxially Applied strain	SWOF [kJ/m <sup>2</sup> ] for (15%) Biaxially Applied strain	SWOF [kJ/m <sup>2</sup> ] for (20%) Biaxially Applied strain	SWOF [kJ/m <sup>2</sup> ] for (30%) Biaxially Applied strain
2	51.074	35.375	25.221	17.485
4	53.168	49.771	38.754	20.919
6	59.213	48.115	47.876	29.929
8	76.864	71.082	58.543	35.14
10				
10	107.428	87.975	64.975	43.041
12				
12	126.728	107.92	70.214	47.178
14				
14	137.101	120.442	99.714	68.829

**Data for figure 6.7(a)**

{Thickness} <sup>2</sup> [mm] <sup>2</sup>	Tearing force [N] For Control Samples Dried Freely
1.3689	28.194
1.2544	15.944
1.0816	16.877
1.3689	17.816
0.8649	14.659
0.8836	14.962
0.81	12.11
0.9025	12.695
0.6241	12.301

**Data for figure 6.7 (b)**

{Thickness} <sup>2</sup> [mm] <sup>2</sup>	Tearing force [N] For Samples dried at 30% Uniaxial Strain
0.9025	15.773
1.1025	16.383
0.5476	9.218
0.5329	8.481
0.5476	8.839
0.5776	10.23
0.6889	11.937
0.5184	9.474

**Data for figure 6.8 (a)**

Ligament-Length [mm]	SWOF for SENT Specimens
5	38.68
10	63.712
15	70.735
20	81.978
25	99.099
30	120.767
35	138.812

**Data for figure 6.8(b)**

Ligament length [mm]	SWOF for (DENT) Specimens.
8	40.754
14	58.786
20	68.234
26	79.917
32	99.099
38	122.839
44	132.621